NASA Contractor Report 158920

Study of Thermal Insulation For Airborne Liquid Hydrogen Fuel Tanks

F. E. Ruccia, R. S. Lindstrom
and R. M. Lucas

Arthur D. Little, Inc.
Cambridge, Massachusetts 02140

CONTRACT NAS1-14157
SEPTEMBER 1978

National Aeronautics and
Space Administration

Langley Research Center
Hampton, Virginia 23665

NASA CONTRACTOR REPORT 158920

STUDY OF THERMAL INSULATION FOR AIRBORNE LIQUID HYDROGEN FUEL TANKS

F. E. RUCCIA, R. S. LINDSTROM,
AND R. M. LUCAS

ARTHUR D. LITTLE, INC.
CAMBRIDGE, MASSACHUSETTS 02140

CONTRACT NAS1-14157
SEPTEMBER 1978

NATIONAL AERONAUTICS AND
SPACE ADMINISTRATION

LANGLEY RESEARCH CENTER
HAMPTON, VIRGINIA 23665

TABLE OF CONTENTS

TABLE OF CONTENTS (Continued)

LIST OF FIGURES

APPENDICES

LIST OF FIGURES (Continued)

LIST OF TABLES

LIST OF TABLES (Continued)

APPENDICES

STUDY OF THERMAL INSULATION

FOR AIRBORNE LIQUID HYDROGEN FUEL TANKS*

F. E. Ruccia, R. S. Lindstrom, and R. M. Lucas**

SUMMARY

With the need for developing alternative jet aircraft fuels becoming more obvious, NASA has determined that liquid hdyrogen has the potential of being technically feasible, economical, and compatible with the environment. However, if liquid hydrogen were to be used in an aircraft, a reliable, light-weight thermal insulation would be required for the fuel tanks. Thus, the contract was undertaken for (1) development of a concept for thermally insulating the outside of liquid hydrogen fuel tanks that would meet certain life and reliability requirements; and (2) for the determination of the requirements of the system concept and identification and development of materials required to implement the concept.

Arthur D. Little, Inc., directed its efforts toward developing and screening light-weight foam materials which would meet stipulated requirements and also be capable of machine production. In its foam evaluation and selection program, Arthur D. Little subjected the foam materials to a series of tests and analyses, including porosity, cold shock, high-temperature deformation, gas diffusion, thermal strain and contraction evaluation, 0.3- and 0.6-meter-square cold panel tests and thermal conductivity measurements. In addition, tests and/or evaluation of adhesives and vapor barriers were conducted.

The test program resulted in the selection of two foams, Stafoam AA1602 and Upjohn 452, both of which were reinforced with 10 percent, 1.6-mm-long milled glass fibers (OCF Style 701). Crest 7410 percent, was selected from among several adhesives evaluated, for use with the foam and vapor barrier. The selected vapor barrier consists of a laminate of three layers of aluminum foil, two layers of Mylar film and a scrim material.

---

* Use of commercial products or names of manufacturers in this report does not constitute official endorsement of such products or manufacturers, either expressed or implied, by the National Aeronautics and Space Administration.

**Members of the staff of Arthur D. Little, Inc., Cambridge, Mass.

INTRODUCTION

Looking ahead to the need for alternative jet aircraft fuels, NASA has found [1,2] that liquid hydrogen has the potential for being technically feasible, economical, and compatible with the environment. However, the use of liquid hydrogen in aircraft requires a reliable, light-weight, thermal insulation for the fuel tanks.

The purpose of this study was to develop a concept for thermally insulating the outside of liquid hydrogen fuel tanks that would meet certain life and reliability requirements. A secondary purpose was to determine the requirements of the system concept and to identify the materials needed to implement the concept.

Arthur D. Little, Inc., had worked previously on a ground-hold, thermal insulation system for launch vehicle, liquid hydrogen propellant tanks. A concept making use of reinforced polyurethane foam and an outer gas-vapor barrier was developed and demonstrated experimentally [3]. This concept showed great potential for the present application. It was mutually agreed, therefore, that our present work would enlarge upon this concept and pursue the development of a thermal insulation that would meet the requirements for the liquid hydrogen fuel tanks of a jet aircraft.

At the beginning of the program, we reviewed Brewer's [4] work in which the liquid hydrogen jet aircraft requirements were developed for a 400-passenger, 5,500-nautical mile mission. From this, we obtained the full-scale fuel tank and insulation requirements as well as the expected operational conditions for the fuel storage system. With this as a basis, and enlarging upon our previous work, we developed an insulation concept consisting of a plastic foam insulation bonded to the outside of the liquid hydrogen tank and containing both an inner and outer gas-vapor barrier.

In the following sections, we describe the liquid hydrogen fuel storage system requirements and the new insulation concept in detail. In addition, we identify the material requirements needed to implement the concept and make it viable. The largest part of our program was concerned with the development and screening of light-weight foam materials which would meet the requirements and also be capable of machine production. Thus, we conducted a large variety of tests and analyses to both identify and screen acceptable foam materials.

In subsequent sections, we deal with the selection of adhesive and vapor barrier systems. Finally, we provide a summary of results.

*No. in [ ] refer to references on page 113.

REQUIREMENTS

The requirements for a thermal insulation for an airborne liquid hydrogen fuel tank are presented in this section. Two sets of requirements have been considered: (1) general requirements dealing with the aircraft size and mission from which tank size and configuration, environments, and conditions are obtained; and (2) requirements dealing with the insulation system and materials that evolved from the insulation concept being considered in this program.

General Requirements

Liquid hydrogen aircraft. - The aircraft upon which the tankage requirements are based is taken from the Lockheed Aircraft Company "Study of the Application of Hydrogen Fuel to Long-Range Subsonic Transport."[4] The aircraft and mission details are summarized in Table 1 and the aircraft configuration is shown in Figure 1.

The exterior configuration resembles a conventional, wide-body, subsonic jet passenger aircraft. The interior configuration, however, is significantly different in that the fuel is stored within the fuselage. Two fuel tanks are provided. The forward tank is located between the flight crew compartment and the passenger compartment; the rear tank is located in the tail section of the fuselage behind the passenger compartment.

A typical mission for the hydrogen-fueled aircraft is as follows. On the ground, the aircraft will be subject to the prevailing climatic conditions with temperatures ranging between 244K and 347K and atmospheric pressure. In flight, the aircraft climbs to an altitude of about 11.27 km and achieves a speed of Mach 0.85. At these conditions, the minimum air temperature is 218K; and the minimum atmospheric pressure is 24mPa. The average cruise period of the mission is 10.3 hours, and fuel is consumed at a rate of about 0.45 kg/sec (1 lb/sec).

The aircraft is designed for a life of 50,000 hours extending over a period of 15-20 years. In this period, the aircraft will accomplish about 6,000 missions. One of the anticipated operational modes of the aircraft is to maintain the fuel tanks cold with liquid hydrogen on a full-time basis, except at yearly intervals when the tanks are warmed for inspection and maintenance. Thus, the tanks will undergo at least 20 full temperature cycles. Initially, the fuel tanks of test aircraft may be warmed and inspected at shorter intervals.

Tank size and configuration. - The rear tank is the largest of the two fuel tanks. It is nearly cylindrical with a mean diameter of 5.6 m and a length of about 12.9 m, resulting in a capacity of 16,690 kg. The tanks are capable of internal pressures of 124-137mPa above and up to

Table 1 - Aircraft and mission details -- liquid-hydrogen-fueled, long-range, subsonic, transport aircraft.

Mission	Units	Customary Units
Range	10,190 km	5500 n mi
Payload	39,900 kg	88,000 lb
Passenger Equivalent	400	400
Cruise Mach Number	0.85	0.85
Altitude (Maximum Cruise)	11.27 km	37,000 ft
Flight Duration	11.7 hours	11.7 hours
Aircraft Utilization Factor	0.375	0.375
Aircraft Life	50,000 hours	50,000 hours
Aircraft		
Gross Weight	177,000 kg	391,700 lb
Operating Weight, Empty	109,200 kg	242,100 lb
Fuel Weight	27,900 kg	61,600 lb
Fuselage Length	67.8 m	219 ft
Wing Span	53.0 m	174 ft
Engine Thrust (each of 4 engines)	127,800 N	28,700 lb
Average Fuel Consumption Rate (approximate total)	0.45 kg/sec	1.0 lb/sec

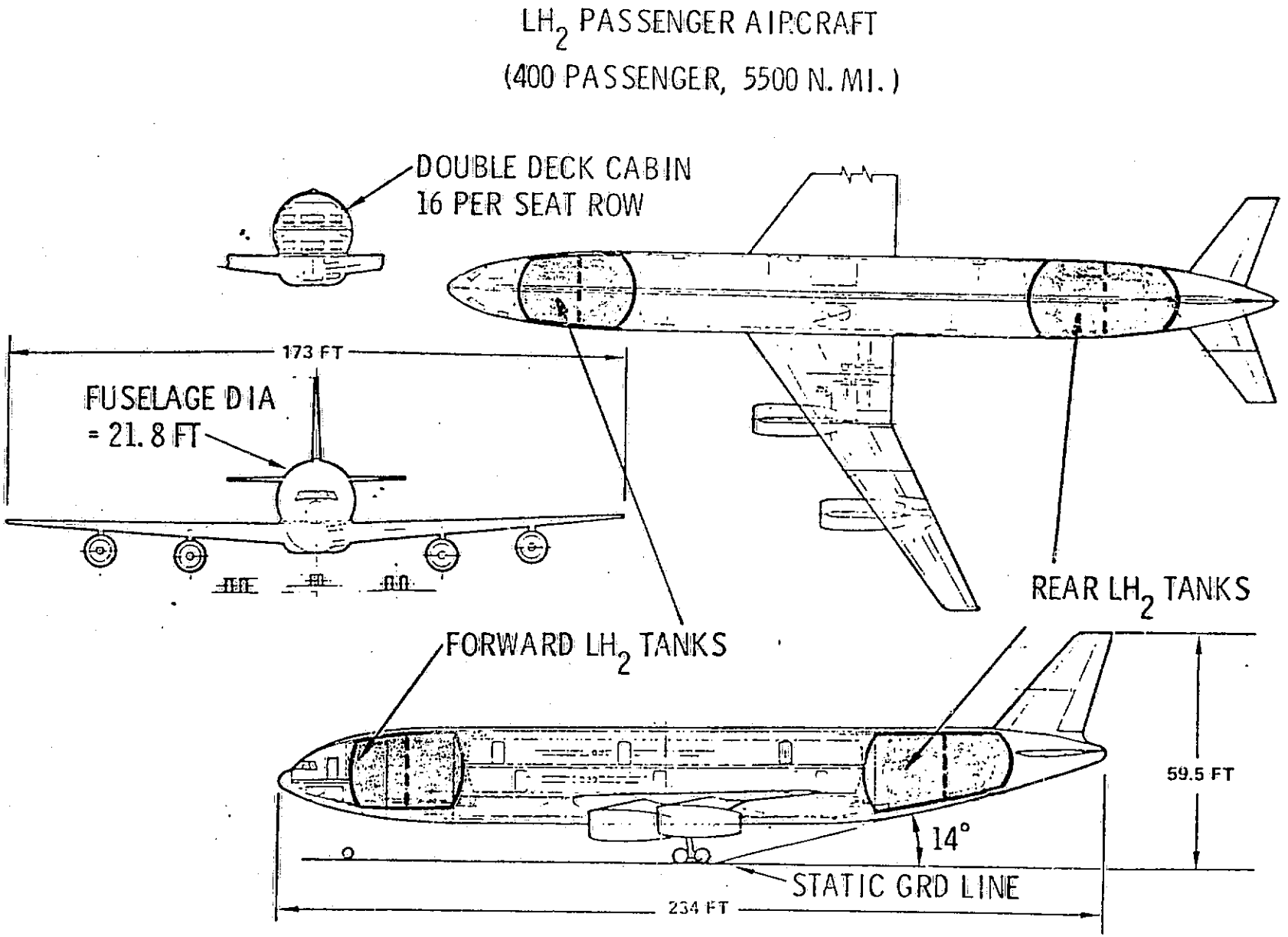

Courtesy of Lockheed Aircraft Co.

Figure 1. - Selected internal tank configuration.

14mPa below the external pressure. Further, the tank material has been designated as aluminum alloy 2219-T85. The outer surface is assumed to be smooth, while the interior surface may be webbed or formed with rings and stringers.

The tank will be of the non-integral type mounted within the airframe. Supports to the tanks will be provided within the airframe and allowances made for dimensional changes in the tanks due to temperature and pressure. These supports are not presently defined and several configurations are possible. Provisions will also be made for the removal of the tanks from the aircraft for extensive and thorough tests and inspections necessary for recertification.

Tank Insulation. - The insulation optimization by Brewer [4] establishes the requirement for a foam insulation thickness of approximately 152 mm (6.0 inches). This is based on nominal densities and thermal conductances of presently available polyurethane foam materials.

The outer insulation surface temperature will vary in accordance with the operational environment. In the extremes, this variation occurs between 220°K (-65°F) and 347°K (165°F). However, for 95 percent of the aircraft life, the temperatures are expected to remain between 261°K (10°F) and 311°K (100°F).

Purge Space. - The space within the airframe surrounding the fuel tanks is called the purge space. It is assumed that this space is maintained at cabin pressure during all phases of flight operations, except during emergency situations when cabin pressure is lost or when hydrogen is detected. For the present, no statement is made relative to the operations and purge gas, if any, that may be used for inerting and otherwise diluting any hydrogen leakage into this space.

The amount of water vapor in the atmosphere that condenses and/or freezes onto the outer surface of the tank insulation is dependent upon climatic and operational conditions and upon the fuel tank and airframe configurations. For many situations, the quantity of condensation and/or freezeout will be zero. However, there are many other situations when there will be condensation and/or freezeout of water vapor. Therefore, provisions must be made to condition the air in the purge space, or to eliminate water accumulation with hot air or other appropriate dry gas-purge methods.

System Description

Liquid hydrogen containers require thermal insulation to minimize evaporative losses. In general, large volumes of hydrogen are stored and shipped as a liquid at 21 K saturated at a pressure of 1 atmosphere. Because the ambient environment is always warmer, there is a constant inward heat flow to the stored liquid which causes boiling and loss of liquid by evaporation. Thermal insulations are necessary to limit this loss to acceptable levels.

The thermal protection system for a liquid hydrogen container must physically and thermally isolate the tank surfaces from the ambient atmosphere and structures. The liquid hydrogen tank can be isolated physically in two principal ways. The first of these, and the one common in ground-based storage tanks, is to place around the liquid container a separate shell that can be evacuated. In this case, several types of insulations, including powders and multilayer types, can be placed in the evacuated space to provide the thermal isolation. The second isolation method is to attach a closed-cell insulating foam to the liquid container outer surface, so that there are no fluid flow paths between the surrounding atmosphere and the liquid container. The foam and the gas barrier membrane provide the physical isolation. The low conductance of the gas within the closed cell foam provides the thermal isolation required.

At the direction of NASA/LRC, the thermal insulations considered in this program were to be the latter type, consisting of a non-evacuated foam material applied to the external surfaces of the liquid hydrogen tanks. The concept we developed consists basically of a bonded composite of two plastic foam layers and two vapor barriers, as shown in Figure 2. The basic objective of this design is to provide a system in which diffusion, flow, and the accumulation of the atmospheric gases within the foam insulation are reduced to the lowest possible levels and inhibited in every way possible so as to eliminate all the destructive tendencies which their presence entails.

The two foam layers provide the thermal insulation and because of their rigidity act as support for the vapor barriers. Also, because of their closed-cell characteristics, they provide a physical isolation as well. The first layer of foam is made up of separately formed pieces that are continuously bonded to the liquid hydrogen tank and to each other. A flexible membrane is then continuously bonded to the exposed surface of the first foam layer. The vapor barriers are necessary because foams are porous to a small degree, and they are also permeable to gases over long periods of time. The second layer of foam, like the first, is made up of separately formed pieces that are then continuously bonded to the first gas barrier and to each other. A second flexible membrane is then continuously bonded to the exposed outer surface of the second foam layer.

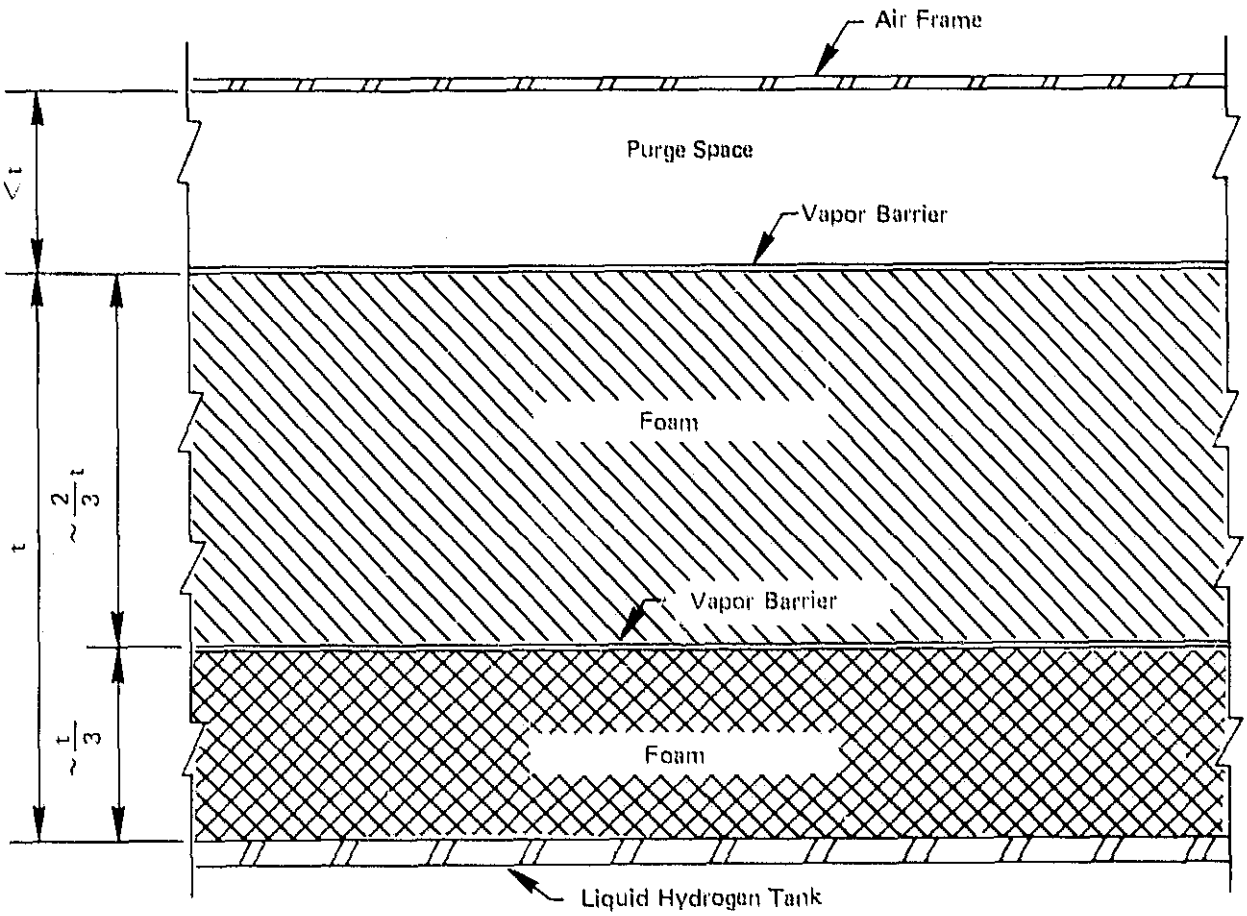

Figure 2. – Insulation concept

The first or inner gas barrier is intended to isolate the inner foam layer from any atmospheric gases that may succeed in penetrating the outer barrier and foam layers. The position of this shield is determined from the thermal conductance of the foam material and from the lowest environmental temperature that can be imposed at the outer insulation surface. The inner gas barrier position is such that its temperature is always above the normal condensing temperatures of the significant atmospheric gases such as oxygen, argon, and nitrogen. This position is determined from the steady-state temperature distribution within the foam. For a typical polyurethane foam and an outer surface temperature of 219K, the foam has a temperature of about 100 K at a depth representing about 15 percent of the total thickness. To provide a factor of safety, a depth representing about 25 to 35 percent of the total thickness is recommended for the location of the inner barrier.

The temperatures within the inner foam layer are below 100K. This is sufficient to cause the liquefaction and freezing of the blowing agent and any atmospheric gases within the cells. Thus, the gas pressure within the cells is expected to be subatmospheric. This produces a pressure driving force across the boundary of the inner foam layer. The inner vapor barrier is the primary seal which prevents the migration of any external gases into the inner foam; such migration can cause failure of the insulation in a number of ways. Because of its location, this barrier is physically protected by the outer foam and outer vapor barrier. Unless it fails in a significant manner, the entire insulation will be adequate indefinitely. Minor failures in the inner vapor-barrier, i.e., small sparce perforations, will be prevented from causing the failure of the insulation for some time by an intact outer foam layer and outer vapor barrier.

The outer gas barrier is intended to isolate the outer foam layer from the atmospheric gases. The cells of polyurethane foam are filled with Freon 11. This gas has a thermal conductance approximately one-third of the thermal conductance of air. Diffusion of air into the cells over a period of time causes an increase in the thermal conductance of the foam and subsequently an increase in the insulation heat flow. This is inhibited by a vapor barrier membrane at the outer surface of the foam insulation.

Under the conditions cited in the previous section, the concept described above should achieve acceptable performance and high reliability as an insulation system when the material properties meet the requirements noted below.

Specific Requirements

Foam. - The insulation material is to be a rigid, closed-cell, plastic foam with a density in the range of 32-48 kg/m^3. On the basis of previous experience the maximum acceptable level of porosity was arbitrarily set at 5 percent. The permeability of the foam

to the principal atmospheric gas must be sufficiently low, so that pinholes in the vapor barrier will not produce significant changes in the thermal conductivity over a 20-year period. The foam is required to have sufficient strength so that it does not crack or delaminate at the foam-tank boundaries or elsewhere in the system. The foam has to have adequate strength and not be degraded or take on permanent deformation after it is placed into the system and subjected to the static and dynamic temperature and pressure environments.

In addition, the foam must meet a number of fabrication requirements. Chief among these is that large quantities of the foam be continuously manufacturable in production equipment. When fiber reinforcement is necessary to achieve the appropriate properties, its use must be compatible with available production machinery. The use of toxic or carcinogenic materials necessary for the production of any foam is sufficient reason for discarding this material.

Adhesives. - Extensive use of adhesives is made in the application of this insulation concept. The adhesive must remain non-brittle over a temperature range from 20 to 347 K. It must be non-corrosive to 2219-T87 aluminum and compatible with the foam selected for the insulation systems. Because of the large surface areas to be covered, it must be sufficiently fluid for easy application of thin, even coatings to the foam and vapor barriers. It must be free of toxic and carcinogenic materials, and its bond strength must be greater than the foam and vapor barrier strengths.

Vapor barrier. - The properties of the vapor barrier which are required in this application are near-zero permeance, high tensile strength, and high tear strength. In the event of accidental puncture, the barrier must have a rip stop that will limit the extent of the damage. The barrier must be flexible and have a low weight. In addition, the barrier must be compatible with the selected adhesives and with temperature-induced strains occurring within the foam system. Finally, the barrier must not be subject to corrosion or pitting when in contact with the atmosphere.

FOAM EVALUATION AND SELECTION PROGRAM

Introduction

The purpose of this phase of the program was to identify at least one and possibly two plastic foam materials that would meet the requirements demanded by the insulation concept. This was done by performing a variety of tests with a number of plastic foams. We utilized standard test methods wherever possible and we developed some tests specifically for this program. In some cases, we had to rely upon the literature for data and information on generic foam properties. We evaluated both commercial materials and materials which were developed or modified within this program to achieve our goal of finding at least one and possibly two acceptable plastic insulating foams.

Foam materials are difficult to characterize because of their many complex interactions, including the chemical reactions, processing methods, and final foam structures. Foams are anisotropic. The directional properties are based upon the size and shape of the mold and upon the rise direction. Temperature plays an important role at all stages of manufacture, including metering, mixing, and foaming. The rise time built into the foam is another important factor which causes variability in foam characteristics.

To obtain candidate materials for this program, we utilized in-house information based on our previous work in developing cryogenic and insulation systems technology. We conducted a literature search and surveyed (by telephone and letter) more than 50 manufacturers of potentially useful materials. The foams evaluated in this program fall into two general classifications: (1) those available as board stock, and (2) those available as liquid systems which can be mixed and formed to the desired configuration with or without additives, such as reinforcing fiber.

Foam materials evaluated. - The foams evaluated in the program are listed in Table 2. The Dow Thurane is a board stock which has been used as insulation in some land-based LNG storage tanks. Several groups of General Latex board stock foams were studied as well, because they represented a range of densities and combinations of polyurethane (PU) and polyisocyanurate (PI) foam. They provided a useful means for determining whether the density variations represented and the PU/PI foam have any advantage over the more conventional polyurethanes. The Owens Corning Fiberglas (OCF) T-300 and T-500 are two board stock foams recommended by OCF as useful for cryogenic applications. Cellulair, a PU/PVC foam, formerly known as Klegecell, is available only from France and is very expensive. It was evaluated because it has been used

Table 2. - Insulating foam materials evaluated in program

	Foam Designation	Supplier	Type	Comments
1.	Thurane	Dow Chemical	Board Stock	32.0 kg/m^3 (2 lb/ft^3), PU
2.	XR493	General Latex	Board Stock	27.7 kg/m^3 (1.7 lb/ft^3), PU
3.	XR493	General Latex	Board Stock	32.8 kg/m^3 (2.05 lb/ft^3), PU
4.	XR493	General Latex	Board Stock	38.9 kg/m^3 (2.43 lb/ft^3), PU
5.	XR493	General Latex	Board Stock	43.2 kg/m^3 (2.7 lb/ft^3), PU
6.	XR1061	General Latex	Board Stock	28.8 kg/m^3 (1.8 lb/ft^3), 50/50 PU/PI
7.	XR1061	General Latex	Board Stock	32.0 kg/m^3 (2.0 lb/ft^3) "
8.	XR1061	General Latex	Board Stock	40.0 kg/m^3 (2.5 lb/ft^3) "
9.	XR1005	General Latex	Board Stock	90/10 PU/PI
10.	XR1006	General Latex	Board Stock	25/75 PU/PI
11.	XR1060	General Latex	Board Stock	50/50 PU/PI
12.	T-300	Owens Corning Fiberglas	Board Stock	33.6 kg/m^3 (2.1 lb/ft^3) PU
13.	T-500	Owens Corning Fiberglas	Board Stock	48.0 kg/m^3 (3.0 lb/ft^3), PU
14.	Cellulair H.917	L'Air Liquide	Board Stock	44.8 kg/m^3 (2.8 lb/ft^3), PU/PVC
15.	Rohacell 31	Rohm GmBh	Board Stock	30.4 kg/m^3 (1.9 lb/ft^3), Acrylic
16.	Rohacell 51	Rohm GmBh	Board Stock	51.2 kg/m^3 (3.2 lb/ft^3), Acrylic
17.	Rochcell 71	Rohm GmBh	Board Stock	70.5 kg/m^3 (4.4 lb/ft^3) "
18.	Rohacell 41S	Rohm GmBh	Board Stock	41.6 kg/m^3 (2.6 lb/ft^3) "
19.	Rohacell 61S	Rohm GmBh	Board Stock	50.9 kg/m^3 (3.8 lb/ft^3) "
20.	Rohacell 91S	Rohm GmBh	Board Stock	41.3 kg/m^3 (5.7 lb/ft^3) "
21.	ADL-1	ADL	Liquid System	T-221 polyol (1)
22.	ADL-2	ADL	Liquid System	NASA Ames fire-retardant foam
23.	ADL-3A	ADL	Liquid System	Catalyst change - ADL-1
24.	ADL-3B	ADL	Liquid System	None
25.	ADL-4	ADL	Liquid System	None
26.	ADL-UC	ADL	Liquid System	BE-375 polyol
27.	Stepanfoam BX249N	Stepan Chemical	Liquid System	Polymeric Isocyanate
28.	Stepanfoam BX289	Stepan Chemical	Liquid System	Polymeric Isocyanate
29.	Stafoam AA1602	Expanded Rubber & Plastics	Liquid System	TDI Based
30.	Upjohn 452	CPR Div., Upjohn	Liquid System	Polymeric Isocyanate
31.	Upjohn 492	CPR Div., Upjohn	Liquid System	Polymeric Isocyanate

Nomenclature

PI: Polyisocyanurate
PU: Polurethane
TDI: Toluene Diisocyanate based
PVC: Polyvinyl Chloride

(1) ADL liquid systems based on polymeric isocyanate

in cryogenic applications, particularly for LNG insulations in France. Rohacell is an acrylic foam which is available only from Germany and which has also been used in cryogenic work.

The ADL liquid system formulations (represented by ADL-1, 3A, 3B, and 4) are derived from the basic formulation that was highly successful in the program for NASA/Lewis [3] in 1964. A polyurethane liquid system consists basically of two components--the isocyanate and the polyol. Unfortunately, the primary polyol used in the NASA/Lewis formulation was discontinued by Union Carbide in the late 1960's. At that time, it recommended a substitute polyol, T221, which we have used successfully in foams for several cryogenic applications. Soon after we started work on this program, we found that the T221 polyol also had been discontinued by Union Carbide, and it recommended another substitute polyol, BE-375, for use in its place. The formulation utilizing the BE-375 was designated as ADL-UC. The ADL-2 formulation is a foam developed by NASA/Ames for good fire resistance. It is a polyisocyanurate foam with flame-retardant additives. The two Stepanfoam formulations are, according to Stepan Chemical (the supplier), variations of the Nopco BX250 foam which has previously been used in liquid hydrogen applications. Stepan acquired this business from Diamond Shamrock, which had previously acquired Nopco.

The Staform AA1602 is based on toluenediisocyanate (TDI), whereas all of the other liquid systems are based on polymeric isocyanate, commonly known as MDI. The TDI-based foams are more difficult to handle because the liquid always contains a small amount of free toluenediisocyanate, which is a very toxic chemical. These foams frequently are less brittle, but also less resistant to elevated temperatures and more flammable than the MDI-based foams. The manufacturer, Expanded Rubber and Plastics Company, recommended Stafoam AA1602 as having cryogenic properties, and we felt that it would be useful to evaluate at least one TDI-based foam in the program to determine whether this type of foam had any significant advantages over the more common MDI-based types.

Both of the Upjohn liquid systems have been used for cryogenic applications, primarily in the LNG area.

Fiber reinforcements evaluated. - Our previous experience with plastic foams used in cryogenic systems for insulation purposes indicated that commercially available foams failed primarily because of cracking. We found that this could be remedied by adding about 10 percent by weight of 6.0-mm-long chopped glass fibers to one of the chemicals of the two-part liquid systems prior to mixing and foaming. Anticipating similar difficulties with the commercial foam materials, this program included modified foam liquid systems which incorporated fiber reinforcement.

Glass fibers are widely used for reinforcement of organic plastics. Several sizes and finishes have been developed for glass fibers to make them compatible with various organic reins. The two finishes used are OCF Style 630 and Style 701. Style 630 finish is a starch-based treatment and Style 701 is a cationie-based treatment. No only do the glass fibers generally impart desirable physical properties, but they also produce composites with lower coefficients of thermal expansion. This is advantageous, particularly when plastics are combined with metals to form composites--the metals having expansion coefficients between those of glass and plastics.

Fibers can be added to the foam after the two-part liquid system has been mixed. This is done using a roving chopper mounted on a foam spray gun. The chopper cuts the glass and throws it into the fan of the spray gun so that the fiber is deposited with the liquid urethane and becomes a part of the structure as the liquid foams. We have found, however, that in using this technique, good quality control is difficult to achieve because the fibers can entrap air in the foam and create voids which would be extremely detrimental in the insulation concept under evaluation in this program. We did not, therefore, pursue this processing method in our program.

Chopped glass strands. - Glass fiber is generally supplied in a bundle of parallel glass filaments called a roving. The individual filaments are about 8 microns (0.3 mil) in diameter and are designated as "G Filament." The roving, chopped to a given length, is called chopped glass strand. We used chopped lengths of 7 and 5 mm in our program and they are denoted as c.s.

Milled glass fiber. - For a number of applications where glass fiber is to be dispersed in a liquid resin system, milled fiber, rather than chopped strand, is used. The milled fiber is made by ball-milling chopped strand of a given length to break the strands down to the individual fibers. In the course of the ball-milling, some of the fiber is also broken into shorter lengths and even ground to a glass dust; therefore, milled fiber contains a range of fiber lengths. The milled fiber is classified according to its ability to pass through a standard size mesh sieve. In our evaluation, emphasis was placed on 1.6 and 0.8 mm grade. Grade refers to sieve opening dimensions and not to fiber length.

Nylon fiber. - The availability of synthetic organic fibers in a range of lengths, diameters, and surface finishes is limited, except on custom order for a large quantity. Therefore, we selected one commercially available fiber for evaluation--a nylon fiber of 30 denier and 4 mm long. This is a relatively coarse fiber and is somewhat longer than we would have desired, but we were not readily able to obtain a more suitable fiber. We felt that nylon would be a desirable type of fiber because the chemistry of the nylon provides the possibility of a chemical bond between the polyurethane and the fiber surface.

Foam tests and analysis. - In the sections which follow, we present the information derived from a variety of tests. From this information, we attempted to establish whether any foams have the collective properties that would suit them for a liquid hydrogen tank insulation. We found the foam properties extremely variable, dependent upon many factors and showing no clear trends. We did not attempt to include all of this information because, at this point, much of it cannot be correlated with specific conditions and/or factors. However, we have presented the relevant information. The remaining material, which may be useful in future work, is contained in Appendix 3.

The tests that were conducted and the analyses that were made are as follows:

- Porosity,
- Cold Shock,
- High-Temperature Deformation,
- Gas Diffusion,
- Tensile Strength and Thermal Contraction,
- Cold Panel Tests (0.3m x 0.3m),
- Cold Panel Tests (0.6m x 0.6m), and
- Thermal Conductivity Measurements

Porosity

Foam porosity is a measure of the open-cell content of the material. The porosity of a "solid" object or loose material (such as foam, powder, pellets, etc.) is determined from the ratio of its air displacement volume (DV) to its geometric volume (GV). It can be determined from the equation:

$$\text{Porosity} = 1 - \frac{DV}{GV}$$

The geometric volume is obtained from measurements of the dimensions of the "solid" object, or of the space containing the loose material. The air displacement volume is measured with a pycnometer.

Low foam porosity is desirable and zero foam porosity is ideal in the application considered here. A non-porous foam will inhibit the permeation of vapor into the foam (assuming a failure in the vapor barrier) and prevent the loss of the low-thermal-conductance blowing agent. Thus, the foam insulation is less subject to physical failure due to the accumulation and freezing of atmospheric gases. Therefore, its thermal conductance is more constant with time.

ASTM Standard D2341-72, "Standard Specification for Rigid Urethane Foam," establishes a maximum porosity of 20 percent for a foam having a density of 40 kg/m^3 (2.50 lb/ft^3). This level is unacceptable for

cryogenic service. Therefore, we investigated the literature to establish actual levels of porosity for polyurethane foams. Because the available data were inadequate, we made porosity measurements in our program.

We measured the porosity of many foam samples with a Beckman air pycnometer in accordance with ASTM D2856-70, Standard Method of Measurement. Each sample was approximately 16.4 cm^3. The pycnometer measured the amount of air displaced by the sample.

Because the foam samples contain a large number of open cells at the surface, a correction for this surface volume was necessary. For this, we utilized Procedure B of the ASTM Standard, which involved measuring the specimen, making an initial reading with the pycnometer, cutting the specimen into a series of smaller pieces, and remeasuring the displaced volume. When introduced into the appropriate equation, the double measurement of the displaced volume automatically eliminates the volume of the surface cells from the calculation of the porosity value.

In cases where the porosity is very low, this procedure sometimes leads to negative values for porosity or open-cell content, because of the small errors in the measurements and the cutting of the samples. In cases where negative values were found, these are reported as zero open-cell content or porosity in our data tabulations.

Sample preparation. - The pycnometer samples were of two types. Some were board stock and others we prepared from liquid chemicals and are called pour-type foams. When the latter was being prepared, the fibrous reinforcement, when used, was first mixed into the polyol component. The isocyanate portion of the system was then added and the mixture was quickly blended manually or with a mechanical stirrer. The mixing was done in an 800-ml cup, and the foam was allowed to rise and cure in the cup. Sample cubes, 25 mm on each side, were then cut from the cured foam, measured, and prepared for the porosity measurements. The samples prepared from the board stock were cut, measured and prepared in the same manner.

Results. - The results obtained with 17 materials are presented in Table 3. Half of the materials tested were obtained from board stock and the other half were pour-type foams. Most foams were polyurethane and a few were acrylic and polyurethane/polyvinyl chloride. The highest porosity value measured was 4 percent and the lowest, 1 percent. For all 17 sets of data, the average porosity measured was 2 percent and the probable maximum porosity expected was 4.5 percent. These results are consistent with the 31 porosity measurements we made after cold shock to 77k (see next section). Thus, the foam porosity levels determined in this test series are compatible with the insulation concept requirements. Further, we found no correlation in the data between porosity and foam density.

The first five materials listed in Table 3 were selected for this test on the basis of availability and density only. These materials were not considered further in the program.

Table 3. - Foam porosity at 300 K

	Foam Sample	Measured Density kg/m^3	Porosity (%)	Type (1)
1.	Dow Thurane	29.2	2	Board
2.	Gen. Latex XR 1061	30.5	1	Board
3.	Gen. Latex XR 1061	43.6	1	Board
4.	Gen. Latex XR 493	27.4	2	Board
5.	Gen. Latex XR 492	44.9	2	Board
6.	ADL-1	39.1	3	Liquid
7.	ADL-2	32.9	3	Liquid
8.	ADL-3	30.5	1	Liquid
9.	ADL-3B	35.1	2	Liquid
10.	ADL-4	34.8	2	Liquid
11.	Stepanfoam BX289	30.0	4	Liquid
12.	Stepanfoam BX249N	30.3	3	Liquid
13.	Stafoam AA1602	30.3	2	Liquid
14.	OCF T-300	34.8	2	Board
15.	OCF T-500	42.0	2	Board
16.	Rohacell #71	34.6	1	Board
17.	Upjohn 452, Glass Reinforced (2)	35.2	3	Liquid

(1) Board refers to board stock and liquid refers to liquid or pour foam system.
(2) The glass reinforcement is 10 percent by weight of 1.6mm-grade milled glass fiber, Style 701.

Cold Shock

We next looked at 31 foam materials to determine if cold shocking produced any structural deterioration of the foam cell structure. If the foam crumbled or broke up internally when cycled to liquid nitrogen temperatures, it would be a poor candidate for a 20-year life system which was expected to be temperature-cycled at least once per year. Such deterioration can be detected with the air pycnometer measurement method. Thus, we conducted a series of tests on foam samples before and after cold shocking in liquid nitrogen.

Sample treatment. - For this test series, we used six samples of each foam type. Each sample was initially cut into 25-mm cubes. Half were tested directly without being subjected to cold shock. These samples were treated in the same manner as those tested for porosity (Table 3) and they were measured in the same instrument as well.

The samples from the second group of each foam type were treated as follows: First, the linear dimensions of each sample cube were measured. Next, the cubes were immersed in liquid nitrogen for a minimum of one minute. The cubes were then removed from the liquid nitrogen bath and allowed to warm up. The samples were then immersed a second time following the procedure used in the first immersion. This was repeated again until each cube had been cycled three times in the liquid nitrogen bath. The choice of three cycles was arbitrary. After the final warm-up, the linear dimensions of each cube were remeasured.

Note that the three specimens of each foam subjected to the shock cooling yield the "after" porosity and percent volume change data. Different specimens must be used for the "before" and "after" tests, because the specimens are cut as part of Procedure B of the ASTM Standard to obtain the cut surface cell volume correction.

Test results. - The test data are summarized in Table 4. The porosities before cold shock are in column 4, and those after cold shock are in column 5. The volume changes noted after cold shock are tabulated in column 6.

Generally, a lower porosity was measured after the foam materials were cold-shocked. The average porosity of the 31 foam materials was 1.76 percent before cold shock and 0.66 percent after cold shock. The data on only three materials (Nos. 4, 14, and 25) contradict this trend. We concluded that cold shocking has produced a measurable amount of internal damage in only 10 percent of the foams tested. The remaining materials apparently were not damaged at all by the cold treatment.

Generally, cold-shocking produced a permanent reduction in the foam volume. The average decrease was 0.7 percent and one material (Item 15) showed a volume decrease of 1.6 percent. It is possible that this volume reduction had some effect on the porosity as well. We believe that the permanent decrease in foam volume after immersion in liquid nitrogen may be a form of stress relief or cell contraction. Consideration must be given to preconditioning at 77K all thermal-structural foams before their application to cryogenic tank walls.

Table 4. - Foam volume and porosity changes after cold shock to 77 K

	(1) Foam Sample	(2) % by Weight of Reinforcement	(3) kg/m^3 Density	(4) (5) Porosity (% Open Cell) Before	After	(6) % Volume Change
1	Stepanfoam BX249N	0%	30.5	3	0	-0.4
2	Stepanfoam BX249N	10% 3.2 mm MG	35.3	2	0	-0.8
3	Stepanfoam BX249N	10% 3.2 mm CS	38.5	4	0	-0.6
4	Stepanfoam BX249N	15% 3.2 mm MG	40.1	2	3	-1.1
5	Stepanfoam BX249N	15% 3.2 mm CS	40.1	4	2	-0.3
6	Stepanfoam BX289	0%	30.5	4	0	0
7	Stepanfoam BX289	10% 1.6 mm MG	33.7	1	0	-0.9
8	Stepanfoam BX289	10% 3.2 mm MG	33.7	2	0	-0.6
9	Stepanfoam BX289	15% 1.6 mm MG	38.5	1	0	-0.6
10	Stepanfoam BX289	15% 3.2 mm MG	36.7	1	0	-1.1
11	Stepanfoam BX289	20% 1.6 mm MG	38.5	1	0	-0.6
12	Stafoam AA1602	0%	30.5	2	1	-0.3
13	Stafoam AA1602	10% 1.6 mm MG	33.7	0	0	+0.3
14	Stafoam AA1602	10% 3.2 mm MG	35.3	0	4	-0.7
15	Stafoam AA1602	10% 3.2 mm CS	35.3	2	1	-1.6
16	Stafoam AA1602	10% 6.4 mm CS	35.3	2	0	-0.4
17	Stafoam AA1602	15% 3.2 mm MG	35.3	0	0	-0.6
18	Stafoam AA1602	15% 3.2 mm CS	38.5	4	1	-0.7
19	Stafoam AA1602	15% 6.4 mm CS	35.3	4	3	-0.9
20	Stafoam AA1602	20% 1.6 mm MG	35.3	0	0	+0.1
21	ADL-1	0%	40.1	2	0	-0.6
22	ADL-1	10% 3.2 mm MG	40.1	1	1	-0.3
23	ADL-1	10% 3.2 mm CS	44.9	4	0	-1.0
24	ADL-1	5% 6.4 mm CS + 5% 3.2 mm MG	40.1	0	0	-0.8
25	ADL-1	15% 3.2 mm MG	41.7	1	3	-1.3
26	ADL-1	15% 3.2 mm CS	43.3	1	0	-0.7
27	OCF T-300		35.3	2	0	-0.1
28	OCF T-500	-	41.7	2	1	-0.4
29	Rohacell 71	-	35.0	1	0	+0.1
30	Dow Thurane	-	28.8	2	0	-0.9
31	Upjohn 452	10% 1.6 mm MG	34.4	3	1	-0.8

High-Temperature Deformation

The requirements for the foam insulating system define an upper working temperature of 347 K (165°F) at the outside surface of the insulation system. Several different foam insulation materials were placed in an oven to determine the effect of elevated temperature on their dimensional statility.

Test procedure. - This series of tests was conducted with samples 25 x 25 x 150 mm. Initially, the specimens were placed in an oven at 333K for 12 hours to assure full cure and stabilization. The oven temperature was then increased in a series of daily steps to 400K. The intermediate steps were 339, 334, 353, 367, 378, and 389 K. The specimens were inspected at room temperature, after soaking at each temperature for 24 hours, before the temperature was raised to the next level. The inspection was performed by placing each specimen on a flat surface and measuring its deformations. The specimen was considered deformed when it was distorted more than 6.4 mm in any dimension, and that temperature at which the deformation occurred was reported as the deformation temperature. All specimens were returned to the oven after each measurement cycle and subjected to the next higher temperature level. After the final soak at 400 K, the actual length of each specimen was measured at room temperature and the percent change from original temperature length was calculated. These data are shown in Table 5.

Results. - Half of the foams tested had deformation temperatures below 347 K. Of the remaining acceptable samples, the two Rohacell foams showed the highest deformation temperature. The next acceptable materials in decreasing order were the Dow Thurane, Upjohn 452, and Stepanfoam BX249N.

The dimensional stability obtained after soaking at a temperature of 400 K indicates that about half of the foams show changes of less than 5 percent. The remaining samples have changes in the 8-16 percent range and are considered unacceptable. The former and acceptable materials consist of Stepanfoam BX249N, Rohacell #31 and #51, Stafoam AA1602, Stepanfoam BX289, and Upjohn 452.

The materials which show the highest deformation temperature and greatest dimensional stability at 400 K in decreasing order of acceptability are Rohacell #31 and #51, Stepanfoam BX249N, and Upjohn 452.

Gas Diffusion

The diffusion of gases through closed cell foams, such as polyurethane, is not well understood and few experimental measurements are available to verify proposed theories. The generation of this type of

Table 5. - Heated-foam deformation tests*

	Foam Sample	Deformation Temperature (°K)	Percent Change in RT Length after Soak at 400°K
1.	Stafoam, AA1602, No Fiber Added	339	-4.2
2.	Stafoam AA1602, 10% 1.6 mm MG, Style 630	339	-4.2
3.	Stepanfoam BX249N, No Fiber Added	353	+8.3
4.	Stepanfoam BX249N, 10%, 1.6 mm MG, Style 630	353	0
5.	ADL-UC, No Fiber Added	344	+16.7
6.	ADL-UC, 10%, 1.6 mm MG, Style 630	344	+10.4
7.	ADL-UC, 15%, 3.2 mm CS	339	+12.5
8.	Stepanfoam BX289, No Fiber Added	344	+4.2
9.	Stepanfoam BX289, 10%, 1.6 mm MG, Style 630	344	+14.6
10.	Dow Thurane, Boardfoam	389	+12.5
11.	Rohacell 31, Boardfoam	400	-2.0
12.	Rohacell 51, Boardfoam	400	-2.0
13.	Upjohn 452, 10% 1.6 mm MG, Style 701	367	+1.0

*The heat deformation tests were performed with samples 25 x 25 x 150 mm.

Abbreviations:

MG: Milled Glass
CS: Chopped Strands
Percent: By weight of filler material
mm: Chopped strand or milled fiber length classification.
RT: Room Temperature

experimental data is both complex and costly. No attempt was made within our program to obtain gas diffusion measurements. Rather, we summarized the present state of knowledge on the diffusion of gases in polyurethane foams and based our conclusions on the existing data.

Foam Properties. - When originally blown, the foam cells contain a gas such as Freon 11 (F-11). The cells are not identical in size or shape, the cell walls are not of uniform thickness, and the original F-11 pressure undoubtedly differs from cell to cell. Thus, the properties of such foams are likely to vary somewhat from batch to batch. Some properties are also a function of time because, in contact with ambient air, oxygen and nitrogen tend to diffuse into the foam structure, while F-11 counter-diffuses out. Evidence indicates that F-11 diffuses at a slower rate, and so the pressure in the cells may increase above the ambient level, and properties, such as thermal conductivity, actually increase as the cells fill with air (see Figure 3).

With such a complex, heterogeneous structure, most theoretical correlations have assumed that one can average out the properties and assign a bulk property, such as diffusivity, to permeating gases. Because we believe that the movement of a gas within the foam is rate-limited by solution into and diffusion across individual cell walls, the important correlating parameter is the product of D and S in the solid polyurethane wall. (D is the diffusion coefficient, and S is the solubility.) This product is called the permeability, K_p. It is a function of the gas-foam system and of temperature.

The flow of gas from one cell to another, N, is given by

$$N = K_p A \, \Delta P / \Delta x$$

where A is the area, ΔP is the pressure across the cell wall, and Δx is the cell wall thickness. This equation may be numerically integrated to estimate the permeation rate of gases at various depths (5, 6, 7, 8, 9, 10, 11).

Experimental measurements of K_p in polyurethane foam are scarce. Harding's values [5] are given in Table 6 and are compared to Norton's data [6]. There are significant differences. In both cases, however, it is evident that air has a much higher permeability than CCl_3F (F-11). Water has a still higher permeability and will diffuse rapidly into foam; the few data on hydrogen [6] indicate that $K_p(H_2)/K_p(O_2) \sim 0.23$.

Except for water, the effect of temperature on K_p of oxygen and nitrogen is large. The few data available suggest that

$$d \ln K_p / d(1/T) = -\Delta H/R$$

with $\Delta H/R$ in the order of 4000 K. Thus, at low (cryogenic) temperatures, K_p is very small. As an example, $K_p(293\ K)/K_p(20\ K) \simeq 8.5 \times 10^{80}$! Clearly,

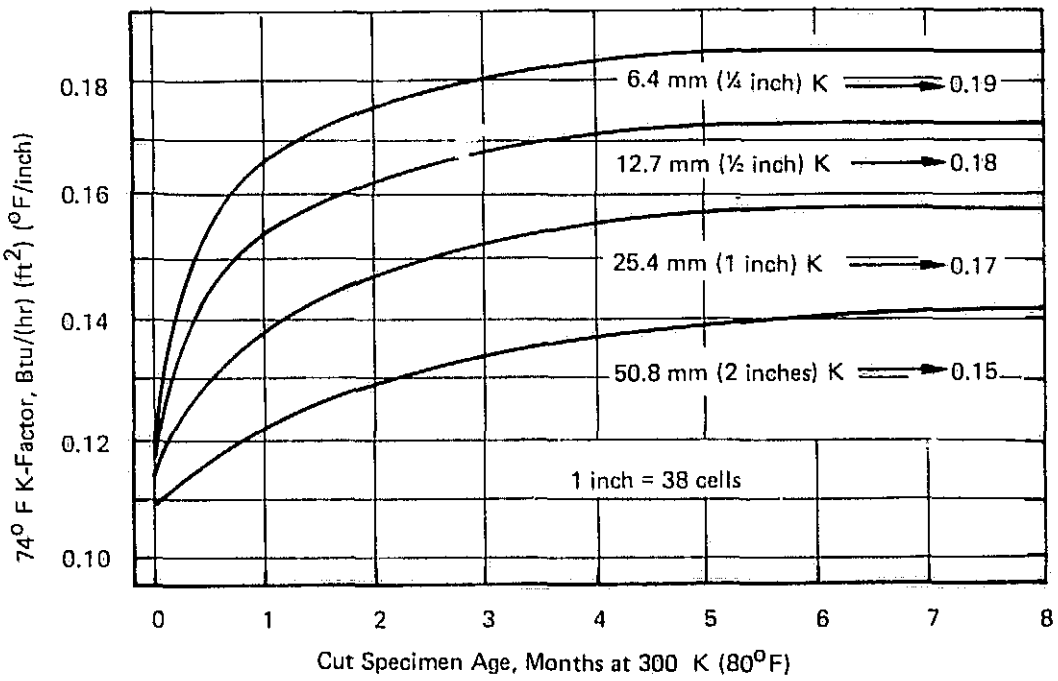

Harding (Reference 11)

Figure 3. — Effect of foam thickness on K-factors of a unicellular isotropic CCl_3 F-blown urethane

Table 6. - Gas permeation coefficients for polyurethane foam having a density of 32 kg/m^3 (2 lb/ft^3)

Gas	Temperature (K)	Temperature (°F)	K_p CGS Units*	Reference Source
CCl_3F	255	0	5.6×10^{-15}	Harding (5)
CCl_3F	278	40	2.5×10^{-14}	Harding (5)
CCl_3F	300	80	1.2×10^{-13}	Harding (5)
Air	255	0	1.2×10^{-13}	Harding (5)
Air	278	40	5.6×10^{-13}	Harding (5)
Air	300	80	4.0×10^{-11}	Harding (5)
CCl_3F	298	76	4.4×10^{-11}	Norton (6)
CCl_3F	323	121	1.4×10^{-10}	Norton (6)
CCl_3F	333	140	2.2×10^{-10}	Norton (6)
CCl_3F	348	166	4.3×10^{-10}	Norton (6)
CCl_3F	363	193	7.2×10^{-10}	Norton (6)
N_2	298	76	3.4×10^{-10}	Norton (6)
N_2	323	121	8.0×10^{-10}	Norton (6)
N_2	333	140	1.2×10^{-10}	Norton (6)
N_2	348	166	1.8×10^{-9}	Norton (6)
N_2	363	193	2.7×10^{-9}	Norton (6)
O_2	298	76	1.5×10^{-9}	Norton (6)
O_2	323	121	4.4×10^{-9}	Norton (6)
O_2	333	140	6.9×10^{-9}	Norton (6)
O_2	348	166	1.1×10^{-8}	Norton (6)
O_2	363	193	1.8×10^{-8}	Norton (6)

*CGS: cm^3 (STP)-cm/cm^2 sec cm Hg.

permeation at low temperatures must be considered negligible. Unpublished data at Arthur D. Little, Inc., verify this estimation. Long term (circa 4 months) immersion of polyurethane foam in liquid methane (or liquid natural gas) indicated essentially no hydrocarbon permeation.

Conclusions. - Considering a polyurethane foam applied to a liquid hydrogen tank exposed to the ambient environment without a gas barrier, we found that permeation of the atmospheric gases into the warm regions of a non-porous foam was limited to depths of 25 mm after several months. This figure was obtained during proprietary work performed at an earlier time by Arthur D. Little, Inc. If on the other hand, a non-permeable gas barrier is bonded to the outer foam surface and causes it to be completely sealed, it can be reliably predicted that the thermal conductance properties of the foam will remain constant for many years, provided the foam and the barrier are not mechanically degraded.

Further, in the event that the inner vapor barrier is degraded, the insulation will not fail catastrophically if the outer foam layer and outer vapor barrier are intact. Similarily, if the outer foam layer and outer vapor barrier are degraded the insulation will not fail catastrophically if the inner foam layer and vapor barrier are intact.

Finally, we concluded from the above that all closed-cell polyurethane foams have an acceptably low gas diffusion rate. This characteristic is consistent with the requirements of the hydrogen fuel tank insulation and increases the system reliability.

With regard to the other plastic foams investigated in this program, we have no information on their gas diffusion properties. The tentative assumption is that their diffusion properties are similar to that of the polyurethane. When any of these foams become serious candidates for liquid hydrogen tank insulations, a definitive study of this property can be conducted.

Thermal Strain and Contraction Evaluation

We performed an analytical study to ascertain the critical properties of the metal-foam systems that contribute to the generally observed cracking and delamination behavior of foam when a metal-foam composite is cooled to cryogenic temperatures. The results (presented in Appendix 2 of this report) indicate that the foam fails at the interface because the bonded metal induces a strain which exceeds the proportional limit strain of the foam at the existing temperature. This induced strain is directly related to the difference between the contraction of the metal and of the foam when both are cooled from room to cryogenic temperatures. If this difference is less than the proportional limit strain of the foam, then the foam is expected to survive. On the other hand, if this difference is larger than the proportional limit strain, then the foam

is expected to fail. Therefore, a series of tests was undertaken to measure the proportional limit strains of three each of a number of foam materials and to note the contribution, if any, made by the fiber reinforcement to this property. We also measured the thermal contraction (one sample each) of a number of foams between room temperature and 77 K. Both measured properties were used to obtain an estimate of the survivability of the metal-foam system when subjected to cryogenic temperatures.

The foam materials used for the proportional limit tests were also used to obtain compressive and flexural strength data. This information was developed to further characterize the foam materials, but it was not used in the selection of the foam materials best suited for liquid hydrogen tank applications.* Thus, the data are presented in Appendix 3 for informational purposes only.

Test Method. - For the test method used to determine the proportional limit strain refer to Appendix 3.

Results. - The results on the measurements of the foam proportional limit strains are presented in Table 7 for 10 different foam materials with and without reinforcement at 300 and 77 K. We find no correlation between the proportional limit strains and the presence or absence of reinforcing fiber or with fiber length.

The average value of $\varepsilon_{P.L.}$ at 300 K is 0.024 m/m, and the standard deviation is $\pm$ 0.008 m/m. All results are within 1 standard deviation, except for Rohacell 51 which has an exceptional proportional limit strain of 0.042 m/m.

The average value of the strain at the proportional limit ($\varepsilon_{P.L.}$) at 77 K is approximately 0.016 m/m and represents a general decrease for the materials tested of almost 40 percent. The data have a standard deviation of about $\pm$ 0.005 m/m which includes all but few values; again, Rohacell 51 at 77 K has a significantly larger proportional limit strain, 0.027 m/m, than any other material.

The data are contradictory on whether fiber reinforcement improves the proportional limit strain. From the data at 300 K, it is not possible to distinguish between reinforced and non-reinforced foams. At 77 K, the Upjohn 452 is significantly improved when reinforcing fibers are added; e.g., compare results from Sample No. 1 with Nos. 2, 17, and 19. However, Upjohn No. 492 and Stepan BX249N show little improvement, and Stafoam AA1602 is improved or degraded by reinforcing fibers; e.g., Sample No. 13 versus Nos. 14 and 18.

From the measurements of the proportional limit at 300 and 77 K, a straight line extrapolation was used to estimate the proportional limit at 20 K. This result, listed in the last column of Table 7, shows that there is a slight but definite decrease in the proportional limit with decreasing temperature. This decrease with temperature for

* No correlating factors between properties and requirements could be established. The data were extremely variable.

Table 7 - Tensile modulus and strain measured at 300 and 77 K; and proportional limit strain at 20 K obtained by straight line extrapolation.

Sample No.	Foam Description	Filler Reinforcement Material	Tension Parallel to the Rise** (300 K) E	(300 K) $\varepsilon_{P.L.}$	(300 K) $\varepsilon_{0.2\%}$	(77 K) E	(77 K) $\varepsilon_{P.L.}$	(77 K) $\varepsilon_{0.2\%}$	(20 K) $\varepsilon_{P.L.}$
1	Upjohn 452	None	5.50	0.029	0.039	27.78	0.005	Fail	0.000
2	Upjohn 452	10% 1.6 mm MG, Style 630	7.41	0.025	0.030	11.64	0.014	Fail	0.011
17	Upjohn 452	10% 1.6 mm MG, Style 701	13.18	0.019	0.027	20.31	0.014	Fail	0.013
19*	Upjohn 452	10% 1.6 mm MG, Style 701	10.94	0.022	0.029	16.23	0.012	Fail	0.009
5	ADL-UC	None	8.19	0.020	0.029	15.47	0.019	Fail	0.019
6	ADL-UC	10% Nylon	4.64	0.024	0.034	12.42	0.021	Fail	0.020
7	ADL-UC	10% 1.6 mm MG, Style 630	7.88	0.022	0.030	15.02	0.013	Fail	0.011
8	ADL-UC	10% 0.8 mm MG, Style 630	9.89	0.017	0.026	17.73	0.010	Fail	0.008
9	ADL-UC	10% 1.6 mm MG, Style 701	10.15	0.017	0.025	12.98	0.015	Fail	0.014
10	ADL-UC	10% 0.8 mm MG, Style 701	8.01	0.020	0.030	14.49	0.015	Fail	0.014
11	Stepanfoam BX249N	None	8.90	0.029	0.040	14.49	0.014	Fail	0.010
12	Stepanfoam BX249N	10% 1.6 mm MG, Style 630	12.53	0.026	0.033	16.94	0.013	Fail	0.010
13	Stafoam AA1602	None	7.75	0.024	0.030	21.30	0.014	Fail	0.011
14	Stafoam AA1602	10% 1.6 mm MG, Style 701	8.87	0.022	0.029	19.32	0.021	Fail	0.021
18	Stafoam AA1602	10% 1.6 mm MG, Style 701	17.31	0.018	0.022	23.75	0.010	Fail	0.008
3	Upjohn 492	None	10.27	0.028	0.038	19.41	0.012	Fail	0.008
4	Upjohn 492	10% 1.6 mm MG, Style 630	12.04	0.025	0.033	16.55	0.013	Fail	0.010
15	Rohacell 31	None	25.56	0.030	Fail	15.38	0.017	Fail	0.014
16	Rohacell 51	None	30.04	0.042	Fail	18.95	0.027	Fail	0.023

Notes and Nomenclature:

E: Youngs Modulus, MPa

$\varepsilon_{P.L.}$: Strain at Proportional Limit, m/m

$\varepsilon_{0.2\%}$: Strain at 0.2 percent offset, m/m

*Machine-mixed foam.

**Average of three samples

most foams is contrary to the general results obtained from the literature (see Appendix 2),which suggested no consistent trend in this important material property. However, for foams 5,6,9 and 14, the decrease is so slight as to be in accord with the result reported in Appendix 2.

Sample 6 was made with nylon fibers available at the time from our supplies of experimental and commercial fibers. The fiber used was coarse nylon fiber about 1 cm long. The proportional limit strain obtained with the nylon-reinforced foam was the same as the average for all foams tested and above the average for all foams tested at 77 K, i.e., 0.021 versus 0.016 mm/mm. However, no further testing was performed with nylon fibers because there is a very limited choice in the number of grades and surface finishes available commercially.

Table 7 indicates the use made of OCF Style 630 and 701 fiber finishes in the foams tested. According to our experience in combining fibers, with these finishes, and polyurethane foams, the Style 701 is preferable because it disperses more readily in the polyol component than the Style 630.

The present tests indicate two significant properties of Rohacell. First, as noted from the data presented in Table 7, Rohacell, and particularly Rohacell No. 51, has a high proportional limit strain; and second,Rohacell, unlike the other foams, has a brittle failure mode at room temperatures. This is exhibited by the fact that tensile failure occurs immediately after the proportional limit is reached, i.e., prior to the 0.2 percent offset.

Thermal Contraction. - A foam material with thermal contraction values comparable to that of 2219 aluminum over the operating temperature range would be desirable. A foam material having the same thermal contraction as aluminum would experience no significant tangential or axial temperature strains or stresses at the boundary. However, because plastic foams contract up to six times as much as aluminum, severe strains induced in the foam at the boundary can cause cracking in the foam perpendicular to the tank wall and/or delamination of the foam at the foam-to-wall boundary.

Because the addition of glass and other fibers was expected to affect the thermal contraction of plastic foams, we measured foam samples at 294 and 77 K to determine the dimensional changes that occur between these two temperatures. The majority of the data presented in Table 8 was obtained from measurements of samples about 15 cm (6 inches) long and 2.5 cm (1 inch) square. Their length was measured at room temperature and after immersion and equilibration in liquid nitrogen at 77 K.

Table 8. - Insulating foam materials thermal contraction from room temperature to 77 K (1)

Sample No.	Description Foam/Filler	$-\frac{\Delta L}{L} \times 10^5$ 294-77 K	$-\frac{\Delta L}{L} \times 10^5$ 294-20 K[2]
1.	Upjohn 452/no fiber added	1066	1115
2.	Upjohn 452/10%, 1.6 mm M.G., Style 630[4]	1054	1105
3.	Upjohn 492/no fiber added	1319	1515
4.	Upjohn 492/10%, 1.6 mm M.G., Style 630	1049	1100
5.	ADL/no fiber added	2441	3000
6.	ADL/10% nylon	1601	1814
7.	ADL/10%, 1.6 mm MG, Style 630	1813	2090
8.	ADL/10%, 0.8 mm MG, Style 630	1715	1975
9.	ADL/10%, 1.6 mm MG, Style 701	1707	1960
10.	ADL/10%, 0.8 mm MG, Style 701	1692	1950
11.	Stepanfoam BX249N/no fiber added	1427	1635
12.	Stepanfoam BX249N/10%, 1.6 mm MG, Style 630	935	1080
13.	Stafoam AA 1602/no fiber added	1647	1890
14.	Stafoam AA 1602/10%, 1.6 mm MG, Style 701	1176	1345
15.	Rohacell No. 31 (Boardfoam)	696	960
16.	Rohacell No. 51 (Boardfoam)	631	770
17.	Upjohn 452/10%, 1.6 mm MG, Style 701	1171 (1229)[4]	1195
18.	Stafoam AA 1602/10%, 1.6 MG, Style 701	1088 (1142)	1145
19.	Upjohn 452/10%, 1.6 mm MG, Style 701 Machine Made	1171	1195
	Other Materials		
	Crest Adhesive 7343	2258	-
	Aluminum 2219-T87[3]	366	412

Notes:

1. For rapid measurement of the thermal contraction of samples 1 through 16, a simple fixture was constructed which permitted the length of a foam sample to be measured both at room temperature and after immersion in liquid nitrogen for 12 minutes. The nominal dimensions were 2.5 x 2.5 x 15 cm (1 x 1 x 6 inches). The Crest adhesive sample was a 2.5-cm-diameter x 15-cm-long (1 in. x 6 in.) cylinder. The contractions for Samples 17 and 18 were obtained from tests performed by Dynatech R&D Company. No data were taken with sample 19. It is assumed that the contraction values for 19 are the same as for 17.
2. Contraction to 20°K was estimated by extrapolation.
3. Aluminum contraction was obtained from the literature.
4. Bracketed values were obtained by outside laboratory (see Table 9).
5. Abbreviations:

   Percent: Percent by weight of filler material
   Length: Milled fiber grade classification
   MG: Milled glass fiber

Table 9. - Linear thermal expansion

Temperature		Thermal Expansion $(\Delta L/Lo) \times 10^4$		Coefficient of Thermal Expansion $10^6/K$	
(K)	(°F)	A	B	A	B
77	-321	0.0	0.0	-	-
98	-283	2.0	4.6	9.5	21.9
123	-238	6.2	10.6	13.5	23.0
148	-193	12.4	17.4	17.5	24.5
173	-148	20.8	26.2	21.7	27.3
198	-103	33.2	36.0	27.4	29.8
223	-58	49.2	48.5	33.7	33.2
248	-13	69.2	64.7	40.5	37.8
273	32	93.7	87.2	47.8	44.5
298	77	122.9	114.2	55.6	51.7
323	122	156.9	148.2	63.8	60.2
348	167	195.3	189.5	72.1	69.9

Notes:

Material A: CPR Upjohn 452, 10%, 1.6-mm MG, Style 701,
Density = 35 kg/m^3, Batch-Produced, No. 17 of Table 8

Material B: Stafoam AA1602, 10%, 1.6-mm MG, Style 701,
Density = 35.5 kg/m^3, Batch-Produced, No. 18 of Table 8

Results. - In general, the addition of 10 percent fiber reduced the thermal contraction about 30 percent over the fiber-free material. Samples 2 and 17 are the exceptions. In Sample 2, the addition of fiber produced an insignificant change over Sample 1. We do not have a theory to fit these circumstances. These exceptions could be the result of the variability demonstrated by different batches as mentioned in the introduction to this chapter.

In addition, the results obtained with Rohacell 31 and 51 are approximately half of the average of all measured foam values and about twice the thermal contraction value for 2219 aluminum.

Table 9 presents the thermal contraction and thermal contraction coefficients measured by an outside laboratory over the range of temperatures 77 and 348 K. When thermal contraction data, thus obtained, are compared with the Arthur D. Little, Inc., data, there is reasonable agreement (see samples 17 and 18 in Table 8). The data shown in Table 9 are also presented in Figure 4 for comparison with the data obtained from our literature search and for comparison with 2219 aluminum and polyester film (Mylar).

Because all of our testing was performed with liquid nitrogen at 77 K, we were interested in determining the additional strain that would be experienced by the reinforced Upjohn 452 and the reinforced Stafoam AA1602 when cooling to 20 K temperature level. We estimate from the extrapolated data on Figure 4 that in lowering the temperature from 77 to 20 K, the Upjohn materials experience a strain increase of 2.1 percent, and the Stafoam material experiences a strain increase of 5.2 percent.

On the basis of the foregoing data for proportional limit strain and thermal contractions, we prepared an estimate of which foams are expected to survive the bonding to 2219 aluminum and cooling to cryogenic temperatures. The basis for this estimate is the following relationship:

$$SF = \frac{\varepsilon_{PL,\,T}}{\left[\left(\Sigma \frac{\Delta \ell}{\ell}\right)_{foam} - \left(\Sigma \frac{\Delta \ell}{\ell}\right)_{Al}\right]_{300\ K}^{T}}$$

where:

SF = Safety Factor

$\varepsilon_{PL,T}$ = strain in the foam at the proportional limit at temperature T

$\left(\Sigma \frac{\Delta \ell}{\ell}\right)_{foam}$ = thermal contraction of foam between 300 K and T

$\left(\Sigma \frac{\Delta \ell}{\ell}\right)_{Al}$ = thermal contraction of 2219 aluminum between 300 K and T

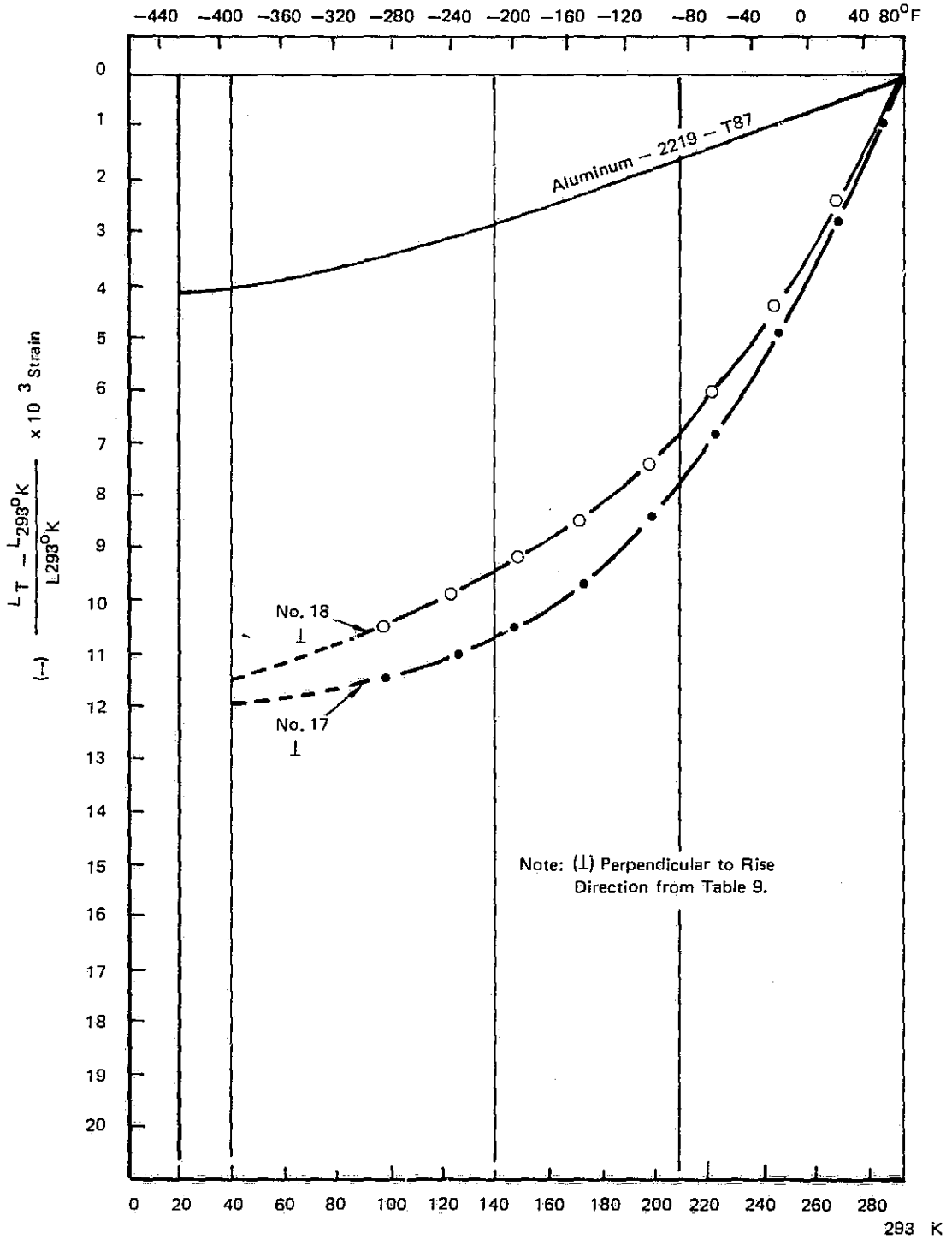

Figure 4. — Thermal contraction of Upjohn 452 and Stafoam AA1602 both reinforced with 10 percent, 1.6-mm style 701 milled glass fibers

The strain in the foam at the proportional limit was obtained from the measurements reported in Table 7. The value of $(\Sigma \frac{\Delta \ell}{\ell})$ foam was obtained from the tests reported in Table 8. The value of $(\Sigma \frac{\Delta \ell}{\ell})_{Al}$ was obtained from data reported in the literature (see Table 8).

The mechanical suitability of a foam as an insulation for an aluminum tank for liquid hydrogen can be determined, in part, by comparing its elastic properties with a requirement based on a worst case of thermal strain compatibility at the aluminum-foam interface. This worst case is one where the foam must withstand the total thermal differential strain between the aluminum and the foam. Since all foams contract more than aluminum (at any reduced temperature), it is obvious then that any foam will be strained in tension at the boundary with the aluminum. Therefore, to prevent the developed tensile strain or stress from causing eventual structural failure, it would be desirable to select foams whose elastic capability in tension, that is, the proportional limit in tension, exceeds the worst case requirement.

The ratio of the proportional limit strain in tension to the differential thermal strain requirement results in a number which can be called a safety factor and, further, can be used to rank-order the structural capability of the foams. In Table 10, this rank-ordering and safety factor in tension is presented in Columns 4 and 5. In Column 4, the calculation is based on actual test data as determined from measurements of the foams at liquid nitrogen temperatures. In Column 5, the calculation is based on the data obtained at liquid nitrogen extrapolated to liquid hydrogen temperatures.

Except for secondary effects such as bi- or triaxial strain effects, and unknown low-cycle fatigue characteristics, the numbers and rank orders in Columns 4 and 5 are true representations of the capability of the various foams considered in this project.

A safety factor of 2 at 77 K was arbitrarily selected as the value separating the materials most expected to survive from those least expected to survive. The safety factor at 20 K was not used as the basis for selection because the extrapolated data are less reliable. Except for Sample No. 17, the rank-ordering is similar. The ranking in Table 10 indicates that five foam materials could be selected on the basis of these criteria. The two highest ranked are Rohacell 51 and Rohacell 31. These are followed by Stafoam AA1602, Stepanfoam BX249N and Upjohn 452, all with 1.6-mm milled glass fiber reinforcement.

Table 10. – Ranking of 19 foam materials in order of safety factor

Sample No.	Foam Description	Filler Reinforcement Material	Safety Factor at 77K	Estimated Safety Factor at 20K	Sample No.
16	Rohacell 51	None	10.2	6.42	16
15	Rohacell 31	None	5.15	3.12	15
14	Stafoam AA1602	10% 1.6 mm MG, Style 701	2.59	2.25	14
12	Stepanfoam BX249N	10% 1.6 mm MG, Style 630	2.28	1.66	17
2	Upjohn 452	10% 1.6 mm MG, Style 630	2.03	1.59	2
4	Upjohn 492	10% 1.6 mm MG, Style 630	1.90	1.50	12
17	Upjohn 452	10% 1.6 mm MG, Style 701	1.74	1.45	4
6	ADL-UC	10% Nylon	1.70	1.43	6
19*	Upjohn 452	10% 1.6 mm MG, Style 701	1.49	1.15	19*
18	Stafoam AA1602	10% 1.6 mm MG, Style 701	1.39	1.09	18
11	Stepanfoam BX249N	None	1.32	0.91	10
3	Upjohn 492	None	1.26	0.90	9
10	ADL-UC	10% 0.8 mm MG, Style 701	1.13	0.82	11
9	ADL-UC	10% 1.6 mm MG, Style 701	1.12	0.74	13
13	Stafoam AA1602	None	1.09	0.73	3
5	ADL-UC	None	0.92	0.73	5
7	ADL-UC	10% 1.6 mm MG, Style 630	0.90	0.66	7
8	ADL-UC	10% 0.8 mm MG, Style 630	0.74	0.51	8
1	Upjohn 452	None	0.71	0.00	1

*Machine-mixed foam.

Cold Panel Tests - 0.3 Meter Square

In the previous section, we attempted to rate the structural performance of insulating foam materials in the cold environment on the basis of their proportional limit strain and on their thermal contraction properties. However, we did not rely on this method completely, but augmented it with a series of tests in which foam samples approximately 25-mm thick and 0.3-m square (Figure 5) were tested directly on a plate which was cooled to 77 K and temperature-cycled several times. The tests were conducted by bonding or foaming the urethane foam in place on the aluminum test plates, through which liquid nitrogen could be circulated. Two foam materials were utilized for each test, one on each side of the plate.

Test phases. - The samples were subjected to four test phases:

(1) The sample was first cooled as quickly as possible by circulating liquid nitrogen through the aluminum plate.

(2) After temperature equilibrium was achieved with the liquid nitrogen in the plate, the outer surface of the sample was shock-cooled by immersion in a bath of liquid nitrogen.

(3) The sample was then warmed to room temperature and the first test was repeated with the sample in an atmosphere of Halon 1301. In this test, if any cracks which were not visually detectable occurred in the foam or if any significant voids or porosity were found in the foam, the Halon 1301 would condense within the foam and then boil off when the plate was warmed so that such defects could be detected.

(4) After the sample was again warmed to room temperature, it was shock-cooled by immersion in a bath of liquid nitrogen.

The fourth test of this series may be considered too severe. In the operational environment, the exterior surface of the foam experiences a large decrease in temperature in a short period when the aircraft completes the ascent portion of the flight mission. The rate and degree of cooling accomplished in the fourth test phase are, admittedly, more severe than the mission environment. However, we believe that the ability of a foam material to withstand the shock cooling from the outside is an indication of an additional margin of safety possessed by the foam. Thus, this part of the test was retained, and we consider it to represent significant data.

Results. - The test results are summarized in Table II. A number of the ADL-I formulations passed the 0.3-meter-square-panel cold test,

Figure 5. – Three 0.3-meter-square cold plates and mounted samples

These tests were the first that we performed. However, as noted previously, the ADL-1 formulations are no longer available commercially and, therefore, cannot be reproduced.

More than half of the samples survived the test regime without cracking or delaminating from the cold plate. It is noteworthy that several foam systems with no reinforcements, including Stafoam AA1602, Stepanfoam BX249N, Upjohn 452, and several of the ADL-UC formulations, survived this test series. On the basis of past experience, we would not have anticipated this result and must conclude that in recent years there have been significant changes in polyurethane foams which make them more suitable for cryogenic applications.

Generally, all fiber-reinforced foams survived the cold panel tests, except the Upjohn 492 which developed a crack in the second step of the test series.

The safety factors developed in the previous section are shown for the corresponding foams tabulated in Table 11. The ratings indicate that, although in many cases both the fiber-filled and fiber-free foams survived the cold panel tests, the fiber-filled materials have a better chance for survival.

Rohacell 31 and 51, the two highest-rated foams on the basis of proportional limit strain and thermal contraction developed failures during the fourth phase of the test series. There is reason to believe that the brittleness of this material, which we identified in the previous section, may make it susceptible to mechanical failure in the presence of transient temperature distributions within the material. This characteristic could lead to catastrophic failure in a tank insulation system.

Candidate Foam Selection

The two foams best suited as candidate materials for the hydrogen tank insulations have been selected. These are Stafoam AA1602 (No. 14) and Upjohn 452 (No. 2), both reinforced with 10 percent, 1.6-mm-long, milled glass fibers, Style 701. The selection was based upon the summary presented in Table 12 as well as on the handling experience we developed in working with each foam system. Nineteen sample materials representing six basic foam formulations were evaluated in detail. Numerous others were eliminated for various reasons.

We have selected these two fiber-reinforced foams as our primary candidates. We fully recognize that the glass fiber reinforcement causes some problems in foam processing.

In addition to the tabulated results, the Stafoam AA1602 and Upjohn 452 are low-viscosity systems that remain processable with as much as 20 percent glass fiber added to the polyol side of the system. The Stafoam system is superior to the Upjohn system in this respect, and

Table 11. - Summary of thermal shock tests[1]

Cold Plate Test No.	Foam Identification	Density (kg/m^3)	Type Filler and Percent by Weight	Foam to Plate[3] Bond Method	Test Results[2] and Observation	From Table 10 Foam Safety Factor	From Table 10 Foam Sample No.
1A	ADL-1	48.1	None	Foamed to Plate	No Failures		
1B	ADL-1	64.1	5%, 6.4 mm CS[4] 5%, 3.2 mm MG, Style 630[5]	Foamed to Plate	Slight Separation at Edges		
2A	ADL-1	32.1	None	Crest 7410	Crack through Center		
2B	ADL-1	32.1	10%, 6.4 mm	Crest 7410	Slight Separation at Edges		
3A	ADL-1	32.1	10%, 6.4 mm	Foamed to Plate	No Failures		
3B	ADL-1	32.1	None	Foamed to Plate	No Failures		
4A	OCF-T300	33.7	N/A	Crest 7410	Crack through Center		
4B	OCF-T500	48.1	N/A	Crest 7410	No Failures		
5A	Stepan BX289	35.3	None	Crest 7410	Crack 3" from Edge		
5B	Stepan BX289	35.3	10%, 3.2 mm MG, Style 630	Crest 7410	No Failures		
6A	Stepan BX289	35.3	10%, 6.4 mm	Crest 7410	Short Edge Cracks		
6B	Cellulaire H-917	44.1	N/A	Crest 7410	Short Edge Cracks		
7A	Rohacell 51	50.0	N/A	Crest 7410	Crack Failure [4]	10.3	16
7B	Rohacell 31	30.5	N/A	Crest 7410	Crack Failure [4]	5.09	15
8A	Stafoam AA1602	30.5	None	Crest 7410	No Failures	1.09	13
8B	Stafoam AA1602	30.5	10%, 1.6 mm MG	Crest 7410	No Failures	2.57	14
9A	Stepanfoam BX249N	40.1	None	Crest 7410	No Failures	1.28	11
9B	Stepanfoam BX249N	40.1	10%, 1.6 mm MG	Crest 7410	No Failures	2.19	12
10A	Rohacell 91S	85.0	N/A	Crest 7410	Serious Crack Failures [4]		
10B	ADL-UC	44.9	10%, 6.4 mm CS	Crest 7410	No Failures		
11A	ADL-UC	33.7	None	Crest 7410	No Failures	0.93	5
11B	ADL-UC	40.1	10%, 1.6 mm MG	Crest 7410	No Failures	0.89	7
12A	ADL-UC	44.9	10%, 6.4 mm Nylon	Crest 7410	No Failures	1.72	6
12B	ADL-UC	33.7	No Fibers, Flex Load Void	Crest 7410	Crack Failure [2]		
13A	ADL-UC	44.9	10%, 1.6 mm MG, Style 701	Crest 7410	No Failures	1.12	9
13B	Upjohn[6]	35.7	N/A	Crest 7410	Large Cracks over Surface [2]		
14A	Upjohn 452	40.7	No Fiber Added	Crest 7410	No Failures	0.87	1
14B	Upjohn 452	41.2	10%, 1.6 mm,	Crest 7410	No Failures	2.08	2
15A	Upjohn 492	44.6	No Fiber Added	Crest 7410	No Failures	1.28	3
15B	Upjohn 492	48.4	10%, 0.8 mm,	Crest 7410	Crack Failure [2]	1.87	4

Notes:

1. These tests were performed with the 0.3 m square aluminum test plate. One sample is placed on each side of the test plate. These samples progress through a series of four test phases, i.e.; 1) the warm samples are cold shocked by cooling the plate with LN_2; 2) after temperature equilibrium is achieved, the plate and samples are immersed in a bath of LN_2; 3) after warm-up of the sample to room temperature, test No. 1 is repeated with the foam samples in a Halon 1301 atmosphere; and 4) if the sample survives the previous tests, it is warmed to room temperature and then immersed in an LN_2 bath.
2. The bracketed number after the failure descriotion indicates the test phase during which the failure occurred.
3. Test pieces of foam were bonded to 0.3 m sq. test plate with Crest adhesive No. 7410 which was then cured at 353 K for 24 hours.
4. 6.4 mm CS identifies 6.4-mm-long chopped strands of Fiberglas.
5. 3.2 mm MG identifies 3.2 mm milled Fiberglas strands.
6. This sample consisted of one 3 m layer of Upjohn board stock with aluminum/Kraft paper covers on each surface. The covers are laminates of aluminum foil/Kraft paper/aluminum foil.

Table 12. - Foam evaluation and selection.

Sample No.	Foam Description	Filler Reinforcement Material	Porosity	Cold Shock	High Temp. Deformation	Gas Diffusion	Strain-Contraction	Machine Processability (1)	Cold Plate
1	Upjohn 452	None	NT	NT	NT	Acceptable	Not Acceptable	Yes	Acceptable
2	Upjohn 452	10% 1.6 mm MG, Style 630	NT	Acceptable	Acceptable	Acceptable	Acceptable	Yes	Acceptable
3	Upjohn 492	None	NT	NT	NT	Acceptable	Not Acceptable	Yes	Acceptable
4	Upjohn 492	10% 1.6 mm MG, Style 630	NT	NT	NT	Acceptable	Not Acceptable	Not Known	Failure
5	ADL-UC	None	NT	NT	Not Acceptable	Acceptable	Not Acceptable	Yes	Acceptable
6	ADL-UC	10% Nylon	NT	NT	NT	Acceptable	Not Acceptable	Not Known	Acceptable
7	ADL-UC	10% 1.6 mm MG, Style 630	NT	NT	Not Acceptable	Acceptable	Not Acceptable	Not Known	Acceptable
8	ADL-UC	10% 0.8 mm MG, Style 630	NT	NT	NT	Acceptable		Not Known	
9	ADL-UC	10% 1.6 mm MG, Style 701	NT	NT	NT	Acceptable	Not Acceptable	Not Known	Acceptable
10	ADL-UC	10% 0.8 mm MG, Style 701	NT	NT	NT	Acceptable		Not Known	
11	Stepanfoam BX249M	None	Acceptable	Acceptable	Not Acceptable	Acceptable	Not Acceptable	Yes	Acceptable
12	Stepanfoam BX249M	10% 1.6 mm MG, Style 630	Acceptable		Acceptable	Acceptable	Acceptable	Not Known	Acceptable
13	Stafoam AA1602	None	Acceptable	Acceptable	Marginal	Not Known	Not Acceptable	Yes	Acceptable
14	Stafoam AA1602	10% 1.6 mm MG, Style 701	Acceptable	Acceptable	Marginal	Not Known	Acceptable	Not Known (2)	Acceptable
15*	Rohacell 31	None	NT	NT	Acceptable	Not Known	Acceptable	Yes	Failure
16*	Rohacell 51	None	NT	NT	Acceptable	Not Known	Acceptable	Yes	Failure
17	Upjohn 452	10% 1.6 mm MG, Style 701	NT	Acceptable	NT	Acceptable	NT	Yes	
18	Stafoam AA1602	10% 1.6 mm MG, Style 701	NT	NT	NT	Not Known	NT	Possible	
19*	Upjohn 452	10% 1.6 mm MG, Style 701	Acceptable	NT	Acceptable	Acceptable	NT	Yes	

NT = Not Tested.
*Machine-made foam.

Notes:

1. It is assumed that all fiber-free liquid systems are machine processable.

2. Not known but expected to be superior to Sample No. 2 of this table.

both are greatly superior to the Stepanfoam materials. The Upjohn 452 can be readily molded into any thickness while the Stafoam AA1602 because of its high exotherm, is limited in thickness of molding to 8 to 10 cm.

An additional basis for selecting the fiber-reinforced Upjohn 452 was the successful machine production demonstration carried out by CPR Upjohn Division (see Appendix 4). For a foam system to be acceptable, it must have good reproducibility in volume production. The demonstration run is a first step only, but it establishes that it is processable by machine. Because the processing properties of the Stafoam AA1602 are considered superior to those of the Upjohn 452, we believe that the Stafoam AA1602 system will also be machine processable.

Toxicity is another concern in processing. All urethane liquid systems have some degree of toxicity due to the isocyanates they contain, and careful handling is necessary. However, the Stafoam AA1602 is based on toluene diisocyanate (TDI), which is highly volatile and therefore much more toxic to handle than systems based on MDI, such as the Upjohn 452. This is true, even though the TDI is reacted to make a prepolymer, because there is always a small percentage of unreacted TDI in the system.

The elevated temperature at which the foam will deform is of concern in this particular application because the tanks may be exposed to elevated temperatures when empty. These temperatures may reach 347 K (165°F) or higher. Our test data indicate that the Stafoam AA1602, even with glass fiber reinforcement, will distort at 339 K (150°F), which makes it marginal in this property. The Upjohn 452 with fiber reinforcement passed this distortion test up to 367 K (200°F). It is, therefore, much superior to the Stafoam AA1602 in this property.

Rohacell was also considered very seriously as a candidate material. It was not included in our final selection for a number of reasons. The principal technical reason is that the material is brittle and may be subject to cracking at room temperature as well as at liquid nitrogen temperature. There were also a number of non-technical reasons. For example, our further evaluation would be redundant, since the NTF facilities at both NASA/Langley and Bell Aerospace Company are evaluating this material in separate programs. The material is presently obtainable only from a foreign source at high cost. Further, the material is available only as board stock which must be machined or formed to obtain shaped pieces.

Cold Panel Tests - 0.6 Meter Square

Tests performed at Arthur D. Little. - A final series of foam tests was conducted on the two foam systems selected. These tests were performed on a scale larger than any of the previous tests, i.e., the thickness was doubled to 50 mm and the area increased to 0.38 m^2. Further, the foam was bonded to an aluminum plate and cycled many times between room temperature and liquid nitrogen temperature to obtain some measure of its structural performance and endurance.

The foam materials used in this series of tests were the CPR Upjohn 45z and the Stafoam AA1602. Both of these foams contain 10 percent by weight of 1.6-mm, milled glass, OCF, Style 701 fibers. The properties of these two materials are detailed in Tables 13 and 14, respectively.

Test apparatus. - The 0.38 m^2 cold plate was constructed from two 3.2-mm aluminum plates sealed at the ends with 6.4 x 6.4 mm aluminum bars. A series of baffles, formed from 6.4 x 6.4 mm aluminum bars, was welded on the interior to direct the cryogenic coolant from the inlet to the outlet, assuring uniform temperature distribution over the plate surface after the initial cooldown.

One foam sample was bonded to each face of the cold plate. The samples were made larger than the cold plate to provide an overlap of about 37 mm at each edge. Each foam sample was installed to the cold plate in the following manner. First, the surfaces of each sample to be attached to the cold plate were coated with a layer of Crest 7410 adhesive. Next, each surface of the cold plate was coated with adhesive. Then, one sample was placed on a flat surface with its adhesive-coated surface facing upward. The cold plate was then placed and centered over this foam sample. Next, the second foam sample was placed, adhesive face down, over the cold plate. This outer layer of foam was then weighted down until the adhesive was cured. The spaces between the samples at the four edges of the cold plate were sealed with cast-in-place urethane foam.

Table 13. - Upjohn 452 foam system - Summary of material properties of 0.6-meter-square cold plate sample.

1.	Manufacturer:	CPR Division of Upjohn Company Alaska Avenue Torrance, CA 90503 (212) 320-3550	
2.	Formulation:		
	2.1 Manufacturer Designation:	Upjohn 452	
	2.2 Chemical Basis:	Polymeric isocyanate	
3.	Foaming Method:	Batch	
4.	Density:	35.2 kg/m^3 (2.7 lb/ft^3)	
5.	Reinforcement:	Owens Corning Fiberglas (OFC), Style 701, 1.6-mm-long milled glass fibers	
	5.1 Fiber Designation:		
	5.2 Fiber Weight:	10 percent of total by weight	
6.	Porosity:	3 percent	
7.	Ultimate Flexural Strength	300 K	77 K
	Strength MPa/(psi):	0.234/(34)	0.380/(55.2)
	Modulus, MPa/(psi):	5.129/(744)	8.384/(1216)
8.	Ultimate Tensile Parallel to Rise Direction MPa/(psi):	0.379/(55)	0.303/(44)
9.	Compressive Strength		
	Parallel to Rise MPa/(psi):	0.207/(30)	0.10/(45)
	Perpendicular to Rise, MPa (psi):	0.152/(22)	0.221/(32)
10.	Thermal Conductivity at 294 K:	0.0265 $\frac{W}{mK}$ (0.184 $\frac{Btu\text{-}in.}{hr\ ft^2\ °F}$)	
11.	Thermal Expansion		
	294 to 77 K:	1171 x 10^{-5} m/m	
	294 to 20 K (est.):	1195 x 10^{-5} m/m	
12.	Heat Treatment Prior to Bonding to Cold Plate:	347 K for 10 hours minumum 77 K for 1/2 hour minumum after cooldown	
13.	Adhesive:	Crest 7410	

Table 14. - Stafoam AA1602 formulation - summary of material properties of 0.6-meter-square cold plate sample.

1.	Manufacturer:	Expanded Rubber & Plastics Corp. 1400 South Western Avenue Gardena, CA 90249	
2.	Formulation:		
	2.1 Manufacturers Designation:	Stafoam AA1602	
	2.2 Chemical Basis:	Toluenediisocyanate (TDI)	
3.	Foaming Method:	Batch	
4.	Density:	36.8 kg/m^3 (2.3 lb/ft^3)	
5.	Reinforcement:	Owens Corning Fiberglas (OCF) Style 701, 1.6 mm long milled glass fibers	
	5.1 Fiber Designation:		
	5.2 Fiber Weight:	10 percent of total by weight	
6.	Porosity:	0 percent	
7.	Ultimate Flexural Strength:	300 K	77 K
	Strength, MPa/(psi)	0.234/(34)	0.414/(60)
	Modulus, MPa/(psi)	5.708/(828)	8.886/(1289)
8.	Ultimate Tensile Parallel to Rise Direction MPa/(psi):	0.386/(56)	0.234/(34)
9.	Compressive Strength		
	Parallel to Rise, MPa/(psi):	0.214/(31)	0.365/(53)
	Perpendicular to Rise, MPa/(psi):	0.117/(17)	0.255/(37)
10.	Thermal Conductivity at 294K:	0.0215 $\frac{W}{mK}$ (0.149 $\frac{Btu\ in.}{hr\ ft^2\ ^\circ F}$)	
11.	Thermal Expansion		
	294 to 77 K:	1088 x 10^{-5} m/m	
	294 to 20 K (est.)	1145 x 10^{-5} m/m	
12.	Heat Treatment Prior to Bonding to Cold Plate	347 K for 10 hours minimum 77 K for 1/2 hour minumum after cooldown	
13.	Adhesive:	Crest 7410	

After the foam materials were installed on the cold plate, thermocouples were placed on the inlet and outlet of the cold plate and at various depths within each foam sample. At one location in each foam, thermocouples were located at the foam-to-cold plate interface, at depths of 6.4, 12.8 25, and 37 mm. and at the outer surface of the foam. The thermocouples were read out on a Kay (Model DR-TCTF) digital multipoint recorder providing temperature readings directly.

No vapor barrier was placed on the outer surfaces of the foam so that the exposed surfaces could be observed and monitored visually.

The cold plate was positioned vertically with liquid nitrogen supplied to the inlet at the bottom and vented from the outlet at the top (see Figure 6). Cooldown of the inlet area of the plate usually occurred 5 minutes after liquid nitrogen flow to the cold plate was initiated. The remainder of the cold plate cooled to liquid nitrogen temperature within the next 10 to 15 minutes. The insulation achieved temperature equilibrium throughout its thickness in approximately 1.5 hours. At this time, the liquid nitrogen flow to the cold plate was discontinued and the plate and insulation allowed to warm to room temperature, usually overnight, requiring a period of about 15 to 20 hours. During cooldown and after warmup, the outside surfaces of the samples were inspected for cracks and other forms of physical deterioration.

Observations during temperature cycle tests. - We performed 20 temperature cycle tests with the 0.6m^2 flat plate apparatus in this program. The visual observations made during and after each test of the outside sample surfaces showed no evidence of mechanical failure or physical deterioration of either foam material.

Figure 7 is a plot of the typical temperature distributions that were obtained in Cycle Test No. 5. In subsequent tests, we extended the cooldown period to as much as 1.5 hours. Because the thermocouples were placed in the foam after the foam installation, the actual depth of each thermocouple varied by as much as 1.6 mm from the stated location. Further, the thermocouples were held in position with Crest adhesive which, in combination with the depth error and the changing K factor, may have resulted in the very steep gradients observed in the cold portions of the foam.

The only observable occurrences associated with the cooldown of the 50-mm-thick samples were the "snap, crackle, and pop" noises which occurred during the first 10 minutes of cooldown cycle. In the first cooldown test, these noises were quite audible and frequent. However, as the number of cycle tests increased, both the audibility and frequency of these sounds decreased significantly.

After completion of the 20 cycle tests, the two foam samples were dismantled from the cold plate and inspected to determine if any internal failures had occurred. We searched for two failure modes in particular: (1) delamination of the foam from

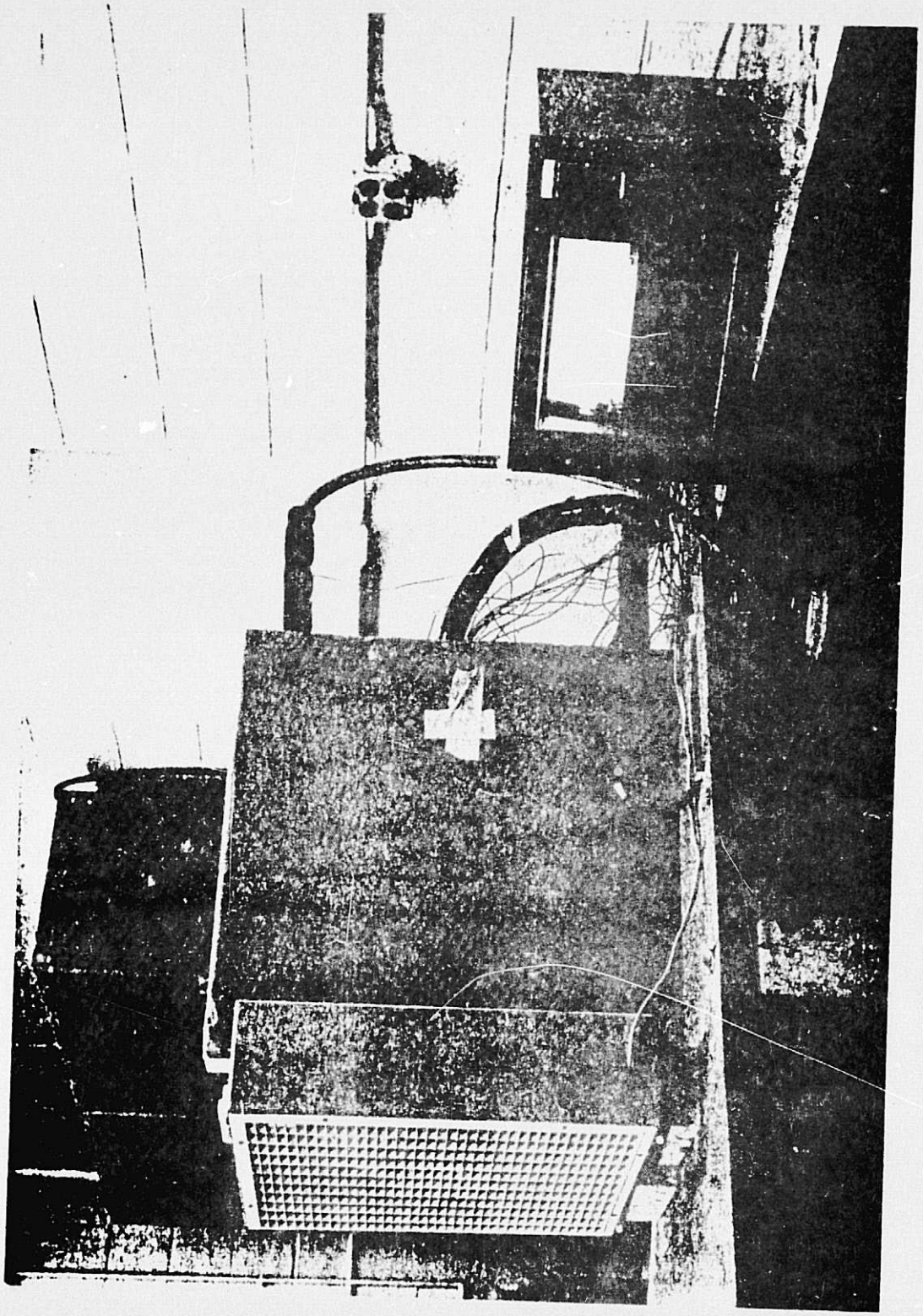

Figure 6. — 0.6-meter-square cold plate — experimental setup

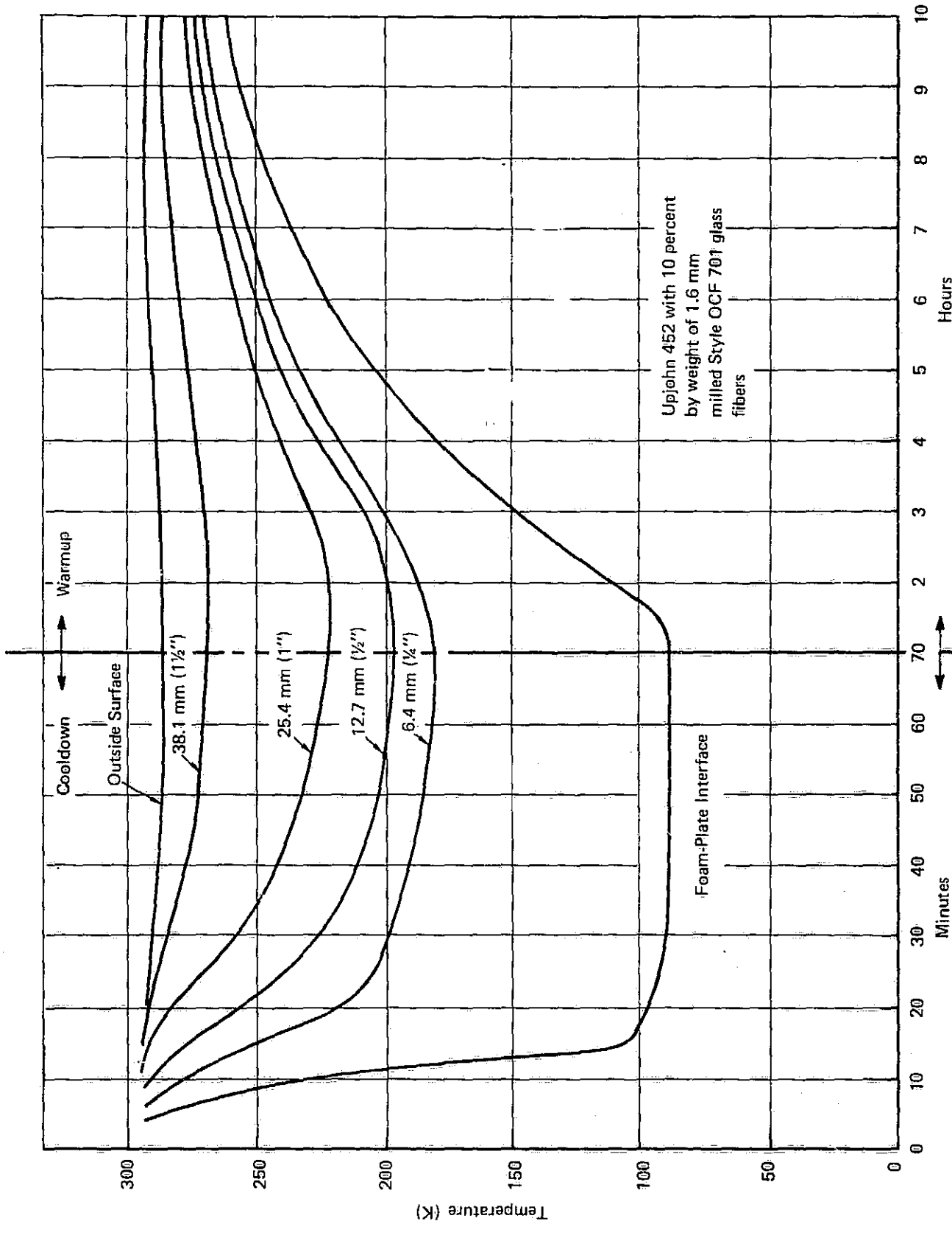

Figure 7. - Typical foam temperature distribution for 0.6-meter-square cold plate, cycle test

the cold plate; and (2) tensile cracks in the foam which would form in a direction perpendicular to the cold plate surface. The results of this analysis follow:.

Observations of foam samples after removal from the cold plate. - Inspection of two foams used in the 0.6-m cold plate was begun by sawing away the 50-mm edge guard foam. Succeeding saw cuts perpendicular to the plate, 50 mm apart, and then parallel to the plate at the foam-metal interface were made in the pattern shown in Figures 8 and 9. Thus 50-mm-square bars of foam were removed beginning at the periphery of the plate and ending with an approximate 100-mm-wide bar at the center. As each bar was successively removed, it was inspected by bending and twisting by hand to open up and reveal the presence of any cracks. The corresponding new surface of the cold plate with its adhered adhesive was also inspected for cracks or delaminations.

The results of this process are shown in Figure 8 for the Upjohn 452 and Figure 9 for the Stafoam AA1602 foams. The solid closed lines indicate areas where there never was a bond between the adhesive coated foam and adhesive-coated aluminum plate during the initial assembly, due to insufficient contact pressure during the adhesive cure. Proof of this initial unbonded condition is the existence of original brush application marks on the cured adhesive surfaces. It is only within these unbonded areas that cracks occurred. These cracks extended through both the adhesive and the foam, extending into the foam 12-25 mm. Such cracks are shown in the figures as terminated lines. Some cracks may have extended only into the saw kerf thickness since they do not appear (or cannot be found) in the 50-mm bars of foam.

That there were no cracks showing through the bonded adhesive thickness (and consequently, the foam) is interesting because it demonstrates that the high thermal contraction of the Crest adhesive is successfully inhibited by the aluminum. This restraint is further projected into the foam, thus preventing foam cracking. In the unbonded areas, there is no restraint to adhesive or foam contraction except at the bond periphery. Thus, the unbonded adhesive-foam behaves like a tensile test specimen and, as noted in the figures, the adhesive and foam crack in the center of the unbonded areas and cause the foam to fail in tension.

From the foregoing test series, we conclude that the two foam systems gave excellent structural performances in those areas where the foam-to-metal bond had been formed. The crack failures which occurred in the foam are believed to be the results of areas unbonded to the cold plate. Or stated in another manner, had the foam been bonded continuously to the cold plate, the cracks which we observed would not have

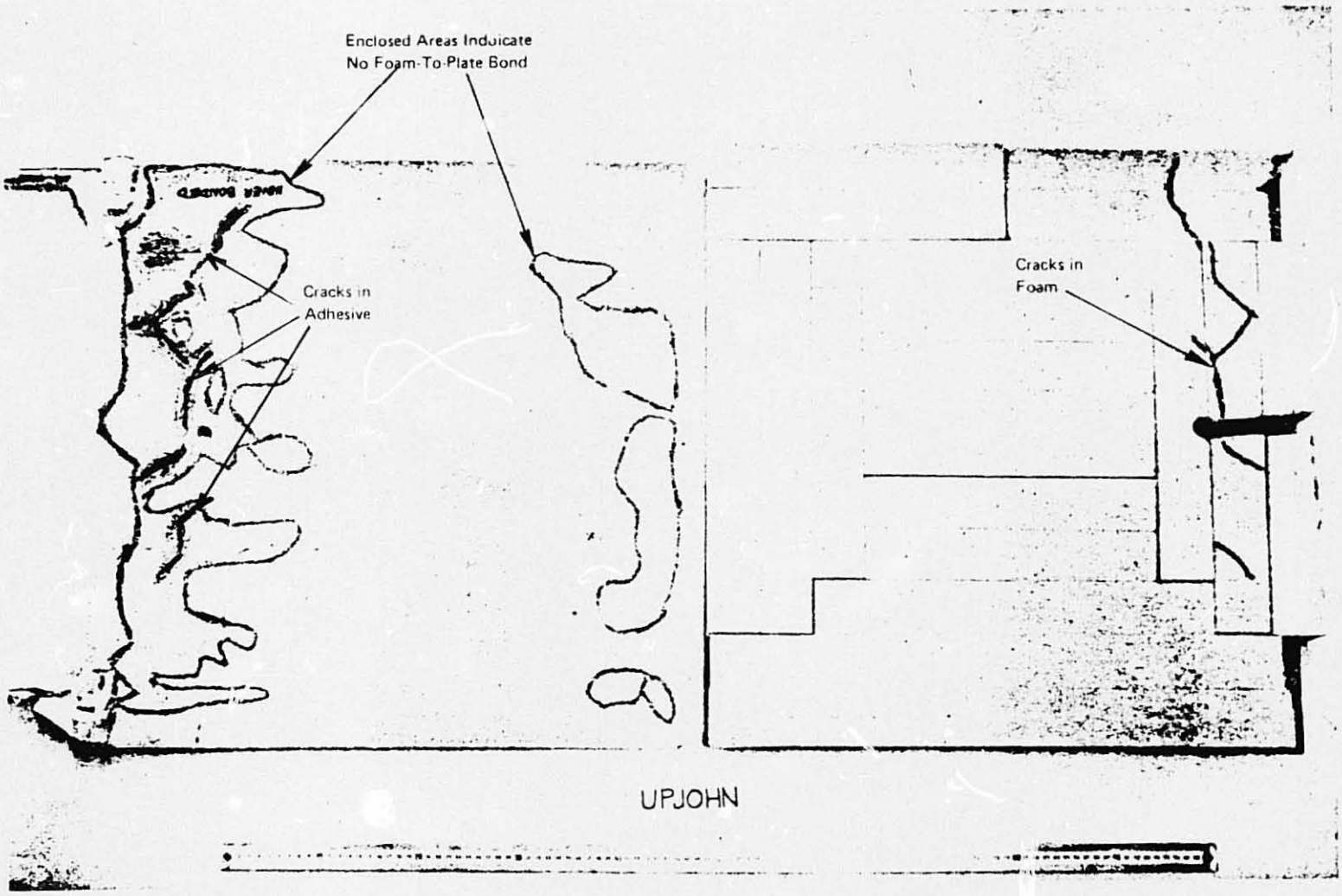

Figure 8. – Upjohn 452 foam system, exhibit of unbonded and cracked foam areas

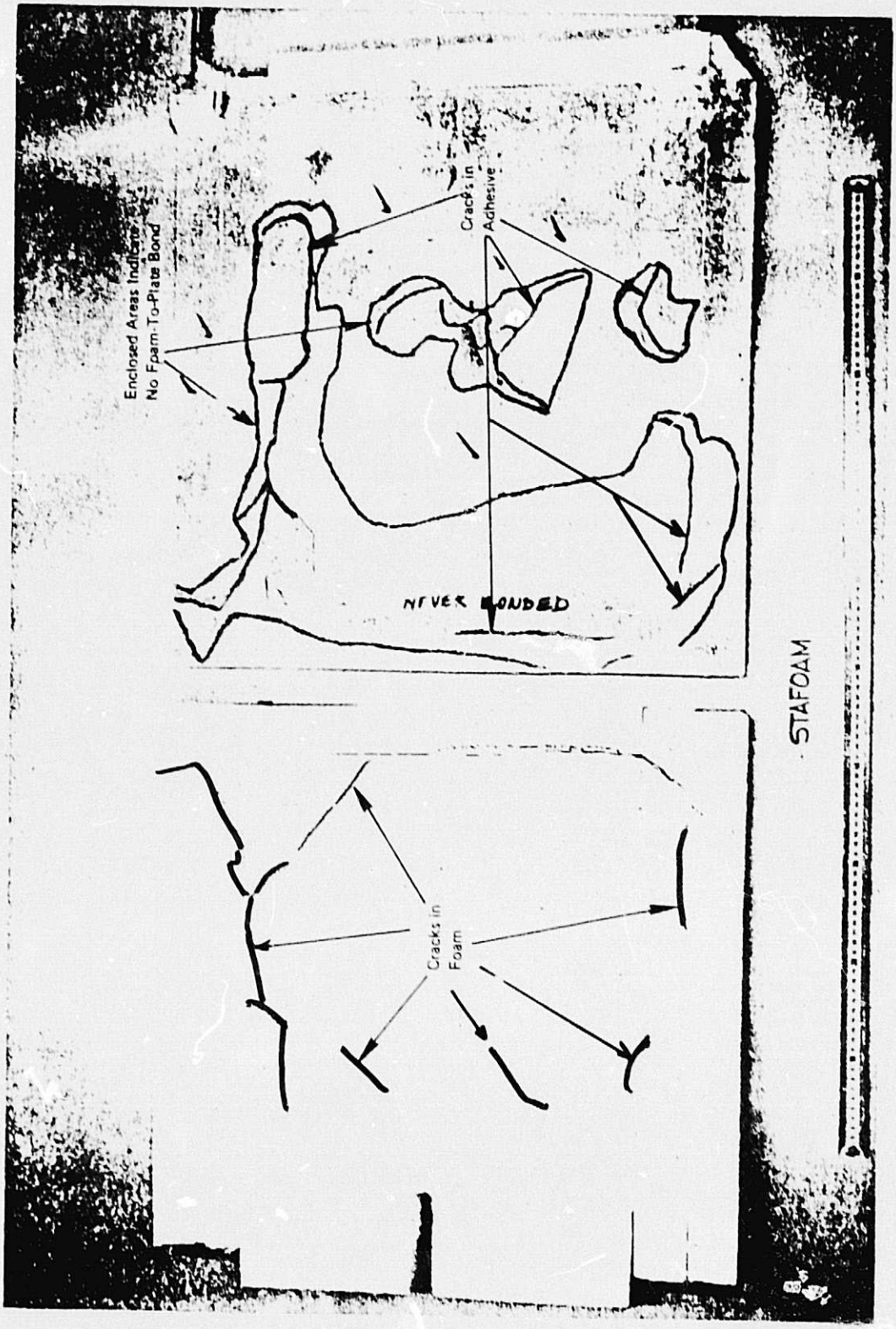

Figure 9. – Stafoam AA1602 foam system – exhibit of unbonded and cracked foam areas

occurred. This emphasizes the importance assigned to the fabrication defects, because the cracks did not penetrate to the outer foam surfaces after 20 temperature cycles and would not be observable during any visual quality control procedure.

Although the foam with defective application survived the repeated 77 K environments, because of the expected accumulation of liquefied and solidified atmospheric gases, we doubt that the system would have survived a 20K cold plate environment. Thus, when future samples are prepared they will have to be pressure loaded during curing of the adhesive to assure adequate bonding of the foam and plate. Even with pressure loading it is important to prevent the entrapment of air at the bond layer, or to assure its removal during the curing period, so that all the adhesive surfaces are in contact with each other.

Conclusions. - 1. The presence of unbonded areas caused the foam samples to develop cracks. Because no cracks developed in either foam sample in the fully bonded areas, we believe that the foam failures are due to faulty assembly of cold plate and samples rather than material failures.

2. Pressure-loading of the foam samples to the cold plate when the bond is formed provides no assurance that all the entrapped air has been removed and that the bonding surfaces are in contact with each other.

Recommendations. - 1. The tests performed with 0.38-m^2 test plate should be repeated using the same foam-adhesive systems and fully bonded surfaces.

2. A technique for removing entrapped air from the bond line and assuring continuous bonding of the surfaces should be developed.

Thermal Conductivity Measurements

Thermal conductivity of the selected foam materials. - The thermal conductance of the materials finally selected was measured by an outside testing laboratory.* As noted previously, these materials were:

1. Upjohn 452, 10%, 1.6 mm MG, Style 701, Batch Produced, Density 35 kg/m^3 (Same material as A.D. Little Sample No. 17)

2. Stafoam AA1602, 10%, 1.6 mm MG, Style 701, Batch Produced, Density 35.5 kg/m^3 (Same material as A.D. Little Sample No. 18)

---

*Dynatech R&D Company.

3. Same as Item 1 except machine produced by CPR Upjohn for Arthur D. Little, Inc.

Item 1 was measured with a guarded hot plate in accordance with ASTM C177 over a temperature range of 77 to 347 K. Items 2 and 3 were measured with a heat-flow meter in accordance with ASTM C518-70. The results which we obtained for these materials are shown in Table 15 and Figure 10.

Inspection of the results shows that the room temperature conductances of the Stafoam AA1602 (batch produced) and Upjohn 452 (machine produced) foams have almost identical values. The Upjohn 452 batch produced foam, on the other hand, has a value approximately 20 percent greater. Our experience in producing the foams indicates that this difference can be attributed to the entrapment of air, primarily during the batch-mixing of the two chemical components just prior to casting. This entrapment, to a large extent, is attributed to the higher viscosity of the Upjohn chemicals. The cells produced by the entrapment of air are generally larger than and intermixed with the cells produced by the Freon blowing agent. Because of the difference in the diffusion rates of air and Freon, we expect that air migrates into the Freon cells, while little Freon migrates into the air cells. Thus, we expect the thermal characteristics of this foam to be determined by a mixture of different cell gases. On the other hand, the mixing of the machine-produced Upjohn 452 is accomplished in an enclosure with no air present. Further, the batch-mixed Stafoam AA1602 does not show the same effects as the batch-mixed Upjohn 452 because its lower viscosity permits the air to be quickly released from the liquids during the mixing operation.

A consequence of the variability of the thermal conductivity of polyurethane insulating foams is the effect upon the temperature gradient in the foam between the cold tank wall and the surface at the ambient environment. In Figure 11, these temperature distributions are shown for the low (219 K), nominal (300 K) and high (346 K) outer surface temperatures. Because of the low thermal conductivity of these foams in the 0-150 K region (values in the 21 to 93 K temperature region are extrapolated, and this procedure is supported by data in the literature), the temperature gradients in the foam adjacent to the tank wall are 2-6 times greater than those at the outer surfaces of the foam insulation.

When applying insulation systems to flight vehicles, the $K\rho$ product is an important consideration. This product evaluates the amount of insulating value obtained per pound of insulating material. All other things considered equal, the material with the lowest $K\rho$ product is also the most efficient for flight.

Summary of $K\rho$ Products. - Table 16 is a summary of $K\rho$ products for materials we selected for final evaluation and other materials previously reported by Lockheed. The first four reported items are actually one material for which four mean thermal conductances, K_m, have been computed,

Table 15. - The thermal conductivity of three foam materials.

Temperature		$W\ m^{-1}\ K^{-1}$			$Btu\ in.\ h^{-1}ft^{-2}{}^{\circ}F^{-1}$		
K	°F	A	B	C	A	B	C
93	-292	0.0123	-	-	0.085	-	-
139	-210	0.0186	-	-	0.129	-	-
183	-130	0.0242	-	-	0.168	-	-
233	-40	0.0297	-	-	0.206	-	-
286	55	0.0257	-	-	0.178	-	-
294	70	0.0265	0.0215	0.0221	0.184	0.149	0.153
336	145	0.0328	-	-	0.227	-	-

Notes:

1. Material A: Upjohn 452, 10% 1.6 mm MG, Style 701, Density = 35.0 kg/m^3, Batch Produced

2. Material B: Stafoam AA1602, 10%, 1.6 mm MG, Style 701, Density = 35.5 kg/m^3, Batch Produced

3. Material C: Same as Material A except machine produced by CPR Upjohn for Arthur D. Little, Inc.

4. The thermal conductance of Material A was measured with the guarded hot plate in accordance with ASTM C177.

5. The thermal conductances of Materials B and C were measured with the heat flow meter in accordance with ASTM C518-70.

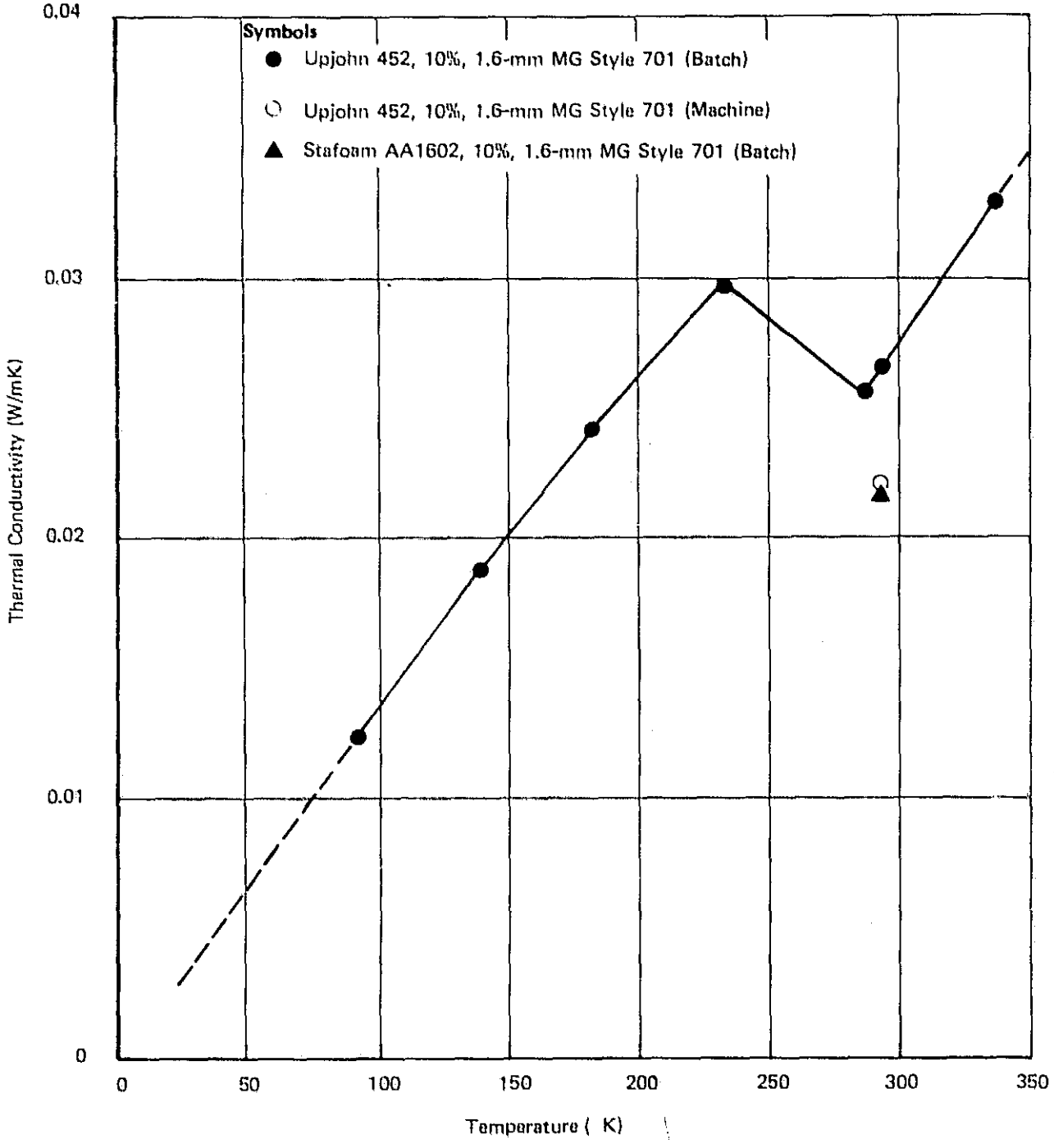

Figure 10. — Thermal conductivity of Upjohn 452 and Stafoan AA1602

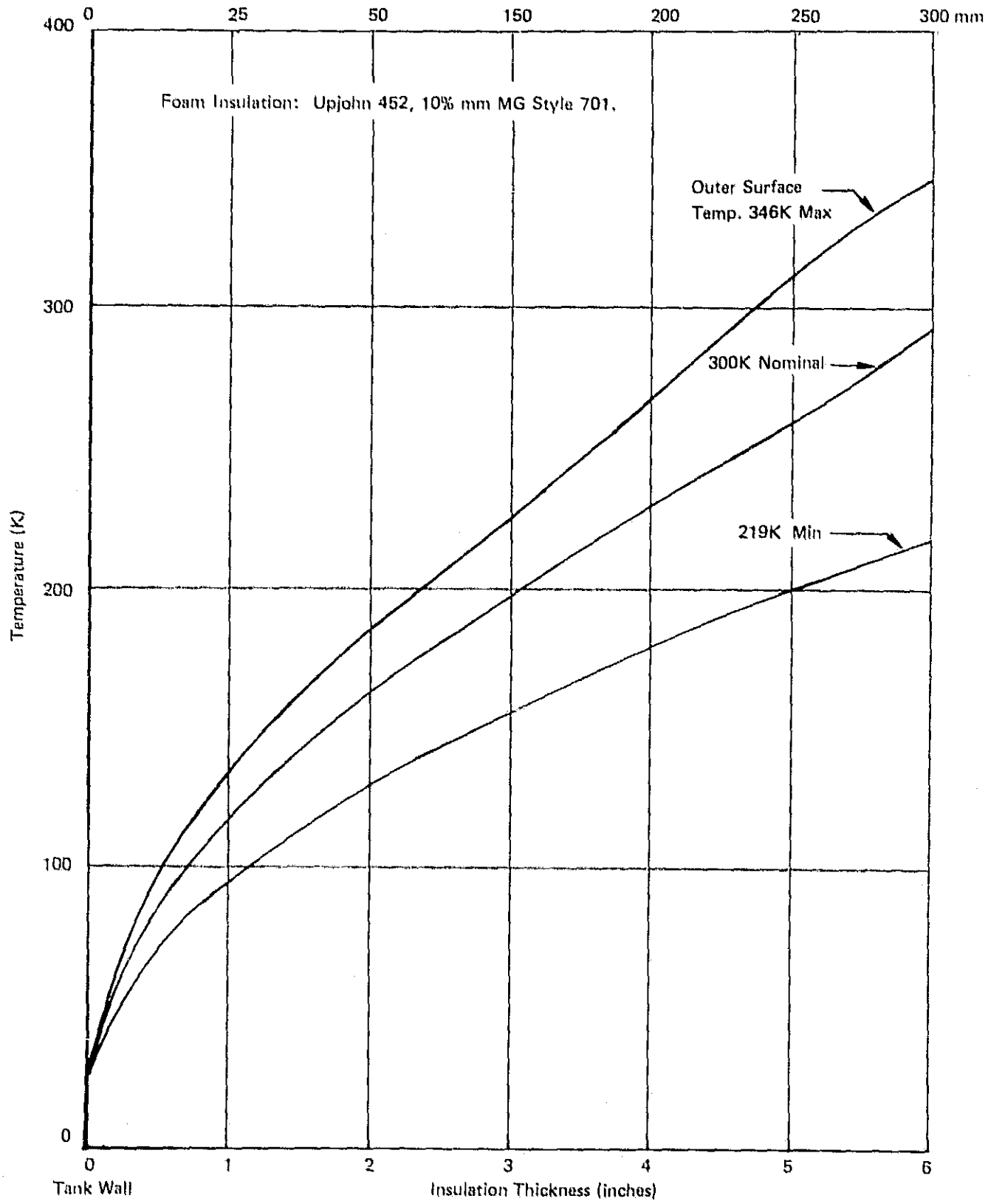

Figure 11. — Thermal insulation temperature gradients

Table 16. - Thermal conductance and $K\rho$ products.

	Material	Temperature and Range (K)	K_m (W/mK)	ρ (kg/m^3)	$K_m\rho$ (Wkg/m^4 K)
1.	Upjohn 452, 10%, 1.6-mm MG, Style 701 (Batch Produced)	21-300	0.0193	35.36	0.68
2.	Upjohn 452, 10%, 1.6-mm MG, Style 701 (Batch Produced)	21-219	0.0160	35.26	0.56
3.	Upjohn 452, 10%, 1.6-mm MG, Style 701 (Batch Produced)	21-347	0.0208	35.26	0.73
4.	Upjohn 452, 10%, 1.6-mm MG, Style 701 (Batch Produced)	77-300	0.0225	35.26	0.79
5.	Upjohn 452, 10%, 1.6-mm MG, Style 701 (Machine Produced)	294	0.0221	35.26	0.78
6.	Stafoam AA1602, 10%, 1.6-mm MG, Style 701 (Batch Produced)	294	0.0215	35.50	0.76

Notes:

1. Data for Items 1 through 6 were obtained in this program.

2. Where a temperature range is noted $K_m = \int_{t1}^{t2} K dt$. Otherwise it is assumed that K_m is the thermal conductance at the temperature indicated.

ADHESIVES

Adhesive Selection for Foam-to-Tank Bonding

A considerable amount of work has been done over the years in the evaluation of various adhesives for cryogenic applications. The two classes of adhesives that have the best combination of properties are epoxies and elastomeric polyurethanes. The polyurethanes have by far the best low-temperature properties, but these tend to soften and lose strength rapidly as temperatures rise to 340 to 370 K. The liquid epoxy systems have better properties at moderate elevated temperatures, but they tend to become more hard and brittle and have less strength at cryogenic temperatures than the elastomeric polyurethanes.

A specific polyurethane adhesive that has proved suitable in our work and the work of others for temperatures below 77 K is Crest 7343, originally developed by a Narmco Division of Whitaker as Narmo 7343. This adhesive was used and performed very satisfactorily in our work for NASA/Lewis in 1964. However, in 1974, the curing agent for this adhesive was cited as a suspected carcinogen, and there are now restrictions on the manner in which it can be used. These restrictions significantly decrease the practicality of using this system.

We have had occasion, as part of this program and other work in the cryogenic area, to evaluate a number of other adhesives for both handling characteristics and low-temperature properties. Table 17 summarizes these data. In our experience, the Crest 7410 has the best combination of properties and was selected as the primary adhesive for use in this program. It has characteristics very similar to the 7343.

The only question regarding the Crest 7410 is the bond strength required at elevated temperatures. The bond strength of Crest 7410 at various temperatures, as shown in a Crest data sheet, is contained in Table 18.

Metal Surface Preparation

With all these adhesives, excellent bond strength to aluminum can be obtained. Because of repetitive use of the jigs and fixtures in this program, and particularly the 300-mm-square cold plates used for the cold shock tests, sandblasting was the standard method of surface preparation utilized. This procedure allowed us to blast off residual adhesive and foam from one test to prepare the surface for the next test. Since sandblasting would probably be an unacceptable method for surface preparation of the actual fuel tank, a series of tests was run to assure that equal or better bond strength could be obtained using a chromate conversion coating for surface preparation. In these tests, lap shear aluminum specimens were bonded with the Crest 7410 adhesive.

Table 17. - Summary of tests of adhesive handling and bonding characteristics

Adhesive	Pot Life at 300 K (hr)	Cure Time at 300K (days)	Mixing	Application	Cured Film	Adhesion
Crest 7450	2	3	Fair	Fair	Rubbery and Tough	Good
Crest 7410	1	3	Good	Good	Rubbery and Tough	Good
Crest 7425	2	3	Fair	Fair	Rubbery and Tough	Good
Crest 3133	2	1	Good	Good	Hard	Fair Adhesion to Mylar
Tra-Con 828/140	2	1	Good	Good	Hard	Fair Adhesion to Mylar
Solithane 113/300	6	4	Good	Good	Rubbery and Tough	Fair Adhesion to Mylar

Table 18. - Data sheet strength values for Crest 7410 tensile shear test.

Test Temperature (K)	Bond Strength (MPa)
20	48.26
77	41.36
217	31.02
300	11.03
356	2.76

One set of specimens was prepared for bonding by sandblasting. The second set was prepared by an Iridite dip. Iridite is representative of the standard type of chemical conversion coating used as a pretreatment for aluminum in many bonding applications. All specimens showed cohesive failure in the bond line. The average value for the Iridite specimens was 5 to 10% above that for the sandblasted specimens and was in the proper strength range indicated by the Crest data sheet. This indicates that the results achieved on the sandblasted surfaces can be achieved or exceeded on the liquid hydrogen tank by the use of a conversion coating for surface preparation.

Bonding Other System Components

The Crest 7410 can be used also for foam-to-foam bonding. We prepared several different types of specimens, which exposed the bond line to various types of stress, using the Crest 7410 to bond the foam to itself. In all cases, failure occurred within the foam, indicating a bond strength higher than the strength of the foam itself.

The third and most critical material which the adhesive might be called upon to bond is Mylar-surfaced vapor barrier. Our tests in this and other programs indicate that the Crest 7410 forms a good bond to the Mylar surface of various impermeable barrier materials. If problems should occur in bonding the Mylar, there are primers that can be obtained from the barrier material manufacturers to prime the Mylar to improve its bondability.

Although Mylar is the most common surface material in barriers, there is sometimes a layer of Dacron cloth or a non-woven fabric as the barrier surface. The Crest 7410 also bonds well to these types of materials. We therefore believe that this adhesive will be suitable for all applications where bonding is required in the insulation system.

VAPOR BARRIER

The vapor barrier is of great importance in the insulation concept selected for this program. The performance and usable life of the insulation systems depend upon almost-zero levels of atmospheric gas permeation. Although the foam has low gas permeability, the primary safeguard against entry of the atmospheric gases is provided by the outer vapor barrier.

In the event that the outer vapor barrier is damaged and becomes permeable, the inner vapor barrier will block entry of the atmospheric gases into the inner foam regions where oxygen and nitrogen can condense and solidify.

Principal Requirements

The principal requirements for both the inner and outer barriers are:

1. negligible gas permeance,
2. low weight,
3. adequate tear strength,
4. adequate tensile strength, and
5. resistance to corrosion and pitting.

Barrier Construction

On the basis of our experience with barrier materials, we selected a composite structure consisting of laminates of Mylar films, aluminum foil, and Dacron or glass netting to meet these requirements. The aluminum foil is the principal vapor barrier. The Mylar imparts strength to the barrier to provide for handling and fabrication. In addition, the Mylar protects the metal laminates against corrosion and pitting. The netting provides rip-stop capabilities to prevent the enlargement of punctures and tears. A description of the materials and their thickness is provided in Table 19.

Mylar laminates have been used as vapor barriers in many cryogenic systems. An analysis was made in this program of the gas-diffusion properties of such barriers, including the presence of pinholes, and we identified the laminations of a high-performance barrier which can meet the requirements of the insulation concept herein developed. Our evaluation of the barrier stresses, when the barrier is bonded to an insulating foam, indicates that it will perform acceptably.* Bonding of the barrier using adhesives for sealing the barrier and attaching it to the foam has been found to be acceptable. Sources of commercially available material have also been identified.

---

* See subsequent section entitled, Barrier Strength.

Gas Permeability

Because a lifetime of 15 to 20 years is desired for the liquid hydrogen tank insulation, the diffusion of gases through the barrier materials was studied. First, it is generally known that metals are superior to plastics and other materials such as gas barriers. Thus, we selected aluminum foil because of its light weight and commercial availability.

The phenomena of the absorption of gases by metals and the diffusion of gases through metals are fundamentally connected. The mechanism of diffusion is explained by the supposition that the gas goes into solution on the high-pressure side of the metal and is subsequently given off on the low-pressure side because it is supersaturated. Solution of the gas, then, must precede diffusion, and only gases that are soluble in the metal can diffuse through it. [12]

The composition of the atmosphere is identified in Table 20, along with the percent by volume of each gas. The noble gases, consisting of argon, neon, helium, krypton, xenon, and radon, are considered first. These gases are not only present in very small concentrations in the atmosphere, but as far as is known, they do not dissolve in metals in either the liquid or solid state. [12] Thus, we can assume that any metal membrane is impermeable in the presence of the noble gases.

Hydrogen is also present in air in small quantities, e.g., 0.5×10^{-4} percent by volume. The percent by volume is identical with the partial pressure of a gas within a mixture. Thus, the driving force for hydrogen permeation is quite small. In addition, hydrogen gas is practically insoluble in solid aluminum and soluble only to a small extent in molten aluminum at 297K [12]. Thus, the diffusion of hydrogen through aluminum can be ignored as a source of gas permeation because of the hydrogen's low solubility.

Nitrogen, of course, is the largest constituent of air, forming 78 percent of the total volume. However, like hydrogen, nitrogen is soluble in molten aluminum and not in solid aluminum. For the same reason, therefore, nitrogen permeation through aluminum can be ignored.

Oxygen, the second largest constituent of air, is soluble to some extent in most metals and, in the case of aluminum, an oxide phase will also appear when the metal becomes saturated with oxygen. At the maximum temperature of the system 347K (165°F), we estimate (from Duchman [12]) an oxygen diffusion rate through a 0.025mm aluminum membrane of about 0.01 atmos-liter/ft^2 over a 20-year period. If this gas were distributed equally throughout the foam, its partial pressure would be on the order of 0.36 Pa. Thus, we conclude that 1-mil aluminum is essentially impermeable to oxygen.

Table 19. - Vapor barrier membrane.

Layer	Material Description
1	0.013mm Mylar, Type A
2	Adhesive
3	0.013mm Aluminum Series 1100-0 Foil
4	Adhesive
5	0.013mm Aluminum Series 1100-0 Foil
6	Adhesive
7	0.013mm Aluminum Series 1100-0 Foil
8	Adhesive
9	0.013mm Mylar, Type A
10	Adhesive
11	Dacron or Glass Net Fabric

Table 20. - Composition of air at sea level.

Gas	Molecular Weight	Percent By Volume	Boiling Point (K)
Nitrogen	28	78.09	77.3
Oxygen	32	20.95	90.1
Argon	40	0.93	87.4
Carbon Dioxide	44	0.02-0.04	263.1
Neon	20.2	18×10^{-4}	27.2
Helium	4	5.3×10^{-4}	4.2
Krypton	83	1.1×10^{-4}	121.3
Hydrogen	2	0.5×10^{-4}	20.4
Xenon	130	0.08×10^{-4}	164.10
Radon	222	7×10^{-18}	211.3
Water	18	Variable	372.2

Pinholes

Metal foil offers the best choice for reducing the vapor transmission to negligible values needed in hydrogen systems. However, it is generally known that metal foils, including those of aluminum under 0.05mm thick, contain pinholes which can severely increase vapor transmission.

The density and size distributions of pinholes in aluminum foil materials are not well documented. A study conducted by one of the aluminum companies many years ago found that pinholes started to appear in the tested foils at a thickness of 0.025mm. In the range of foil thickness 0.025-.0075mm, about 30 pinholes per $0.03m^2$ were measured; below 0.0075 mm thick, the foils had about 33 pinholes per $0.03m^2$. These data represent average values noted at the time of measurement. No information was available on the hole size distribution.

To reduce the effect of pinholes on the vapor transmission properties of metal foils, two or more foils can be bonded together. Assuming a pinhole diameter of 0.025mm and a density of 30 pinholes per $0.006m^2$ for each of two sheets, one coincidence of pinholes should occur in about every $6.5m^2$ of laminated material. When three such foils are laminated together, one coincidence of pinholes should occur in every 6.5 million square meters of the composite. Thus, the vapor transmission through pinholes can be greatly reduced by lamination without excessively increasing the weight of the barrier system.

It is concluded that a vapor barrier material containing two aluminum foil layers is probably adequate. However, because the size and density of the pinholes in aluminum foils are probably quite variable and not accurately known, then the three-foil laminate offers the best chance of obtaining a pinhole-free barrier.

Barrier Strength

An analysis was made on several laminate combinations to determine if the inner barrier could be structurally degraded by the bonding foam at the operational temperature levels. Results were obtained for conditions in which the temperature of the barrier and adjacent foam was reduced from 293 to 100 K. The latter temperature level covers panels approximately to the operational temperature of the inner barrier and the former to the temperature of fabrication.

First, we determined that the operational temperature should not produce failure of either the Mylar or the metal components of the vapor barrier. This was also demonstrated by the immersion in liquid nitrogen of typical laminated barrier materials on hand. The laminates also tend to behave as metal components because the tensile modulus of the metal is significantly greater than the tensile modulus for Mylar. Further, in no instance does the calculated stress of either the plastic

or the metal exceed its yield stress. The results of this analysis are shown in Tables 21 and 22.

Second, we determined that the strain in the barrier materials is much less than the strain in the foam at the same temperature and about one-quarter to one-third of the proportional limit strain of the foam. We concluded from these values that the barrier would yield in compression or wrinkle in a buckling mode. Because of the continuous bond between the foam on either side of the barrier, we expect the compressive yield to be the more probable barrier failure mode. We have not determined if this yielding would also increase the permeability of the membrane.

Multi-layer barrier materials were not available in small quantities for our tests. Therefore, the System tests conducted in this program used S-5 material (Table 22) as a vapor barrier.

From the foregoing, we have reached the following conclusions:

1. A lamination of several materials is necessary to achieve the required barrier properties;

2. A pinhole-free barrier is best achieved with a laminate containing three layers of bonded metal foil;

3. The chosen barrier (See Table 19) is sufficiently strong to meet the requirements for handling and fabrication; and

4. The barrier materials are not expected to fail when subjected to operational temperatures by themselves. However, the inner barrier is expected to yield in compression at operational temperatures when bonded to the foam. It is not known whether this will affect the vapor transmission properties of the barrier.

Table 21. - Summary of barrier stresses.

BARRIER CONSTRUCTION (mm)			Net Thermal Strain	DEVELOPED STRESS			
				Mylar (tension)		Metal (comp.)	
Mylar	Metal	Mylar	mm/mm	MPa	psi	MPa	psi
0.025	0.025 Alum	0.025	0.00391	49.98	2173	29.97	4347
0.025	0.025 S.S.	0.025	0.00291	23.93	3470	47.85	6940
0.025	0.125 Alum	0.025	0.00360	17.67	2563	7.07	1025
0.025	0.125 S.S.	0.025	0.00272	25.61	3715	10.25	1586
1100 Aluminum alone			0.00352		----		----
304 S. Steel alone			0.00267		----		----

Table 22. - Tensile strength of barrier materials.

Manufacturer[2]	Designation	Construction	Tensile Strength[1] (N/m)	Tensile Strength[1] (lb/in.)
Alumiseal Corp.	Zero-Perm	0.013mm Mylar/ 0.025mm Al/ 0.013mm Mylar	39	22
Sheldahl	G-111800	0.013mm Mylar/ 0.013mm 0.013mm Mylar/ 33g/m^2 Polyester Fabric	105	60
Sheldahl	GT-755	0.05mm Mylar/ 0.025mm Al	88	50
Sheldahl	S-5[2] Hi-performance Barrier	0.013mm Mylar/ 0.025mm Al/ 0.013mm Al/ 0.013mm Mylar/ 110g/m^2 Dacron Woven Fabric	121	69

1. Strength is shown in force per unit width of the barrier laminate. This is the actual strength of the laminate construction, not a specific strength.
2. ADL Designation.

SUMMARY OF FINDINGS

The purpose of this investigation was to develop a method for using plastic foams to thermally insulate liquid hydrogen fuel tanks that are to be housed within the airframe of jumbo jet commercial aircraft. The insulation system consists of three major components that include plastic closed-cell foams, adhesives, and vapor barriers. The requirements for each of these materials were developed from the aircraft configurations and mission and from requirements imposed by the insulation concept.

An investigation, principally experimental, but also sometimes analytical, was conducted into the three classes of materials to identify and select those materials with properties suitable for use in the thermal insulation systems. These include closed-cell plastic foams, cryogenic temperature adhesives, and vapor barriers. Our work has produced the following findings.

Closed-cell plastic foams

We evaluated a variety of board-stock and liquid-poured foam systems, including polyurethane foams, combination foams such as polyurethane/isocyanurate foams and polyurethane/polyvinyl chloride foams, acrylic foams and others.

Porosity. - All foams tested had an acceptable porosity of less than 5 percent. The average porosity for all samples was 2 percent.

Cold Shock.- Cold-shocking the foam in liquid nitrogen produced some permanent dimensional changes, but little apparent structural damage. We utilized the measured porosity to determine if the cell walls failed, thereby producing an increase in porosity. We found that the samples shrank about 1 percent in volume. The average porosity decreased, with few exceptions, from an average 1.9 percent to 0.7 percent. We concluded that in most cases no structural damage of the foam occurred.

High-temperature deformation.- The aircarft requirement establishes a maximum operating temperature for the insulation at 347 K. To this we have added the requirement for dimensional stability at 400 K. Acceptable materials have a deformation temperature above 347 K and have dimensional changes of less than 5 percent at 400 K.

The materials that showed the best combined performance are Rohacell No. 31 and No. 51, Stepanfoam BX249N with fiber, and Upjohn 452 with fiber. Stafoam AA1602 showed marginal performance.

Gas diffusion. - All closed-cell polyurethane foams have an acceptably low gas diffusion rate. This finding is based on an extensive search of the literature. No similar information was found for the other plastic foams which have different chemical bases than the polyurethanes. Our tentative assumption at this time is that the diffusion properties are similar to those of the urethanes and therefore conditionally acceptable.

Thermal strain and contraction evaluation. - An analytical technique was developed for estimating the viability of a plastic foam bonded to 2219 aluminum at a cryogenic temperature. This involved the measurement of the thermal contraction and the proportional limit strain in tension of the foams under consideration. A foam with a large proportional limit strain at 77 and 20 K and a small thermal contraction relative to the strain would be expected to survive. A reversal of these properties would correspond to an expectation for foam failure--the failure being defined as either or both a cracking in the foam perpendicular to the metal-foam interface or a delamination of the metal and foam. In general, the addition of 10 percent fiber reduced the thermal contraction about 30 percent over the fiber-free material.

On the basis of these criteria, which included a safety factor arbitrarily set at 2.0, we identified four materials that are expected to survive liquid hydrogen temperatures. In decreasing order of acceptability, these materials are Rohacell No. 51, Rohacell No. 31 Staform AA1602, and Upjohn 452. The latter two foams contain fiber reinforcement.

0.3 meter square cold panel tests. - Tests were conducted with foams bonded to aluminum plates. The plates were designed to be cooled internally with liquid nitrogen. A regime of four tests was developed to evaluate the foam when cooled from the metal side and from the exposed side. The foams were visually observed during the test and visually inspected after each test for any signs of cracks and/or metal-foam delaminations.

Of 15 pairs of foams tested, more than half survived these tests without cracking and/or delaminating. Several foam systems without fiber reinforcement survived. Generally, all fiber-reinforced systems survived. Rohacell, which received high ratings in other tests, did not survive LN_2 immersion.

The foams which both survived the cold panel tests and produced the highest safety factor ratings are the Stafoam AA1602, Stepanfoam BX249N, and the Upjohn 452, all with fiber reinforcement.

The two foams we believe to be best suited as candidate materials for the liquid hydrogen tank insulation are Stafoam AA1602 and Upjohn 452, both reinforced with 10 percent, 1.6-mm milled glass fibers, Style 701. This selection was made on the basis of the tests which each foam underwent and on the handling experience we developed in working with each foam.

The two foams we selected are by no means ideal in all of their properties. Each has certain advantages over the other and both, we believe, have some clear advantages over all the other foams that we considered. Stafoam AA1602 system is superior to Upjohn 452 with regards to the processing of the chemicals and fibers. On the other hand, the Upjohn foam is more readily molded than the Stafoam. The Stafoam toxicity problem is more severe than that of the Upjohn foam. Upjohn foam has better dimensional stability at the maximum use temperature than does Stafoam. Finally, the Upjohn foam is expected to be less flammable than the Stafoam.

Rohacell was seriously considered as a candidate material. However, we did not include it in our final selection because our test results indicate that this foam material is brittle and subject to cracking at room temperature, as well as at liquid nitrogen temperature.

0.6-meter-square cold panel tests. -- The Stafoam AA1602 and Upjohn 452, both with fiber reinforcement, were next bonded to a 0.6-meter-square cold plate having four times the area of the previous test plate and twice the foam thickness, i.e., 50 mm. The Stafoam was bonded to one plate surface and the Upjohn foam to the other. Both experienced identical conditions as the cold plate was cooled with liquid nitrogen and warmed 20 times, over a period of 1-1/2 months.

Throughout this entire series of tests, we observed no structural failures or changes of any kind in the appearance of the two foams. The only observable occurrence associated with these tests was the "snap, crackle, and pop" sounds associated with the first 10 minutes of each cooldown. In the first cooldown test, these sounds were quite audible and frequent. However, as the number of cooldown cycles increased, the audibility, rate of occurrence, and duration of these sounds decreased significantly.

After the series of 20 cycles was completed, we removed the samples one at a time from the plate in small 50-mm wide pieces. The results of this careful inspection revealed that both foams had not bonded completely, over their entire area, to the cold plate. Only about 75 percent of the Upjohn foam sample was bonded, and only about 55 percent of the Stafoam sample was bonded. In both cases, the foam was found to be cracked on the cold side only, and only in the unbounded areas.

The foam survived in all the areas where there was a bond of the foam to the metal. We believe, therefore, that failure was the result of a fabrication defect and not the result of a material defect.

We concluded that both the Stafoam and Upjohn foams should continue as candidates in further work on liquid hydrogen tank insulation.

Thermal conductivity measurement. - The thermal conductivity of the batch-produced Upjohn foams was measured over a range of temperatures from 93 to 336 K. The variation of thermal conductivity versus temperatures was similar to that variation reported in the literature. However, the room temperature value was about 20 percent larger than expected--and larger than the room temperature values of the Stafoam system and a machine-produced Upjohn foam system. We believe this was the result of air entrapment during the batch production of the foam.

Both foams have an excellent k_p product. Both the batch-produced Stafoam and the machine-produced Upjohn foams have values of 0.78 and 0.76 WKg/m^4k, respectively. The batch-produced Upjohn has a value of 0.56 ot 0.79 WKg/m^4K, depending upon the selected temperature range over which the k value is integrated.

Adhesive

Our tests and evaluations indicated that Crest 7410 adhesive offers the best combination of properties, considering toxicity, pot life, cure time, mixing characteristics, ease of application, adhesion and quality of cured film.

Vapor barrier

Our investigation indicates that a vapor barrier laminate consisting of three layers of 0.013-mm aluminum foil with 0.013-mm Mylar covers and a Dacron rip stop will provide gas-tight covers for the foam system.

APPENDIX 1
FULL-SCALE REQUIREMENTS
LIQUID HYDROGEN FUEL TANK
SUBSONIC JET TRANSPORT AIRCRAFT

PURPOSE

The information provided here is to establish the requirements for the thermal insulation for airborne, liquid hydrogen, fuel tanks of a subsonic jet aircraft of the future. Not all of the pertinent information is presently available. However, it is expected that as more information is developed, in the current and in the future programs, that it will be added to this document to both refine and complete the necessary information.

LIQUID HYDROGEN AIRCRAFT

The aircraft upon which the tankage requirements are based is taken from the Lockheed Aircraft Company report, "Study of the Application of Hydrogen Fuel to Long-Range Subsonic Transport." (1) The aircraft and mission details are summarized in Table 1-1 and the aircraft configuration is shown in Figure 1-1.

The exterior configuration identified above resembles a conventional subsonic jet passenger aircraft. The interior configuration, however, is significantly different in that the fuel is stored within the fuselage. Two fuel tanks are provided; the forward tank is located between the flight crew compartment and the passenger compartment. The rear tank is located in the tail section of the fuselage behind the passenger compartment. Each tank has a central bulkhead dividing the tank into two fuel compartments.

The altitude and Mach number of a typical mission for the hydrogen fueled aircraft is shown in Figure 1-2. In the first 30 minutes of flight, the aircraft climbs to an altitude of approximately 35,000 feet and achieves a flight speed of 0.85 Mach. The cruise period of the trip is about 10.3 hours. This is followed by the descent and landing, which occupy another 30 minutes. The figure illustrates an additional but rare flight segment called "Fly to Alternate Field" in the event of poor weather or flight problems.

Table 1-1. - Aircraft and mission details - liquid hydrogen fueled, long range, subsonic, transport aircraft.

Mission	Units	Customary Units
Range	10,190 km	5500 n mi
Payload	39,900 kg	88,000 lb
Passenger Equivalent	400	400
Cruise Mach Number	0.85	0.85
Altitude (Maximum Cruise)	11.27 km	37,000 ft
Flight Duration	11.7 hours	11.7 hours
Aircraft Utilization Factor	0.375	0.375
Aircraft Life	50,000 hours	50,000 hours
Aircraft		
Gross Weight	177,000 kg	391,700 lb
Operating Weight, Empty	109,200 kg	242,100 lb
Fuel Weight	27,900 kg	61,600 lb
Fuselage Length	67.8 m	219 ft
Wing Span	53.0 m	174 ft
Engine Thrust (each of 4 engines)	127,800 N	28,700 lb
Average Fuel Consumption Rate (approximate total)	0.45 kg/sec	1.0 lb/sec

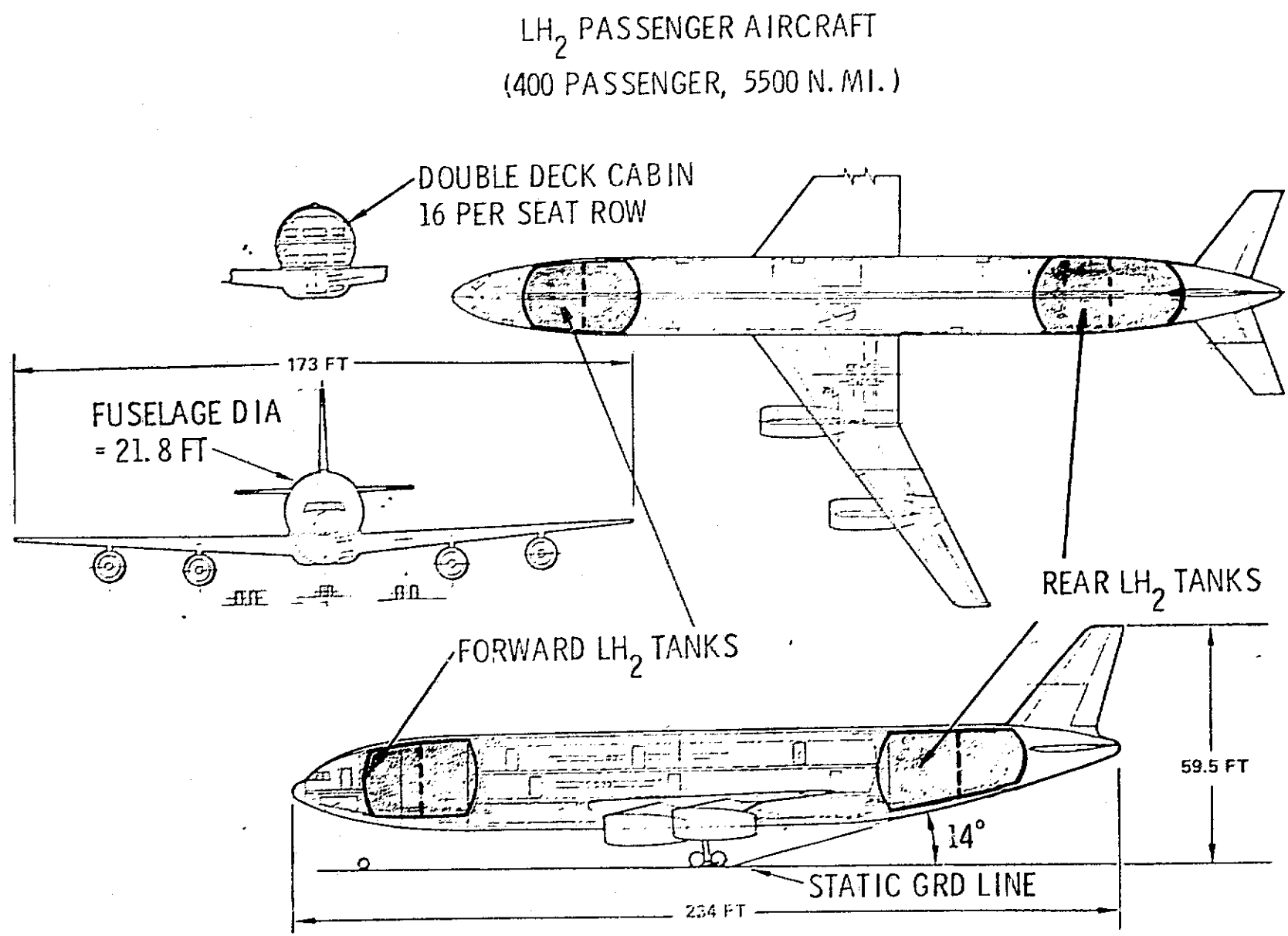

Courtesy of Lockheed Aircraft Co.

Figure 1-1. - Selected internal tank configuration.

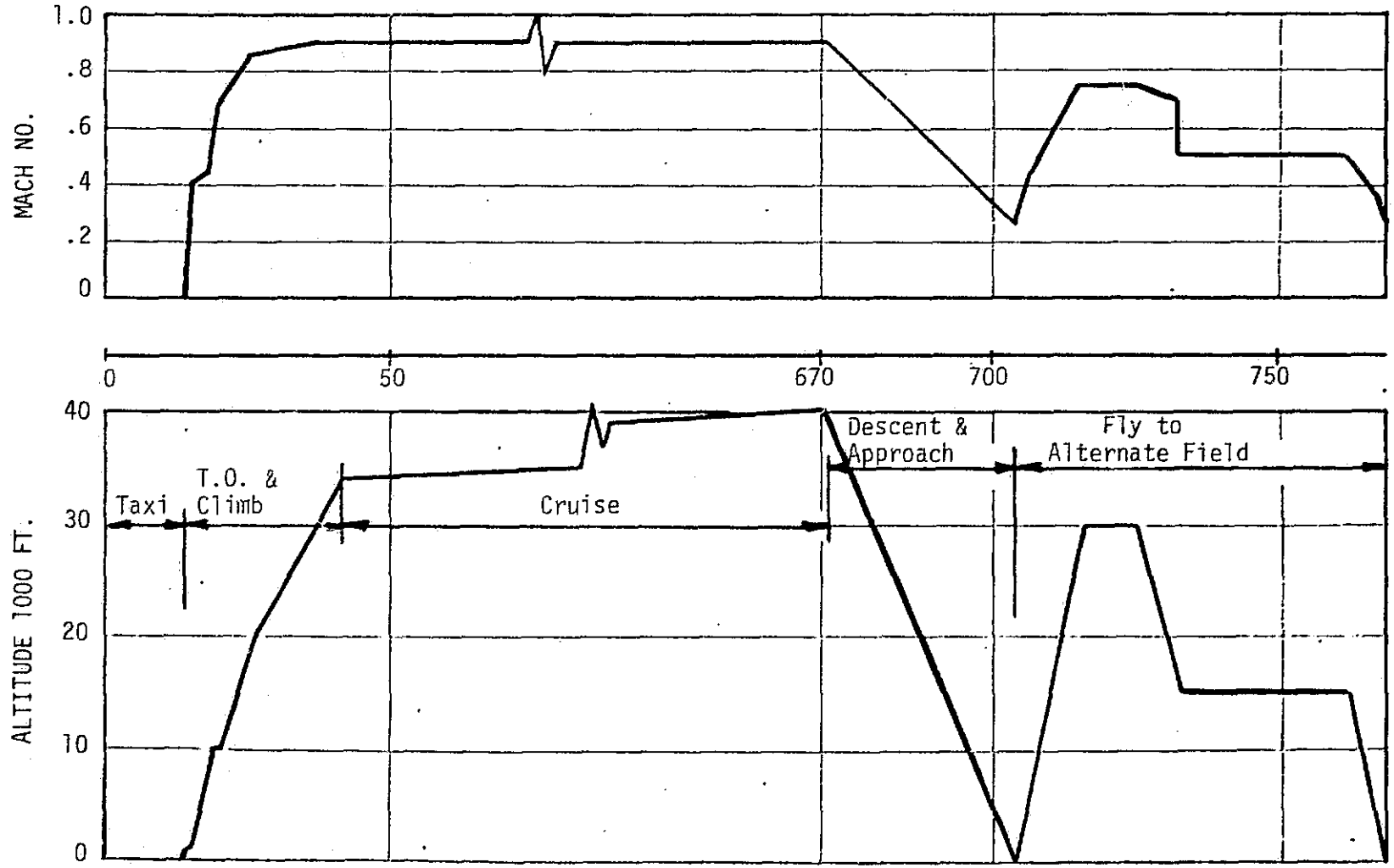

Courtesy of Lockheed Aircraft Co.

Figure 1-2. - Mach No. and altitude vs. time
(5500 n.Mi + 36°F)

LIQUID HYDROGEN FUEL TANKS

Tank Size and Configuration

The fuel tanks will be constructed from high-strength aluminum alloy 2219-T85. The fuel tanks will be almost cylindrical vessels with formed heads. The outer surface will be assumed to be a smooth continuous surface, while the interior surface may be webbed or formed with ring frames and stringers. The tanks will be fitted into the airframe to utilize the maximum space possible. Supports to the tanks will be provided within the airframe and allowances made for dimensional changes in the tanks due to temperature and pressure. These supports are not presently defined and several configurations are possible, one of which is shown in Figure 1-3. Provisions will also be made for the removal of the tanks from the aircraft for extensive and thorough tests and inspections necessary for recertification. The tanks will be capable of resisting maximum differential pressures of about +18 and -2 psi. Additional details for each tank are given in Table 1-2.

Tank Insulation

The liquid hydrogen fuel tank will be thermally insulated with a plastic foam having an overall average density of 2-5 lb/ft. The nominal thickness of this insulation will be 152 mm (6.0 inches). The insulation is to have a life expectancy equal to that of the aircraft.

It is intended that the fuel tanks will contain liquid hydrogen at all times, except when the fuel tanks are being inspected and/or repaired. At the beginning of each mission the tanks will be filled with liquid hydrogen fuel. Thus, the tank and internal insulation surfaces will be at liquid hydrogen temperatures. During the mission the fuel level decreases as shown in Figure 1-4.

Present estimates, based upon an aircraft life of 50,000 hours, are that the hydrogen-fueled aircraft will accomplish approximately 6,000 flights and the fuel tanks will be temperature-cycled between ambient and liquid temperatures approximately 20 times. The exterior surface of the thermal insulation will be cycled once per flight approximately as shown in Figure 1-5.

Also, following the mission and until the tanks are refueled, only a small portion of the tank wall will be submerged in liquid hydrogen. The temperature of that portion of the tank wall in contact with the gas space will increase. The extent of this increase is not defined at this time.

The outer insulation surface temperature will vary depending upon the operational environment. In the extremes, this variation occurs between 220°K (-65°F) and 347°K (165°F). However, for most of the

Table 1-2. - Liquid hydrogen fuel tank data.

Forward Tank	SI Units	Customary Units
Forward Tank	167 m^3	5894 ft^3
Fuel Volume	160.3 m^3	5654 ft^3
Fuel Weight *	11295 kg	24,000 lb
Tank Length	7.16 m	23.5 ft
Mean Diameter	6.00 m	19.7 ft
L/D Ratio	1.19 m/m	1.19 ft/ft
A/V Ratio	1.15 m^2/m^3	0.350 ft^2/ft^3
Ullage Space (percent)	4.0	4.0
Rear Tank		
Tank Volume	246.7 m^3	8712 ft^3
Fuel Volume	236.8 m^3	8363 ft^3
Fuel Weight(1)	16690 kg	36,800 lb
Tank Length	12.92 m	42.4 ft
Mean Diameter	5.55 m	18.2 ft
L/D Ratio	2.33 m/m	2.33 ft/ft
A/V Ratio	1.273 m^2/m^3	0.388 ft^2/ft^3
Ullage Space (percent)	4.0	4.0

*All values in this table are based on fuel weight values and are approximate.

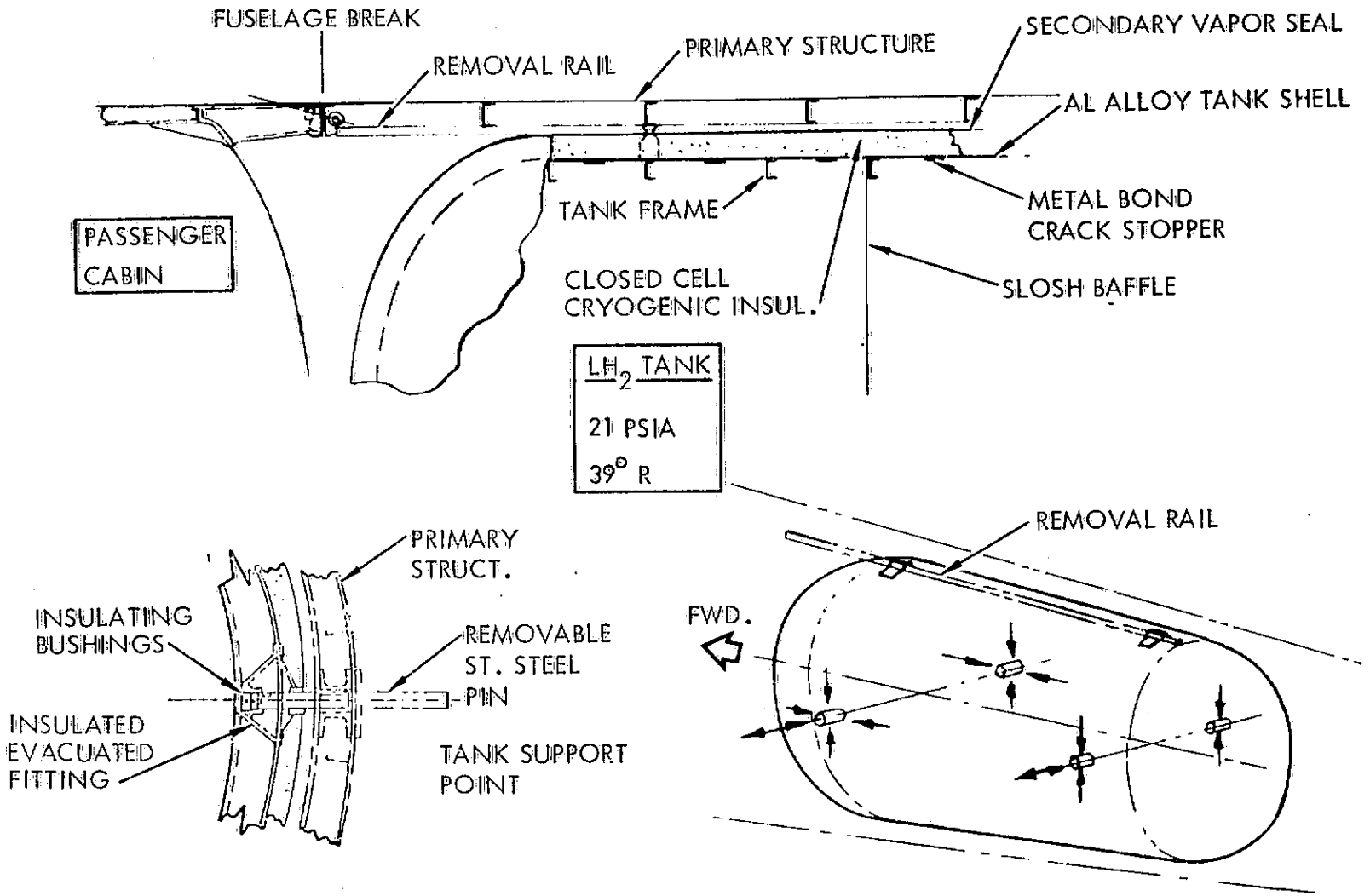

Courtesy of Lockheed Aircraft Co.

Figure 1.3. - Non-integral tank concept.

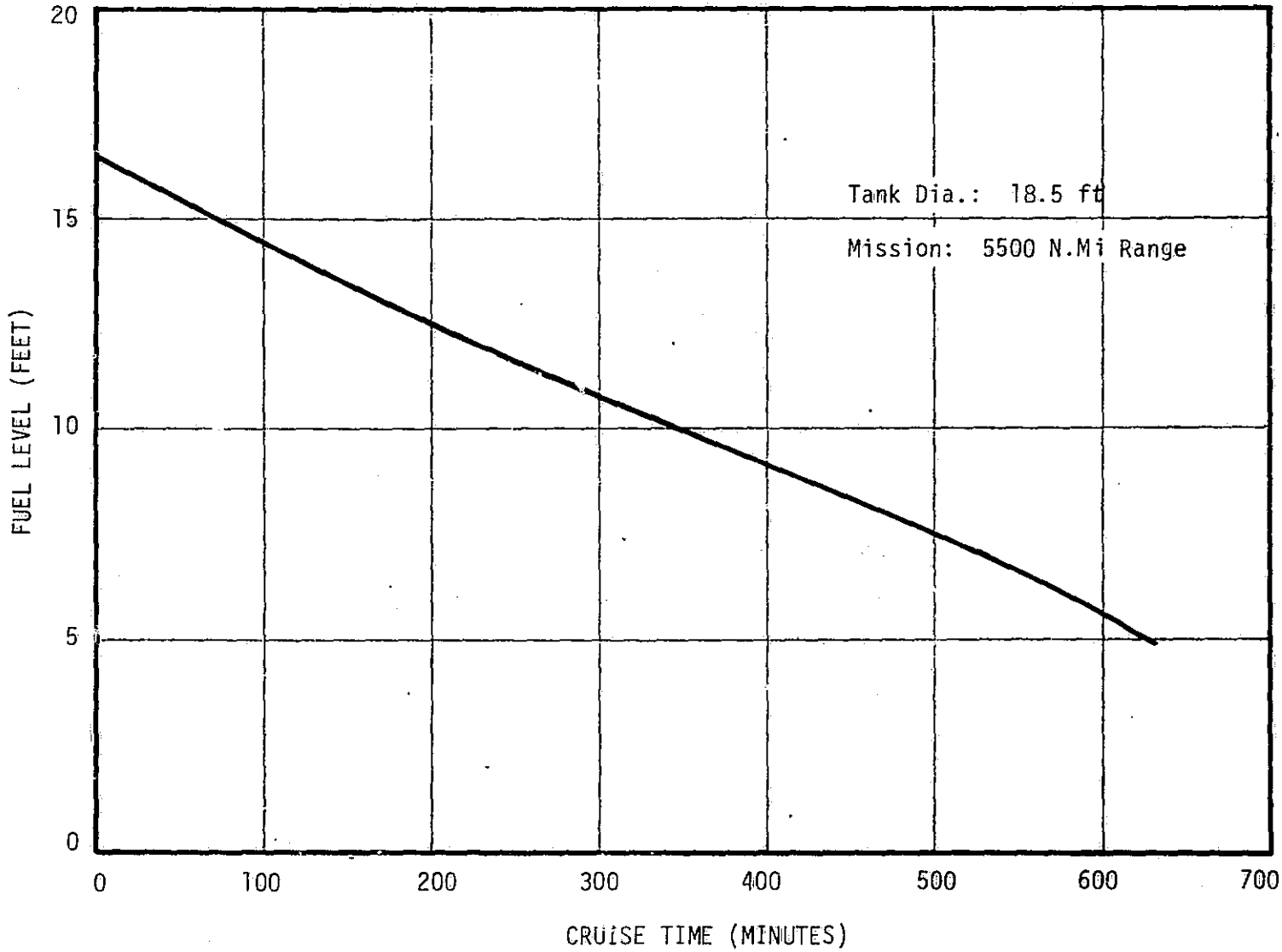

Courtesy of Lockheed Aircraft Co.

Figure 1-4. - Fuel tank liquid level vs. flight time.

aircraft life the temperatures are expected to remain between 261°K (10°F) and 311°K (100°F). (2) The temperature variations during a typical mission are shown in Figure 1-5.

Purge Space

The space within the airframe surrounding the fuel tanks will be identified as the purge space. It is assumed that this space is maintained at cabin pressure during all phases of flight operations, except during emergency situations when cabin pressure is lost or when hydrogen is detected. For the present, no statement is made relative to the operations and purge gas, if any, that may be used for inerting and otherwise diluting any hydrogen leakage into this space.

The amount of water vapor in the atmosphere that condenses and/or freezes onto the outer surface of the tank insulation is dependent upon climatic conditions, operational conditions, and the fuel tank and airframe configurations. For many situations, the quantity of condensation and/or freezeout will be zero. However, there are many other situations when there will be condensation and/or freezeout of water vapor. Therefore, provisions must be made to condition the air in the purge space or to eliminate water accumulation with hot air or other appropriate gas purge methods.

Mechanical Environment

The preliminary three-axis vibration spectra for the liquid hydrogen fuel tank are estimated to be as follows: (3)

10-45 Hz	1 to 10 g ramp
45-2000 Hz	10 g

The aircraft three-axis acceleration data for various flight regimes have not been defined at this time.

TYPICAL AIRCRAFT OPERATIONS

The survival of the fuel tank insulation system is influenced by each environment to which it is subjected. Since proper design and testing of the system must consider all possible environments and their sequence, it is necessary that each aircraft operation be defined with its associated environments. Table 1-3 is an attempt to define these principal operations.

Mission: 5500 N.M. Range
Temp: +36°F Hot Day
Insulation: 6"

Courtesy of Lockheed Aircraft Co.

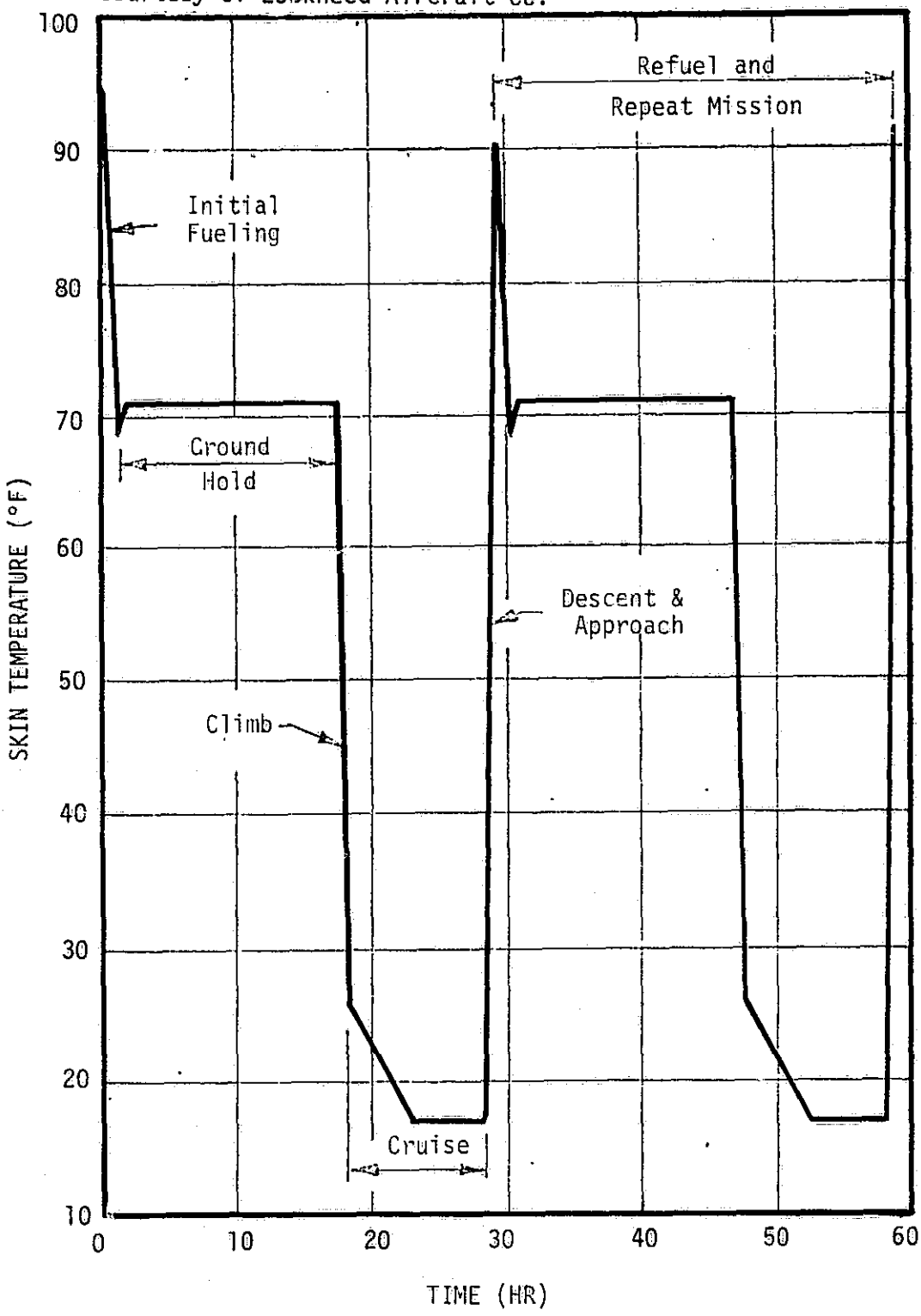

Figure 1-5. - Skin temperature vs. time.

Table 1-3. - Typical aircraft operations -- preliminary.

1. TANK COOLDOWN AND FUELING

1.1 Purge air from fuel tanks and lines with inert gas.

1.2 Purge inert gas from fuel tanks and lines with warm hydrogen gas.

1.3 Cooldown fuel tanks with cold hydrogen gas.

1.4 Fill tank with liquid hydrogen.

1.5 Top fuel tank while the temperatures in the tank insulation are equilibrating.

1.6 Tow aircraft to boarding area.

1.7 Go to Item 3.

2. TANK REFUELING

2.1 Fill tanks with liquid hydrogen.

2.2 Tow to boarding area.

2.3 Go to Item 3.

3. PREFLIGHT (AT BOARDING AREA)

3.1 Flight preparation.

3.2 Make minor repairs and replace, as necessary, instruments & equipment.

3.3 Board passengers, and load baggage and cargo.

3.4 Hold for weather, traffic and other reasons.

3.5 Top fuel tanks if necessary.

3.6 Taxi to runways.

4. FLIGHT

4.1 Take off.

4.2 Climb.

4.3 Cruise

4.4 Descent

4.5 Approach.

4.6 Land

Table 1-3. - (continued)

5. POST FLIGHT

5.1 Taxi to ramp areas.

5.2 Deplane passengers.

5.3 Tow to fueling area.

5.4 Go to Item 2.

6. SCHEDULED MAINTENANCE OF AIRCRAFT AND PROPULSION SYSTEMS, EXCEPT FOR FUEL TANKS WHICH REMAIN PARTLY FUELED WITH LIQUID HYDROGEN

6.1 Tow aircraft to maintenance area.

6.2 Vent fuel tank boil-off to remote area.

6.3 Purge fuel lines with inert gas.

6.4 Perform maintenance tasks.

6.5 Tow aircraft to fueling area.

6.6 Go to Item 2.

7. SCHEDULES TANK MAINTENANCE

7.1 Tow aircraft to defueling area.

7.2 Defuel.

7.3 Warm fuel tanks.

7.4 Purge fuel lines with inert gas.

7.5 Tow aircraft to maintenance area.

7.6 Perform tank inspection and maintenance.

7.7 Tow to fueling area.

7.8 Go to Item 1.0

Operational Sequencing.

Flight Routine (2,3,4,5), (2,3,4,5) ....

Aircraft Maintenance (2,3,4,5), (2,3,4,5,6) (2,3,4,5) ....

Tank Maintenance (2,3,4,5), (2,3,4,5,7), (1,3,4,5), (2,3,4,) ....

REFERENCES

1. Brewer, G.D., R.E. Morris, R.H. Lange and J.W. Moore, "Study of the Application of Hydrogen Fuel to Long-Range Subsonic Transport Aircraft," Final Report, January 1975 prepared by Lockheed for NASA/Langley Research Center. NASA CR 132559.

2. Personal Communication from R.G. Helenbrook, Bell Aerospace Company, January 12, 1976.

3. Barbiere, R. E., and W. Hall, "Electronic Designer's Shock and Vibration Guide for Airborne Applications," December 1958, WADC TR 58-363, ASTIA AD 204095.

APPENDIX 2

EFFECT OF CRYOGENIC TEMPERATURES ON A PLASTIC FOAM AT METAL INTERFACE

The purpose of this appendix is to present a description of the mechanical behavior of plastic foam insulations when bonded with an adhesive to aluminum when the aluminum is cooled from room temperature to 20 K. The results of this work are based upon a review of the literature and lead to a strain criterion for the foam. The comments here are applicable tc a 150-mm-thick foam insulation applied to a 6.15-m diameter liquid hydrogen tank made of aluminum. This discussion is equally applicable to a very large flat plate configuration with the exception that strains perpendicular to the plane of the plate are somewhat different from the radial strain in a cylinder.

Figure 2-1A shows the temperature distribution through the thickness of the insulation. For the initial considerations, it is assumed that at time zero, t_0, there is a step change in temperature in aluminum plate from 293 to 20 K. At some short time later, t_1, there is a very steep temperature gradient in a very thin layer of foam immediately adjacent to the aluminum. As time progresses, this temperature gradient relaxes. At steady-state conditions, the temperature distribution is characterized by the curve t_3.

The primary effect of these temperature gradients is to cause contraction (shrinkage) of the foam of different amounts through the foam thickness, depending upon the local temperature. This differential shrinkage at any one thin layer of foam is restrained or augmented by the contraction of the next adjacent thin layer. At the foam-aluminum surface, the differential shrinkage is the greatest because the aluminum contracts very much less than the foam. If the contraction could be observed at a free edge of the assembly, it would look similar to that shown in Figure 2-1B. At t_0, the aluminum contracts its total amount and pulls the foam interface (not yet cooled) with it. As time increases, the foam cools and attempts to shrink more than the aluminum. Naturally, the foam interface cannot (or should not, unless the shearing bond is broken) contract more than the aluminum, so the interface maintains the same (approximate) contraction as the aluminum. As the foam layers farther away from the plate cool down, the shrinkage becomes greater than that of the aluminum and the distortion shown in Figure 2-1B at large times, t_3, results. In any real case, without edge effects, there is, of course, no net distortion or motion of the foam in the plane of the foam. The result is the development of elastic stresses within the foam in the absence of failure.

The magnitude of these thermally induced stresses depends upon the thermal contraction property, coefficient of contraction, α, and stiffness or Young's modulus, E, of the foam, relative to the α and E of the aluminum. These developed stresses are shown in Figure 2-1C at some long time.

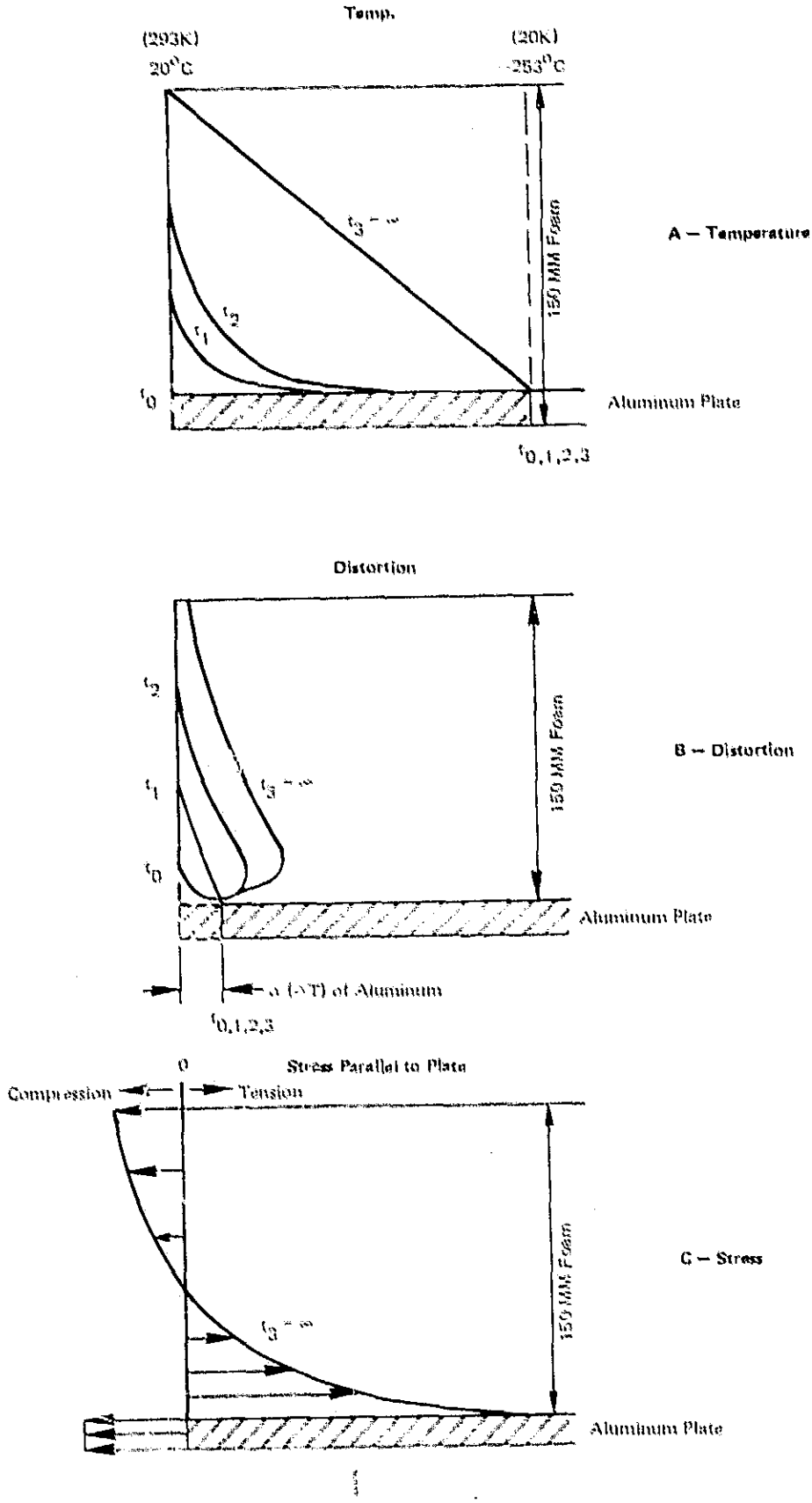

Figure 2—1. — Stress conditions at foam-metal interface

In Figure 2-1C, the tensile stress in the foam is always highest in the infinitesimal layer next to the aluminum plate because of the relatively large, more than 4 to 1, difference in α (this layer of foam is always at the same temperature as the aluminum); that is, the foam is always strained in tension to match the aluminum. Because a layer of colder foam is shorter than the next layer of warmer foam, it tends to pull the layer of warmer foam into a small amount of compression. There is a gradual change, therefore, in the tension of the foam, proceeding from the colder inner layers to the outer warmer layers, until a point is reached where the foam stress is zero. Beyond this point, the outermost layer is in compression. The sense of this action is identical to the action in a cylindrical tank in the following way. The aluminum tank decreases in radius (circumference) as it is cooled. The outer layer of foam is still warm and is pulled inward to a new smaller radius (circumference) because of the developed radial stresses. Hence, the outer layer of foam must be in compression.

It is instructive at this point to develop magnitudes of stresses and/or strains in a simplistic manner.

It has been established that the tank will be stressed to 206.9 MPa (30,000 psi), and it is assumed that this level was established as a proof stress. Considering a safety factor of 2.0, the operating stress will be 103.4 MPa (15,000 psi), and the tank wall will have a corresponding nominal thickness of:

$$t = \frac{\text{Pressure} \times \text{Radius}}{\text{Stress}} = \frac{\sim 0.138\ \text{MPa} \times 304.8\ \text{cm}}{103.4\ \text{MPa}} = \frac{\sim 20\ \text{psi} \times 120''}{15{,}000}$$

$$= 0.407\ \text{cm}\ (0.16\ \text{in.})$$

(The approximate 0.138 MPa (20 psi) differential pressure occurs at operating altitude of about 11.27 km (35,000 ft) with the tank pressurized to about 0.152 MPa absolute (22 psia)).

At the proof stress, the aluminum strain at 20 K will be:

$$+\frac{\Delta \ell}{\ell} = \varepsilon_{AL} = \frac{\text{Stress}}{E} = \frac{\sigma}{E} = \frac{206.9\ \text{MPa}}{8.16 \times 10^4\ \text{MPa}}$$

$$= +2.54\ 10^{-3}\ \text{mm/mm}$$

When cooled to 20 K the 2219-T87 aluminum will develop a total strain of:

$$\frac{L_{20K} - L_{293}}{L_{293}} = \varepsilon_o \Delta T = -4.12 \times 10^{-3}\ \text{mm/mm}$$

Polyurethane foams will contract somewhere between 10 and 19 x 10^{-3} mm/mm and exhibit E's of about 27.6 MPa (4,000 psi) at 20 K.

Taking, for example, the steady-state situation where the tank and a thin layer of foam is at LH_2 and the tank is simultaneously stressed to 206.9 MPa (30,000 psi) (i.e., the proof test), one finds the net strain in the aluminum to be (-4.12 + 2.54) x 10^{-3} or -1.58 x 10^{-3} mm/mm. Using an average foam thermal strain of about -14 x 10^{-3} mm/mm, one can see that the difference of about +12.42 x 10^{-3} mm/mm will be the mechanical strain developed in the foam as it conforms to the length dictated by the significantly stiffer aluminum. If the tank were not pressurized, the developed strain in the foam would be (-4.12 - (-14)) x 10^{-3}, or +9.88 x 10^{-3} mm/mm.

The tensile and compressive forces must be balanced at any cross-section through the foam and the aluminum. Taking a very simplistic, worst-case model which assumes that all of the foam is at 20 K and that the entire thickness of the foam acts as a uniform block of material, one finds that the differential thermal contraction produces a thermal strain in the foam of 9.75 x 10^{-3} mm/mm and in the aluminum of 0.124 x 10^{-3} mm/mm, as shown in Figure 2-2. The corresponding stresses are 10.1 MPa (1463 psi) in the aluminum and 0.27 MPa (34 psi) in the foam. The resulting common force is 41,010 N/m (234 lb/in.) as tension in the foam and compression in the aluminum.

Since, in the real case, all of the foam does not reach 20 K and does not have the high E (due to 20 K through its depth, as assumed), it can be concluded that the foam sees an essentially infinitely stiff plate or the plate is so stiff compared to the foam that the foam strains have a negligible effect on the aluminum plate strains.

Thus, it is concluded that the foam must be able to withstand, at 20 K, a strain that is equal to the differential thermal strain between the foam and aluminum plus the pressure strain or about (14 x 10^{-3}) - (4.12 x 10^{-3}) + 2.54 x 10^{-3}, or a total of 12.4 x 10^{-3} mm/mm.

To meet the suggested criterion, then, a foam must possess a high strain capability at the proportional limit, no particular value of Young's modulus, and a low thermal contraction.

The literature review has revealed the following general properties of foam;

1. As density increases, both ultimate strength and modulus in compression and tension increase.

2. Strength and modulus are greater in the parallel-to-the-rise direction than in the perpendicular directions.* No

---

* The direction in which the foam expands during its formation is the rise direction. The two orthogonal directions are the perpendicular directions.

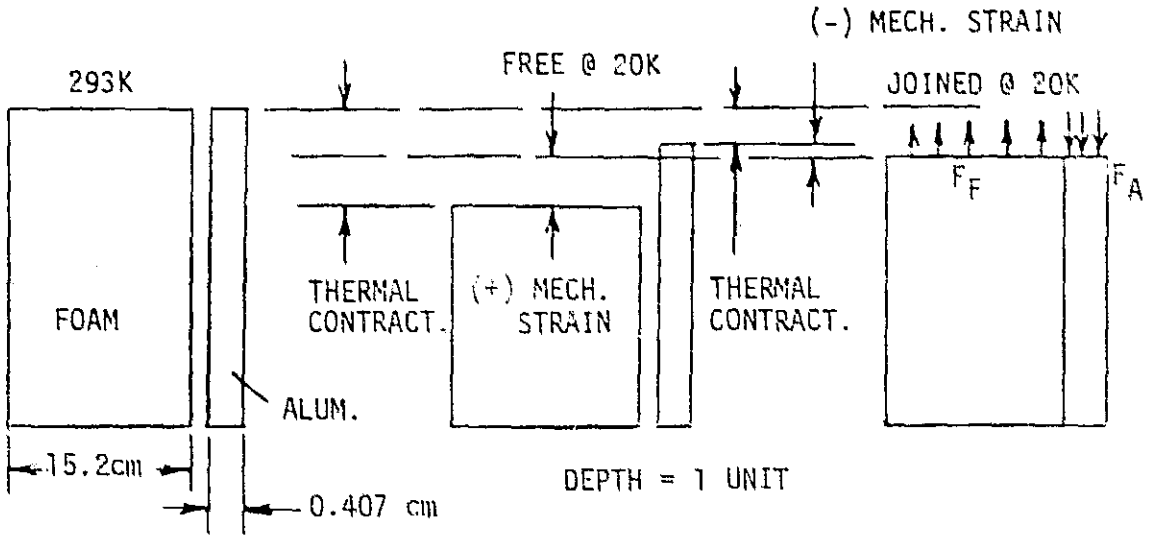

FORCES BALANCED: $F_{FOAM} = F_{ALUM}$ (NOTE: Pressure strains not included)

EQUAL STRAIN: $(\alpha\Delta T)_F - \frac{F_F}{A_F E_F} = (\alpha\Delta T)_A + \frac{F_A}{A_A E_A}$

thermal - mechanical = thermal + mechanical

$$14 \times 10^{-3} - \frac{F_F}{(1)(0.152)(27.6 \times 10^6)} = 4.12 \times 10^{-3} + \frac{F_F}{(1)(0.00407)(8.10 \times 10^{10})}$$

$$9.88 \times 10^{-3} = F_F \frac{1}{(0.00401)(8.16 \times 10^{10})} + \frac{1}{(0.152)(27.6 \times 10^6)}$$

$F_A = F_F = 41{,}010$ N/m (234 lbs/in.)

ALSO: $\sigma_A = \frac{F_A}{A_A} = \frac{41{,}010}{(0.00407)(1)} = 10.1$ MPa (1463 psi)

$\varepsilon_{A,MECH} = \frac{\sigma_A}{E_A} = \frac{10.1 \text{ MPa}}{8.16 \times 10^4 \text{ MPa}} = 0.124 \times 10^{-3}$ mm/mm

$\sigma_F = \frac{F_F}{A_F} = \frac{10.1 \text{ MPa}}{(0.152)(1)} = 0.27$ MPa (39 psi)

$\varepsilon_{F,MECH} = \frac{\sigma_F}{E_F} = \frac{0.27 \text{ MPa}}{27.6 \text{ MPa}} = 9.76 \times 10^{-3}$ mm/mm

Figure 2-2. - Worst-case strain model.

distinction is made between the two perpendicular directions.

3. Strength and modulus increase non-linearly as temperature decreases. Some Upjohn spray foams are just opposite to this trend (spray foam is applied by spray techniques and does not use foams).

4. Thermal contraction data are both insufficient and too contradictory to draw any firm conclusions. In Figure 2-3 is plotted the thermal contraction of various foams, from 293 to 77°K for most cases. The foam with the greatest contraction was 45 kg/m^3 (2.82 lb/ft^3) polyurethane foam *[1]. The data points available are shown down to 105 K. The lesser contraction of Stephan BX-250A polyurethane foam is shown by the solid curves that were drawn with only end-point data at 293 and 88°K, but shaped in the same manner as the Reference [1] data.

   The range of data shown as obtained from Reference [2] represents foams which vary considerably in chemical type and method of foaming (density, ether, ester, Freon, and CO_2 blown). The consistency among these data is that the contraction is less in the parallel-to-the-rise direction. However, the reverse is reported for the Stepanfoam.

   Exhibiting less contraction than any polyurethane foam are the Rohacell and Klegecell foams. The grouped data for Rohacell show no trend with respect to density, but the fire-retardant versions contract more than the non-retardant type.

   Also shown for comparison is the contraction for 2219-T87 aluminum.

5. The induced strain at the proportional limit of the stress-strain curve is almost independent of the kind of foam, density and temperature. The same Upjohn spray foams (see 3 above) do not follow this relationship.

In Figure 2-4, the proportional limit strain of polyurethane foams, in both tension and compression, has been plotted as a function of foam density at various temperatures. In these data the values at any single density represent one foam chemical formulation. Different densities, in most cases, represent different formulations.

The Upjohn bun foam exhibits fairly constant values of compressive strain, regardless of density or temperature, while the spray foam shows a higher strain capability at lower temperatures (bun foam is made by continuous extrusion of foamable plastic which expands to its final dimensions). The more significant strain data, in tension, are unavailable.

---

* Numbers in brackets are references located at the end of Appendix 2.

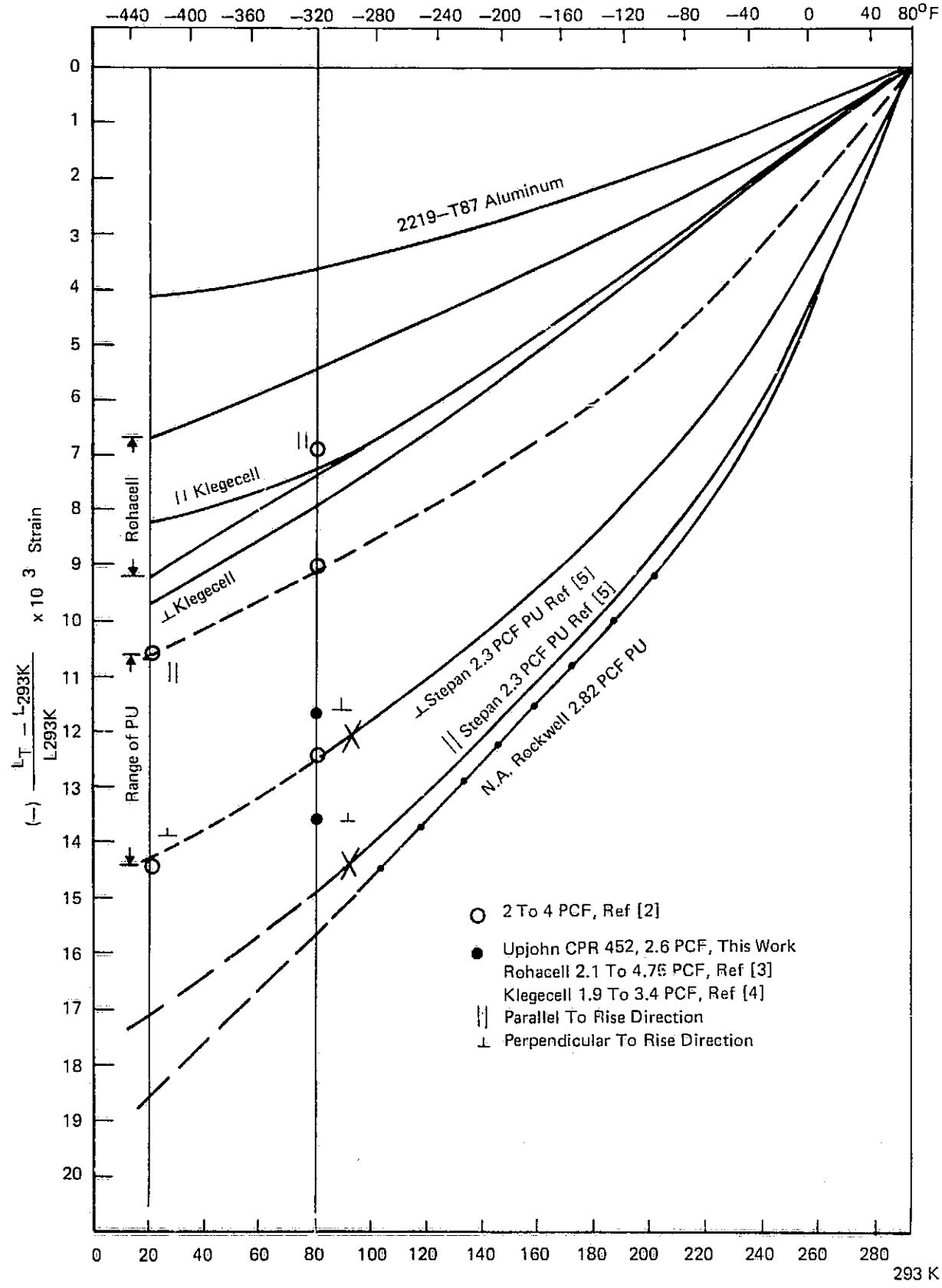

Figure 2−3. − Thermal contractions of foams

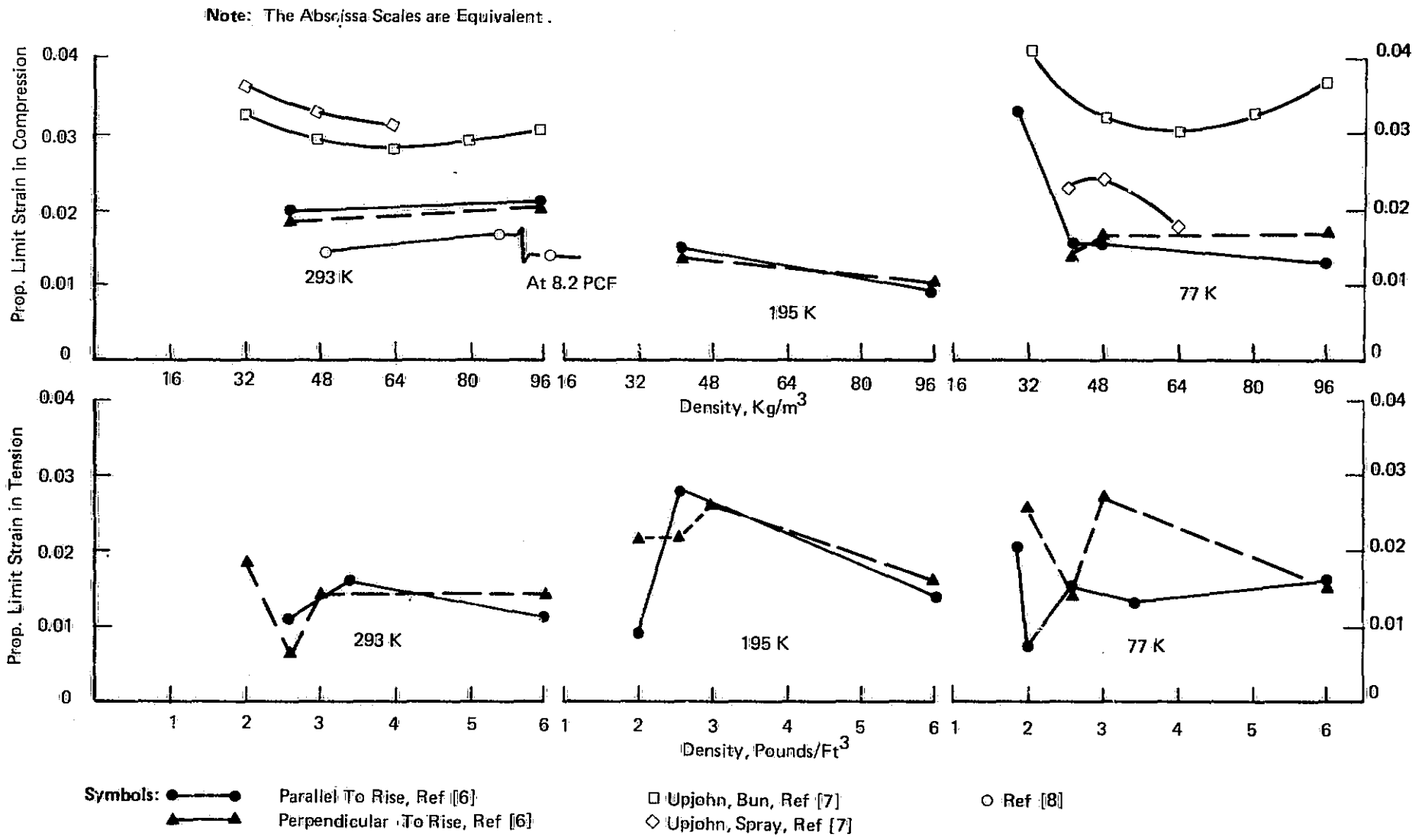

Figure 2–4. – Proportional limit strain for polyurethane foams

Since foams of higher densities, or at lower temperatures, exhibit higher Young's modulus, E, it can be seen that there is no trend related to the modulus of the foams. That is, the proportional limit strain is independent of E. The only effect of E in the application of foams to a cryogenic tank is the magnitude of the internal stresses developed as a result of the thermal contraction (and to a lesser extent the pressure strains).

Figure 2-5 shows the general trend to the stress-strain diagram with changes in temperature. At higher temperatures, the foams behave in a ductile manner. At lower temperatures, the behavior is brittle-like. Because of the brittle-like behavior at lower temperatures, the ultimate strength at breaking is almost identical to the porportional limit.

From the calculations presented earlier, it was determined that the foam would have to withstand a strain differential (thermal plus pressure) of approximately 0.012 mm/mm. From Figure 2-4, it can be seen that some data points fall below this value. Therefore, from the data presented here it could be concluded that during, say, a screening test, these data points would represent yielding of the foam. According to the criterion suggested above, such foams would not be acceptable. In fact, the foams whose proportional limit strain was less than 0.012 mm/mm would exhibit cracking failures at low temperatures due to their brittle-like behavior.

C-2

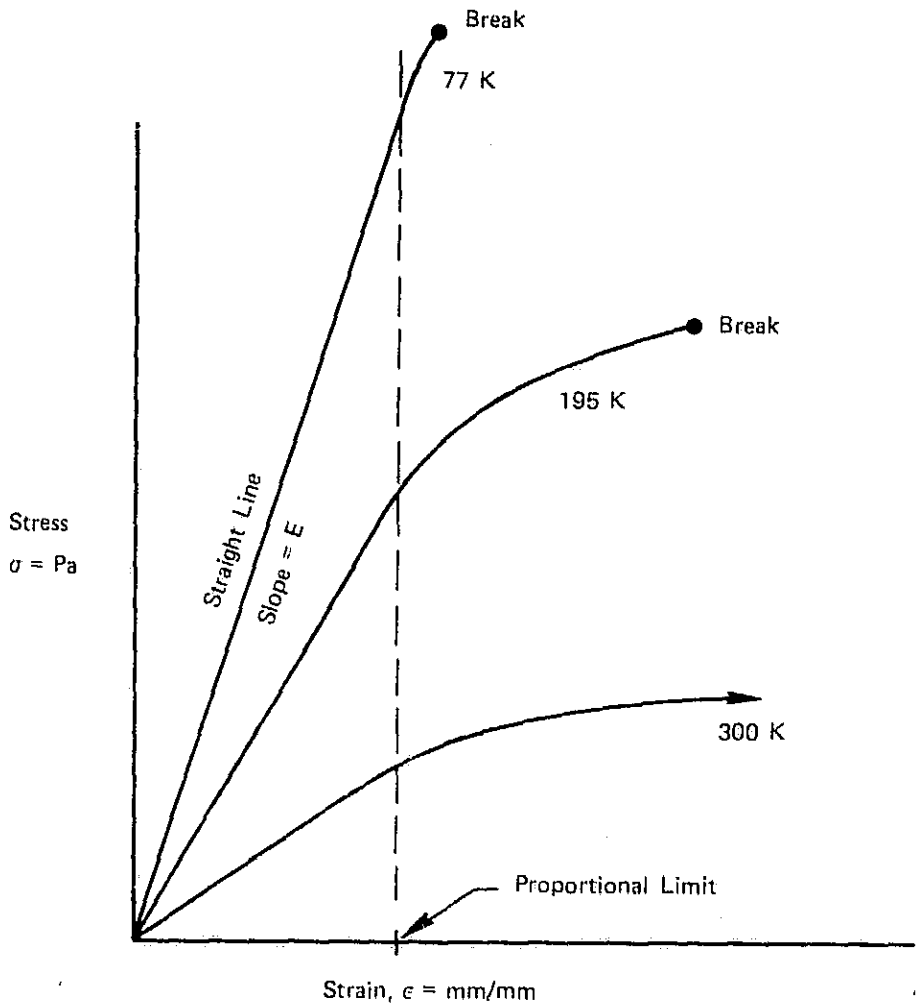

Figure 2–5. — Typical stress-strain diagram for foam materials

APPENDIX 3

MECHANICAL PROPERTY TEST METHODS

The proportional limit of a material is obtained from its stress-strain response. Such data were obtained on the various foams at both 300 and 77 K. The low-temperature tests were run by surrounding the test fixture with an insulated chamber filled with liquid nitrogen. The specimens were cooled for at least 5 minutes in liquid nitrogen and then tested while immersed in liquid nitrogen. All tests were run on an Instron testing machine.

The compression tests were run in accordance with ASTM D-1621 using a 25-mm-square by 25-mm-thick sample. The compressive strength was taken as the strength at yield or at 10% compression of the specimen if a yield point did not occur before 10% strain.

The tensile tests were run in accordance with ASTM D-1623, Type B. In this test, 25-mm cubes of foam were bonded to T-shaped aluminum test jigs. The jigs were then gripped in jaws for tensile testing. This method of test is not the best method, particularly for the 77°K test, because the shrinkage of the foam during cooldown produces some internal stresses. However, the method proved satisfactory for the screening being conducted in this program.

The data are recorded on a strip chart, on which are plotted applied loads versus crosshead motions. Taking into consideration the sample's cross-sectional area and length, such plots then yield the typical stress vs. strain diagram. Figure 3-1 shows the typical forms of these plots (stress vs. strain) for tension and compression at both room temperature and 77 K.

Results

At room temperature, all samples tested in tension showed the usual proportional increase of stress (load) with strain (deflection), an easily defined proportional limit, and a complete fracture at the ultimate stress.

In compression at room temperature, there existed a short initial portion of the stress-strain plot where the cut surfaces, being initially rough and partially unsupported, gradually assumed the applied load until firm support was developed. Because such surfaces do not exist in an infinitely large sample, this initial "settling in" nonlinearity can be ignored.

The linear portion of the plot was easily defined, as was the proportional limit. Failure always occurred as a gradual collapse of the structure.

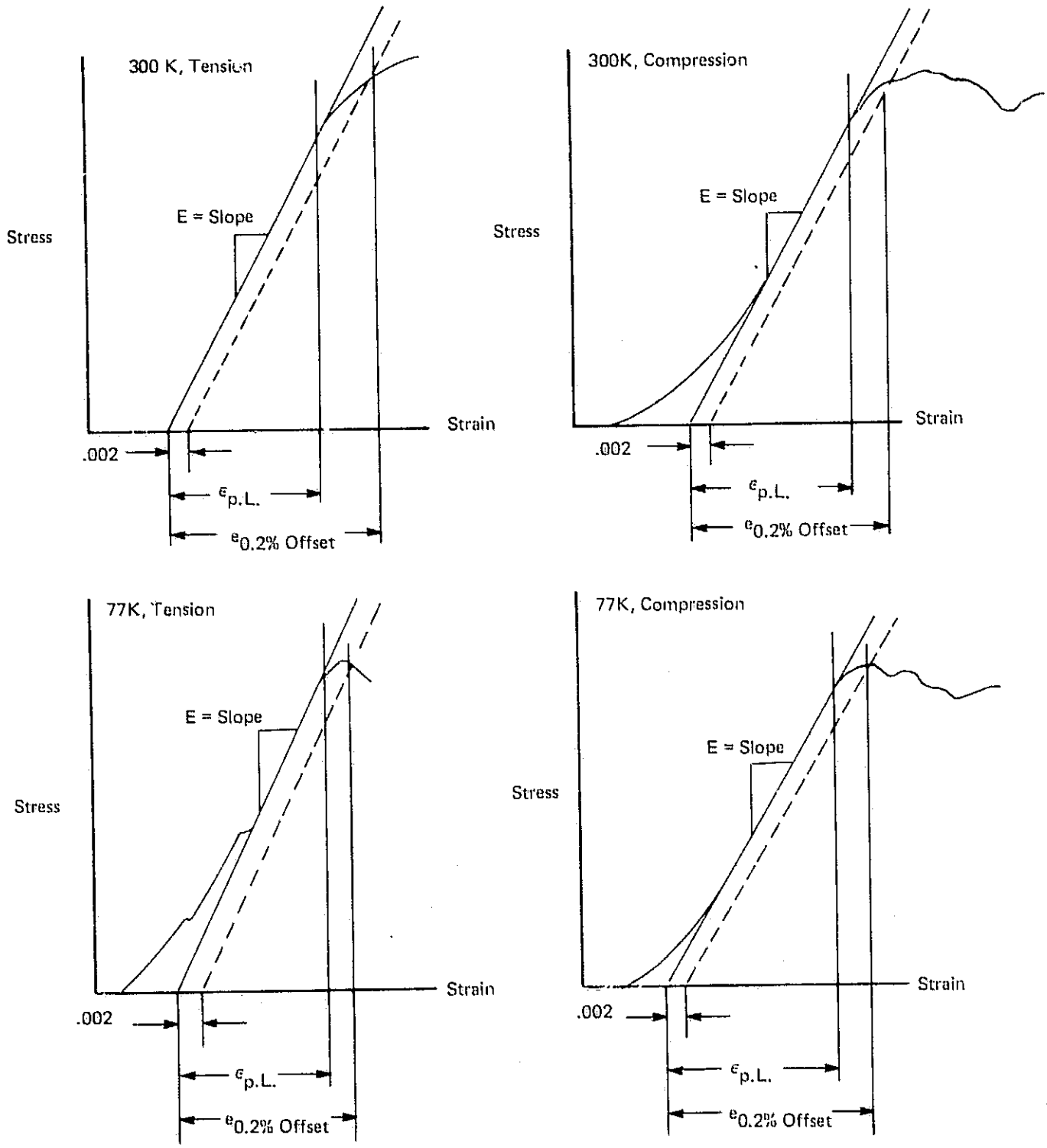

Figure 3.1. — Typical forms of experimental stress-strain diagrams for foam insulations showing Young's modulus, E, and strains at the proportional limit and at 0.2% offset

At 77°K in tension, the form of the stress-strain plot was unusual. As the figure shows, there were steps of increasing slope whose cause could not be determined. Had there been gradual tensile failure, the plot should show gradual, or steps of, decreasing slope, which is not the case. It is possible that inadvertent bending was somehow introduced into the clamps surfaces by ice, formed in the test machine. In any case, since a sample in tension cannot become discontinuously stiffer with increasing load, the initial abrupt changes in slope must be considered as "settling in" artifacts and the greatest slope, which always occurred just before failure, should be a true measure of the sample properties.

In compression, the low-temperature plots were similar to those at room temperature.

Young's modulus was calculated from the slope of the stress-strain diagram. It is a measure of the inherent stiffness of the material. The proportional limit, of course, is the maximum stress or strain for which the stress-strain linearity is still valid. Typically, if a material is not stressed (or strained) beyond this proportional limit, the material will completely recover its shape or dimensions upon relaxation of the loading. Stressing a material beyond this limit implies an inability to recover due to a variety of phenomena, one of which is partial failure. In the case of foam, this failure is the buckling collapse (and eventual bending fracture) of the cell walls due to compression, or the tensile fracture of the cell walls due to direct tension effects. In either case, prudent design requires that the proportional limit not be exceeded, in as much as additional failure on succeeding loading cycles will lead to eventual gross failure--a phenomenon called fatigue.

The strain at 0.2% offset, as described in Figure 3-1, is a measure of the gradual failure. The larger the strain at 0.2% offset, the more tolerant the material is to failure. Alternatively, a higher 0.2% offset strain implies less brittleness and less notch sensitivity. The choice of 0.2% offset is a carryover from metals testing which provides a common design stress criterion when the linear portion of the stress-strain diagram is non-existent.

The experimentally determined values for Young's Modulus E, proportional limit strain, and the strain at 0.2% offset are tabulated. Table 3-1 shows the data for room temperature; and Table 3-2, for 77 K.

At 77 K all foams tested exhibit brittle failure under tension, and about half showed brittle collapse under compression. At 300 K all the foams were ductile under compression. With tensile loading, however, only the Rohacell foams exhibited brittle failure at 77 K and 300 K, which is an indication of the notch sensitivity of this material, possibly over the entire operating temperature range.

Table 3-1. - Uniaxial mechanical properties of insulating foams at 300 K

Sample No.	Foam Description	Filler Reinforcement Material	Parallel to the Rise						Perpendicular to the Rise		
			Tension			Compression			Compression		
			E	$\varepsilon_{P.L.}$	$\varepsilon_{0.2\%}$	E	$\varepsilon_{P.L.}$	$\varepsilon_{0.2\%}$	E	$\varepsilon_{P.L.}$	$\varepsilon_{0.2\%}$
1	Upjohn 452	None	5.50	0.029	0.039	3.76	0.035	0.045	4.06	0.035	0.046
2	Upjohn 452	10% 1/16" MG, Style 630	7.41	0.025	0.030	4.03	0.033	0.040	4.16	0.032	0.038
3	Upjohn 492	None	10.27	0.028	0.038	4.35	0.048	0.058	4.67	0.033	0.042
4	Upjohn 492	10% 1/16" MG, Style 630	12.04	0.025	0.033	7.08	0.031	0.038	6.60	0.028	0.037
5	ADL	None	8.19	0.020	0.029	2.59	0.039	0.050	2.03	0.033	0.044
6	ADL	10% Nylon	4.64	0.024	0.034	1.99	0.042	0.050	2.61	0.033	0.042
7	ADL	10% 1/16" MG, Style 630	7.88	0.022	0.030	2.79	0.033	0.043	2.32	0.030	0.040
8	ADL	10% 1/32" MG, Style 630	9.89	0.017	0.026	3.67	0.034	0.044	2.25	0.031	0.041
9	ADL	10% 1/16" MG, Style 701	10.15	0.017	0.025	3.10	0.034	0.043	1.81	0.032	0.041
10	ADL	10% 1/32" MG, Style 701	8.01	0.020	0.030	2.74	0.034	0.044	2.65	0.028	0.039
11	Stepanfoam BX249N	None	8.90	0.029	0.040	3.88	0.034	0.045	1.67	0.023	0.034
12	Stepanfoam BX249N	10% 1/16" MG, Style 630	12.53	0.026	0.033	4.14	0.029	0.036	3.75	0.030	0.041
13	Stafoam AA1602	None	7.75	0.024	0.030	2.84	0.029	0.038	4.12	0.028	0.037
14	Stafoam AA1602	10% 1/16" MG, Style 701	8.87	0.022	0.029	6.95	0.029	0.036	6.67	0.021	0.030
15	Rohacell 31	None	25.56	0.030	Fail	12.91	0.025	0.032	12.91	0.025	0.032
16	Rohacell 51	None	30.04	0.042	Fail	21.16	0.027	0.034	21.16	0.027	0.034
17	Upjohn 452	10% 1/16" MG, Style 701	13.18	0.019	0.027	23.37	0.007	0.010	18.73	0.006	0.009
18	Stafoam AA1602	10% 1/16" MG, Style 701	17.31	0.018	0.022	24.75	0.006	0.010	14.58	0.006	0.009
19[1]	Upjohn 452	10% 1/16" MG Style 701	10.94	0.022	0.029	5.58	0.022	0.029	2.51	0.031	0.039

Notes and Nomenclature

E: Youngs Modulus, MPa

$\varepsilon_{P.L.}$: Strain at Proportional Limit, m/m

$\varepsilon_{0.2\%}$: Strain at 0.2 percent offset, m/m

All values are the average of these tests.

1. Machine-mixed foam.

Table 3-2. - Uniaxial mechanical properties of insulating foams at 77 K

Sample No.	Foam Description	Filler Reinforcement Material	Parallel to the Rise						Perpendicular to the Rise		
			Tension			Compression			Compression		
			E	$\varepsilon_{P.L.}$	$\varepsilon_{0.2\%}$	E	$\varepsilon_{P.L.}$	$\varepsilon_{0.2\%}$	E	$\varepsilon_{P.L.}$	$\varepsilon_{0.2\%}$
1	Upjohn 452	None	27.78	0.005	Fail	6.38	0.049	Fail	5.63	0.054	Fail
2	Upjohn 452	10% 1/16" MG, Style 630	11.64	0.014	Fail	5.03	0.042	Fail	6.07	0.035	Fail
3	Upjohn 492	None	19.41	0.012	Fail	6.92	0.074	Fail	7.48	0.063	Fail
4	Upjohn 492	10% 1/16" MG, Style 630	16.55	0.013	Fail	11.20	0.052	Fail	9.43	0.050	Fail
5	ADL	None	15.47	0.019	Fail	4.41	0.057	0.065	3.21	0.049	0.059
6	ADL	10% Nylon	12.42	0.021	Fail	3.71	0.050	Fail	4.56	0.045	0.053
7	ADL	10% 1/16" MG, Style 630	15.02	0.013	Fail	4.08	0.035	0.043	3.51	0.042	Fail
8	ADL	10% 1/32" MG Style 630	17.73	0.010	Fail	5.30	0.033	0.043	2.99	0.055	Fail
9	ADL	10% 1/16" MG Style 701	12.98	0.015	Fail	5.07	0.042	0.021	3.01	0.051	0.027
10	ADL	10% 1/32" MG, Style 701	14.49	0.015	Fail	4.87	0.036	0.043	4.91	0.037	0.049
11	Stepanfoam BX249N	None	14.49	0.014	Fail	5.97	0.066	Fail	5.76	0.049	0.027
12	Stepanfoam BX249N	10% 1/16" MG, Style 630	16.94	0.013	Fail	6.77	0.037	Fail	7.68	0.035	0.043
13	Stafoam AA1602	None	21.30	0.014	Fail	8.53	0.050	0.054	5.29	0.056	0.062
14	Stafoam AA1602	10% 1/16" MG Style 701	19.32	0.021	Fail	10.21	0.039	Fail	11.35	0.047	Fail
15	Rohacell 31	None	15.38	0.017	Fail	13.31	0.027	0.032	13.31	0.037	0.032
16	Rohacell 51	None	18.95	0.027	Fail	20.37	0.030	0.035	20.37	0.030	0.035
17	Upjohn 452	10% 1/16" MG, Style 701	20.31	0.014	Fail	2.83	0.070	0.078	2.14	0.074	0.077
18	Stafoam AA1602	10% 1/16" MG, Style 701	23.75	0.010	Fail	2.60	0.105	0.108	3.01	0.075	0.084
19(1)	Upjohn 452	10% 1/16" MG, Style 701	16.23	0.012	Fail	3.69	0.066	0.073	2.91	0.006	Fail

Notes and Nomenclature

E : Young Modulus, MPa

$\varepsilon_{P.L.}$: Strain at Proportional Limit, m/m

$\varepsilon_{0.2\%}$: Strain at 0.2 percent offset, m/m

All values are the average of these tests.

1. Machine-mixed foam.

For the two foam formulations selected for the 0.6 meter square cold shock tests, Upjohn 452 and Stafoam AA1602, both reinforced, the data from Tables 3-1 and 3-2 have been extracted and repeated in Table 3-3.

A review of these data yields the following observations.

The batch-to-batch variability of elastic properties is quite pronounced and obviously not predictable. By no means could the formulations and methods of manufacture used here be considered as standardized or optimum. Further, because of the non-isotropic properties, as demonstrated here, the optimization of a foam should include a preferred rise direction on the tank so as to ensure that the two directions corresponding to the highest proportional limit strain in tension appear within the plane of the foam (circumferential and longitudinal).

Independent of the rise direction, stress direction, tension, compression, and temperature, there is a pronounced trend that a lower E, Young's modulus, results in a higher proportional limit strain. In compression, the proportional limit strain increases significantly at lower temperatures. In tension, the proportional limit decreases slightly with lower temperature. This latter trend is probably due to the embrittling effect of low temperatures on plastic materials. Although the glass reinforcement has a general stiffening effect, this trend can be overshadowed by low-temperature effects. The machine-made foam, in general, exhibits better properties.

The flexural strength test was conducted in accordance with ASTM D-790. The specimens used for the test were 25 mm wide, 12 mm thick, and 150 mm long. A 100-mm test span was used with a three-point loading. The data we obtained are summarized in Tables 3-4 and 3-5. Included in these tables are the strength data obtained in accordance with ASTM D-1621 for low pressure and ASTM D-1623, Type B, for tension.

Table 3-3. - Uniaxial mechanical properties of the two selected insulating foams.

Foam Description and Test Temperature Level		Parallel to the Rise						Perpendicular to the Rise		
		Tension			Compression			Compression		
		E	$\varepsilon_{P.L.}$	$\varepsilon_{0.2\%}$	E	$\varepsilon_{P.L.}$	$\varepsilon_{0.2\%}$	E	$\varepsilon_{P.L.}$	$\varepsilon_{0.2\%}$
Upjohn 452, Data at 300K										
Batch Mixed Without Reinforcement	Sample No. 1	5.50	0.029	.039	3.76	0.035	.045	4.06	0.035	0.046
Batch Mixed With Reinforcement	Sample No. 2	7.41	0.025	.033	4.03	0.033	.040	4.16	0.032	0.038
Batch Mixed with Reinforcement	Sample No. 17	13.18	0.019	.027	23.37	0.007	.010	18.73	0.006	0.009
Machine Mixed With Reinforcement	Sample No. 19	10.94	0.022	.029	5.58	0.022	.029	2.51	0.031	0.039
Upjohn 452, Data at 77K										
Batch Mixed Without Reinforcement	Sample No. 1	27.28	0.005	Fail	6.38	0.049	Fail	5.63	0.054	Fail
Batch Mixed With Reinforcement	Sample No. 2	11.64	0.014	Fail	5.03	0.042	Fail	6.07	0.035	Fail
Batch Mixed with Reinforcement	Sample No. 17	20.31	0.014	Fail	2.83	0.070	.078	2.14	0.074	0.077
Machine Mixed With Reinforcement	Sample No. 19	16.23	0.012	Fail	3.96	0.066	.073	2.91	0.066	Fail
Stafoam AA1602, Data at 300K										
Batch Mixed Without Reinforcement	Sample No. 13	7.75	0.024	.030	2.84	0.029	.038	4.12	0.028	0.037
Batch Mixed With Reinforcement	Sample No. 14	8.87	0.022	.029	6.96	0.029	.036	6.67	0.021	0.030
Batch Mixed With Reinforcement	Sample No. 18	17.31	0.018	.022	24.75	0.006	.010	14.58	0.006	0.009
Stafoam AA1602, Data at 77K										
Batch Mixed Without Reinforcement	Sample No. 13	21.30	0.014	Fail	8.53	0.050	.054	5.29	0.056	0.062
Batch Mixed With Reinforcement	Sample No. 14	19.32	0.021	Fail	10.21	0.039	Fail	11.35	0.047	Fail
Batch Mixed With Reinforcement	Sample No. 18	23.75	0.010	Fail	2.60	0.105	.108	3.01	0.075	0.084

Notes and Nomenclature

E: Youngs Modulus, MPa

$\varepsilon_{P.L.}$: Strain at Proportional Limit, m/m

$\varepsilon_{0.2\%}$: Strain at 0.2 percent offset, m/m

All values are the average of these tests.

Table 3-4. - Summary of strength data at 77 K[2] and 300 K - SI units.[3]

Sample No.	Foam Description	Filler Reinforcement Material	Density (kg/m^3)	Ultimate Flexural Strength and Modulus (MPa)				Ultimate[1] Tensile Strength Parallel to Rise Direction (MPa)		Compressive Strength (MPa)			
				Strength (300K)	Modulus (300K)	Strength (77K)	Modulus (77K)			Parallel to Rise Direction		Perpendicular to Rise Direction	
								(300K)	(77K)	(300K)	(77K)	(300K)	(77K)
1	Upjohn 452	None	41.7	0.43	5.58	0.61	31.80	0.34	0.10	0.19	0.37	0.21	0.26
2	Upjohn 452	10% 1.6 mm MG, Style 630	41.7	0.37	9.51	0.57	16.68	0.24	0.19	0.18	0.25	0.21	0.26
3	Upjohn 492	None	46.5	0.46	8.41	0.74	18.47	0.50	0.25	0.27	0.59	0.25	0.50
4	Upjohn 492	10% 1.6 mm MG, Style 630	51.3	0.50	11.37	0.67	15.92	0.41	0.22	0.30	0.58	0.28	0.51
5	ADL-UC	None	32.1	0.23	3.03	0.41	4.82	0.32	0.28	0.17	0.35	0.11	0.21
6	ADL-UC	10% Nylon	35.3	0.24	3.17	0.44	5.34	0.21	0.27	0.14	0.19	0.15	0.27
7	ADL-UC	10% 1.6 mm MG, Style 630	35.3	0.26	5.38	0.42	8.55	0.25	0.20	0.16	0.22	0.12	0.17
8	ADL-UC	10% 0.8 mm MG Style 630	35.3	0.24	3.58	0.32	5.51	0.25	0.18	0.19	0.28	0.11	0.14
9	ADL-UC	10% 1.6 mm MG Style 701	35.3	0.23	3.93	0.47	8.13	0.27	0.19	0.18	0.24	0.12	0.18
10	ADL-UC	10% 0.8 mm MG, Style 701	36.7	0.17	3.79	0.32	6.07	0.27	0.16	0.16	0.22	0.14	0.27
11	Stepanfoam BX249N	None	36.7	0.31	5.79	0.62	10.75	0.41	0.19	0.21	0.42	0.11	0.34
12	Stepanfoam BX249N	10% 1.6 mm MG, Style 701	43.3	0.30	6.76	0.52	14.68	0.38	0.21	0.17	0.27	0.19	0.34
13	Stafoam AA1602	None	35.3	0.15	2.48	0.38	5.24	0.35	0.35	0.14	0.50	0.17	0.37
14	Stafoam AA1602	10% 1.6 mm MG Style 701	38.5	0.25	6.07	0.52	12.68	0.27	0.41	0.26	0.42	0.22	0.56
15	Rohacell 31	None	35.3	0.65	19.10	0.62	33.78	0.78[4]	0.26[4]	-	-	0.45[4]	0.51[4]
16	Rohacell 51	None	54.5	1.03	30.00	1.07	48.80	1.23[4]	0.47[4]	-	-	0.78[4]	0.90[4]
17	Upjohn 452	10% 1.6 mm MG, Style 701	35.3	0.23	5.10	0.38	8.41	0.38	0.30	0.21	0.23	0.15	0.18
18	Stafoam AA1602	10% 1.6 mm MG Style 701	36.7	0.23	5.72	0.41	8.89	0.39	0.23	0.21	0.34	0.12	0.25
19	Upjohn 452 Machine Made	10% 1.6 mm MG, Style 701	35.3	0.24	4.27	0.33	7.51	0.32	0.19	0.21	0.30	0.13	0.19

Notes:

1. The cross sectional area of the test specimen in the plane perpendicular to the direction of the applied force is nominally one square inch.
2. 77K environmental temperature for sample was achieved by immersion in liquid nitrogen (boiling point 77K).
3. Measurements performed with Instron Model TM.
4. Rohacell tested across thickness of sheet only. Rise direction not known.
5. All values are the average of these tests.

Table 3-5. - Summary of stength data at 77 K[2] and 300 K - Cus:omary units

Sample No.	Foam Description	Filler Reinforcement Material	Density (Lb/Ft.^{3})	Ultimate Flexural Strength and Modulus (lb/in.^{2})				Ultimate[1] Tensile Strength Parallel to Rise Direction (lb/in.^{2})		Compressive Strength (MPa)			
				Strength (300K)	Modulus (300K)	Strength (77K)	Modulus (77K)	(300K)	(77K)	Parallel to Rise Direction (300K)	Parallel to Rise Direction (77K)	Perpendicular to Rise Direction (300K)	Perpendicular to Rise Direction (77K)
1	Upjohn 452	None	2.6	62	810	88	2000	49	15	27	53	30	53
2	Upjohn 452	10% 1/16" MG, Style 630	2.6	54	1380	83	2420	35	27	26	37	30	38
3	Upjohn 492	None	2.9	67	1220	107	2680	72	37	39	85	36	73
4	Upjohn 492	10% 1/16" MG, Style 630	3.2	73	1650	97	2310	59	32	43	84	41	74
5	ADL-UC	None	2.0	33	440	59	700	46	41	25	51	16	31
6	ADL-UC	10% Nylon	2.2	35	460	64	920	31	40	20	28	22	39
7	ADL-UC	10% 1/16" MG, Style 630	2.2	38	780	61	1240	36	29	23	32	18	25
8	ADL-UC	10% 1/32" MG, Style 630	2.2	35	520	47	800	37	26	27	40	16	21
9	ADL-UC	10% 1/16" MG, Style 701	2.2	34	570	68	1180	40	28	26	35	17	26
10	ADL-UC	10% 1/32" MG, Style 701	2.3	25	550	47	880	40	31	23	32	20	39
11	Stepanfoam BX249N	None	2.3	45	840	90	1560	60	28	30	61	18	50
12	Stepanfoam BX249N	10% 1/16" MG, Style 630	2.7	43	980	76	2130	55	31	24	40	28	50
13	Stafoam AA1602	None	2.2	22	360	55	760	51	51	20	73	25	53
14	Stafoam AA1602	10% 1/16" MG, Style 701	2.4	37	880	76	1840	39	60	38	61	32	82
15	Rohacell 31	None	2.2	95	2270	90	4900	113[4]	38[4]	-	-	66[4]	74[4]
16	Rohacell 51	None	3.4	149	4350	156	7080	179[4]	69[4]	-	-	114[4]	131[4]
17	Upjohn 452	10% 1/16" MG, Style 701	2.2	34	740	55	1220	55	44	30	38	22	26
18	Stafoam AA1602	10% 1/16" MG, Style 701	2.3	34	830	60	1290	56	34	31	49	17	27
19	Upjohn 452	10% 1/16" MG, Style 701	2.2	35	620	48	1100	47	27	31	43	19	28

Notes:

1. The cross sectional area of the test specimen in the plane perpendicular to the direction of the applied force is nominally one square inch.
2. 77K environmental temperature for sample was achieved by immersion in liquid nitrogen (boiling point 77K).
3. Measurements performed with Instron Model TM.
4. Rohacell tested across thickness of sheet only. Rise direction not known.
5. All values are the average of these tests.

APPENDIX 4

MACHINE PRODUCTION OF FOAM

Need for Machine Production

Batch mixing of foams is commonly used for preparing small quantities of foam for evaluation; in addition, this method provides a convenient approach to the addition of fibers to the polyurethane foam for reinforcement. In fact, we have batch mixed quantities up to several gallons of urethane foam with glass fibers on a limited production basis. Batch mixing was also used in the application of foam to the calorimeter tank in a NASA/Langley program in 1964.

It is obvious, however, that if a standardized reproducible product is to be made in any significant quantity, machine production of foam is a necessity. The extent of mixing in a batch process may vary from one batch to another because of the very limited mixing time available before the foam starts to cream and rise with most systems. In addition, air and moisture may be whipped into the foam in the batch mixing process, thereby making the thermal and mechanical properties of the foam more variable than is the case with foam from a machine where all mixing is done in a closed space.

Function of Machines

There are a number of manufacturers of machines for urethane foam production. The machines range in capacity from units that will produce a fraction of a kilogram per minute up to large-scale equipment for bun lines and other high-volume applications where production may be in the hundreds of kilograms per minute. Basically, these machines perform two functions: (1) metering of two or more components in exact ratio continuously while the machine is operating, and (2) thoroughly mixing the components to achieve complete chemical reaction of the system.

Metering Pumps

The metering pumps are of critical importance in the polyurethane foam machine. They must have positive displacement and continuously meter the exact ratio of components while the machine is operating if consistent foam is to be achieved. With many foams, if the ratio of components varies by more than a few percent, the properties of the foam are significantly affected. To achieve these exacting ratios, double-acting piston pumps or precision gear pumps are commonly used in these machines. Some of these pumps depend for accuracy of their operation on the opening and closing of valves on the cylinders of the pump. Any solids in the liquid polyurethane components can jam the valves or otherwise hinder proper functioning of the pumps.

Mixing Head

Various types of devices are utilized to achieve the necessary intimate mixing of the urethane foam liquid components. The most common type of mixing head utilizes a high-speed rotating cylinder or cone within a slightly larger stator. The liquids are fed into the annular space between the stator and rotor at one end and mixed by the shearing action in the annular space as they pass to the other end and are discharged.

Another type of mixing head utilizes impingement mixing. These mixing heads require that the liquid components be at high pressure as they are fed through small orifices into the mixing chamber. The orifices are positioned very accurately so that the high-pressure streams impinge on each other within the small chamber and are intimately mixed as they discharge from the end of the chamber. Impingement mixers have the advantage that when a shot is completed, the mixing chamber can be purged by a piston moving down the chamber to discharge all of the mixed reactive components. In this type of system, a minimum of solvent flushing of the mixing head is required. With the rotary type mixing head, substantially larger quantities of flushing solvent are required following each shot of foam.

A third type of mixing head is a static mixer, of which there are various configurations. The original static mixer, manufactured by Kenics Corporation of Danvers, Massachusetts, was developed by Arthur D. Little, Inc. Although the mechanical configurations of various static mixers differ, they all consist of a tube which contains various types of baffles and vanes which cut and redirect the liquid stream so that it becomes intimately mixed. Like the rotary mixer, the static mixer must be flushed with solvent to clean it every time the machine is stopped.

Auxiliary Components

Metering and mixing machines frequently contain other components for various purposes. Normally, the liquid components are fed to the mixing head through hoses which are frequently heated to maintain the components at a specified temperature to assure that the metering is not adversely affected by changes in viscosity with changing ambient temperature and that the components are at the optimum viscosity for most effective mixing in the mixing head. Frequently, the hose lines will be loops so that the metering pumps can pump continuously with recycling back to the storage reservoir. When the pouring of foam is started in these recycle systems, a valve simply diverts the flow from the return line into the mixing head.

Sometimes feed pumps are used to supply the liquid components under pressure to the metering pumps.

Use of Reinforcing Fibers

Fillers and fibrous reinforcements have not been commonly used in urethane foams. In those cases where such additives might be desirable, their use has been discouraged by the problems of handling these solids in dispersion in the liquid components through the metering and mixing machines. This problem has been circumvented, as previously noted, for some applications by utilizing a spray system in which the liquid components are sprayed from an internal mix spray gun and particulate or fibrous additives are blown into the spray pattern and deposited with the liquid components to become a part of the foam system.

There are a number of quality control problems in utilizing such a system. Fibers, particularly if they are long fibers (24 mm) cut from a roving chopper mounted on the spray gun, will entrap air in the liquid components, resulting in air voids in the foam as it rises. Although such voids are not desirable, they are acceptable for some applications. Such voids would be completely unacceptable for insulating liquid hydrogen fuel tanks.

Another problem in using the spray technique is the significant difficulty in achieving uniform distribution of the fibers or fillers, so the properties of the foam may vary from area to area.

A third problem is the absence of high shear and intimate mixing of the additives and the liquid foam components. As a result, the wetting and bonding between the additive and the urethane may be marginal and variable, again resulting in variation in properties from area to area. Because of these reasons, we have not considered spray fabrication as an acceptable method for this program.

In the conventional mixing and metering machines, the use of fiber is particularly objectionable, because fibers can bridge in small orifices and valves and cause blockage with possible damage and shutdown of the equipment. If this problem cannot be avoided, the system is unreliable. However, if the problem can be eliminated through the use of a Moyno or some other type of pump that is not dependent on valves and close tolerances for its metering action, a system with reinforcing fibers dispersed in the liquids becomes practical.

In addition to the problems with the metering pumps, the fibers can adversely affect the mixing head and also be adversely affected by it. Because of the abrasive character of glass fibers and the high pressures required in impingement mixing, we do not consider this to be a practical method for making fiber-reinforced foam systems.

The rotary type mixing heads might be satisfactory for making fiber reinforced foam. But we have some concern that the fiber may be balled up or broken and degraded by the high shear generated in that type of head. We

believe that the most practical type of mixing system for the fiber-reinforced foam is the static mixer; however, we have had some reports that static mixers do not work well with high-viscosity systems, and the glass fiber dispersed in the liquid produces a high viscosity.

We believe that it is possible to design a system to handle liquid polyurethane components with glass fibers dispersed in them if the need for such a system arises.

Discussions with Machine Manufacturers

We discussed with several of the leading polyurethane mixing-metering machine manufacturers the feasibility of machine manufacture of the glass fiber-reinforced polyurethane. These manufacturers included: Martin-Sweets Co., Louisville, Kentucky; Graco, Inc., Minneapolis, Minnesota; Pyles Industries, Inc., Wixona, Michigan; Admiral Equipment Division of Upjohn Co., Akron, Ohio; Binks Manufacturing Co., Franklin Park, Illinois; and Kornylac Corp., Hamilton, Ohio. None of these companies indicated significant experience with the use of filled systems, including fiber-reinforced systems, in their equipment. All of them indicated some experimental work had been done with particulate and fibrous fillers, with mixed results. In general, they indicated a willingness to make pilot runs using glass-filled systems. However, they would not be willing to guarantee the equipment for such applications even if the pilot runs were successful because, in daily production, the machine could be adversely affected by wear caused by the glass fiber and/or the build up of fibers at various points in the system, resulting eventually in clogging of the valves, etc.

Several of the manufacturers have utilized static mixers in their equipment, but expressed some concern that the high viscosity of the glass fiber-reinforced systems might cause excessive back pressure in the static mixer. Some of the companies also have experience in using Moyno-type pumps but indicated that these pumps are generally less effective in maintaining the exact ratio of components than are the piston-and-gear-type pumps currently used on the urethane mixing and metering equipment.

As the result of these discussions, it became clear that the development of a truly effective and reliable mixing-metering system for the fiber-reinforced urethane could not be accomplished within the scope of this program. In order to meet the need in the program to demonstrate the feasibility of machine-made foam, we decided to work with one cooperative manufacturer to identify problems in working with his particular equipment and make sufficient foam for test purposes in this program. The CPR Division of Upjohn indicated a keen interest in working with us on this program. We, therefore, concentrated our efforts with it.

CPR Upjohn Foam Machine Runs

The foam machine trial runs were done at the headquarters of CPR Upjohn Division, 555 Alaska Avenue, Torrance, California. The contacts were Mr. Del Holter and Mr. Jack Tupper.

First Trial Run

For the first trial run, CPR used an Admiral, model 120P pour machine capable of mixing and dispensing up to 5.5 kg/min. The metering pumps on this unit are high-precision gear pumps. The mixing head is a motor driven annular stator and rotor type unit.

The system used was the CPR Upjohn 452 with 20% of 1.6-mm milled Fiberglas, Style 701, added to the polyol component. The actual dispensing rate during the run was 3 kg/min. The foam obtained was not satisfactory for two reasons: 1) poor suspension of the milled glass in the polyol component, and 2) inability of the gear pump to handle the polyol component containing the Fiberglas because of the high viscosity.

Second Trial Run

For the second run, a modified model 120P Admiral pour machine was used. An air-driven agitator of the paddle type was utilized in the holding tank for the B (polyol) component to maintain a uniform dispersion of the Fiberglas in the liquid. A non-precision Viking gear pump designed to handle viscous formulations was substituted for the precision Admiral gear pump for the B component. The Viking pump was controlled with a Dodge SCR solid-state controller with a digital RPM readout. Even though this pump is not a precision unit, it was possible to meter the B component to an accuracy of $\pm$ 1 percent with the controller providing accurate RPM control. The storage tanks and hoses on the unit were heated and a recirculating type of hose system was utilized. Methylene chloride was used to flush the mixing head at the end of each shot.

With this equipment, several buns of the 10% glass-reinforced CPR 452 foam were produced at a dispensing rate of 3 kg/min. Upjohn supplied four 760 x 760 x 56 mm panels of this foam for test and evaluation purposes in this program, and this material is referred to throughout this report as Upjohn 452 machine-made foam.

The estimated cost of the modified model 120P Admiral machine with a Viking pump and Dodge controller is $17,000.

Although this equipment was satisfactory for demonstrating machine processability of this formulation, there are still many questions to be answered. We know nothing of the long-term reliability